Federal Aviation Administration

DOT/FAA/AFS400/2017/R/16
Flight Technologies and Procedures Division, AFS-400
Washington, DC 20591

Safety Study on Simultaneous Independent Approaches Using Established on Required Navigation Performance Authorized Approach Procedures with Radius-to-Fix Design

April 2017

Technical Report

NOTICE

This document is disseminated under the sponsorship of the U.S. Department of Transportation in the interest of information exchange. The United States Government assumes no liability for the contents or use thereof.

The United States Government does not endorse products or manufacturers. Trade or manufacturers' names appear herein solely because they are considered essential to the objective of this report.

DOT/FAA/AFS400/2017/R/16

Jason Walls, AFS-450
Logan Branscum, AFS-450
Cody Nichols, AFS-450
Gary Foster, Clancy JG
Blair Dulli, DIGITALiBiz
Flight Systems Laboratory, AFS-450
Oklahoma City, Oklahoma 73169

Submitted by:

X KAREN E LUCKE

Digitally signed by KAREN E LUCKE
Date: 2017.07.20 09:56:28 -05'00'

Karen E Lucke
Manager, Flight Systems Laboratory, AFS-450

Approved by:

X DANNY E HAMILTON

Digitally signed by DANNY E HAMILTON
Date: 2017.07.20 10:16:44 -05'00'

Bruce DeCleene
Manager, Flight Technologies and Procedures Div...

Technical Report Documentation Page

1. Report No.	2. Government Accession No.	3. Recipient's Catalog No.
DOT/FAA/AFS400/2017/R/16		

4. Title and Subtitle	5. Report Date
Safety Study on Simultaneous Independent Approaches Using Established on Required Navigation Performance Approach Procedures with Radius-to-Fix Design	April 2017
6. Author(s)	**7. Performing Organization Code**
Jason Walls, AFS-450; Logan Branscum, AFS-450; Cody Nichols, AFS-450; Gary Foster, Clancy JG; Blair Dulli, DIGITALiBiz	AFS-450
8. Performing Organization Name and Address	**9. Type of Report and Period Covered**
Flight Systems Laboratory, AFS-450 or 6500 S MacArthur Blvd., STB Annex, RM 217 Oklahoma City, OK 73169	Technical Report

10. Sponsoring Agency Name and Address
Federal Aviation Administration
Flight Technologies and Procedures Division, AFS-400
470 L'Enfant Plaza, SW
Washington, DC 20024

11. Supplementary Notes

12. Abstract

The Federal Aviation Administration conducted a safety study on simultaneous independent Established on Required Navigation Performance (RNP) (EoR) operations using instrument approach procedures with a radius-to-fix (RF) design to dual or triple parallel runways. The EoR concept uses RNP technology to safely direct aircraft from initial approach fixes on the downwind leg to simultaneous independent approach paths for dual or triple parallel runways without required vertical separation of aircraft on adjacent final approach courses. The analysis indicates that mid-air collision risk is between 10^{-9} and 10^{-10} per operation for simultaneous independent RF turn procedures to dual parallel runways separated by 3600 ft or greater and to triple parallel runways separated by 3900 ft or greater. The study also assessed nuisance alert rates from the Traffic Alert and Collision Avoidance System and Final Monitor Aid function in the Standard Terminal Automation Replacement System.

13. Key Words	14. Distribution Statement
Required Navigation Performance (RNP) Radius-to-fix (RF) Established on RNP (EoR) Human-in-the-loop Hardware-in-the-loop Simultaneous independent parallel approaches Performance-Based Navigation (PBN) Improved Multiple Runway Operations (IMRO) Area Navigation (RNAV)	Uncontrolled
15. Security Classification of This Report	**16. Security Classification of This Page**
Unclassified	Unclassified

DOT F1700.7

Table of Contents

1 Introduction 8
1.1 Background 9
2 Objectives and Scope 10
3 Modeling and Simulation 11
3.1 Collision Risk 11
3.1.1 Collision Risk Methodology 11
3.1.2 Collision Risk Input Data 14
3.1.3 Collision Risk Results 18
3.2 Implementation Risks 21
3.2.1 Final Monitor Aid Caution Alerts 21
3.2.2 Traffic Collision Avoidance System Resolution Advisories 26
4 Key Findings and Conclusions 27
Appendix A: Equipment Failure Hardware-in-the-Loop Simulation Conditions 31
Appendix B: Pilot Reaction Data from TF Turn Human-in-the-Loop Experiment 34
Appendix C: EoR RF Design Tabulated Mid-Air Collision Risk 37

List of Figures

Figure 1-1: EoR Concept 8
Figure 3-1: TF and RF Mathematical Model Inputs 13
Figure 3-2: Plot of Bank Angle Responses Relative to Failure Initiation with RF legs 15
Figure 3-3: Historical Wind Distributions 17
Figure 3-4: EoR RF Design Mid-Air Collision Risk without Controller Intervention and Bank Changing Ratio equal to 1 19
Figure 3-5: EoR RF Design Mid-Air Collision Risk without Controller Intervention and Bank Changing Ratio equal to 0.5 19
Figure 3-6: EoR RF Design Mid-Air Collision Risk without Controller Intervention and Bank Changing Ratio equal to 0.1 20
Figure 3-7: EoR RF Design Mid-Air Collision Risk with Controller Intervention and Bank Changing Ratio equal to 1 20
Figure 3-8: EoR RF Design Mid-Air Collision Risk with Controller Intervention and Bank Changing Ratio equal to 0.5 21
Figure 3-9: EoR RF Design Mid-Air Collision Risk with Controller Intervention and RF-to-TF Bank Changing Ratio equal to 0.1 21
Figure 3-10: FMA 10 Second Predictor Overshoot Geometry 23

Figure 3-11: FMA Caution Alert Rate Function Composition Diagram 24
Figure 3-12: Established on RNP RF Design – Nuisance FMA Caution Alert Rate 25
Figure A-1: Approach Plate 31

List of Tables

Table A-1: Airbus A330 RF Flight Guidance Failure Observations 32
Table A-2: Boeing B737 RF Flight Guidance Failure Observations 33
Table C-1: Median Winds at 3600' 38
Table C-2: Median Winds at 3900' 39
Table C-3: Median Winds at 4300' 40
Table C-4: Median Winds at 4800' 41
Table C-5: Median Winds at 5300' 42
Table C-6: Median Winds with No Controller Intervention at 3600' 43
Table C-7: Median Winds with No Controller Intervention at 3900' 44
Table C-8: Median Winds with No Controller Intervention at 4300' 45
Table C-9: Median Winds with No Controller Intervention at 4800' 46
Table C-10: Median Winds with No Controller Intervention at 5300' 47
Table C-11: Worst Winds at 3600' 48
Table C-12: Worst Winds at 3900' 49
Table C-13: Worst Winds at 4300' 50
Table C-14: Worst Winds at 4800' 51
Table C-15: Worst Winds at 5300' 52
Table C-16: Worst Winds without Controller Intervention at 3600' 53
Table C-17: Worst Winds without Controller Intervention at 3900' 54
Table C-18: Worst Winds without Controller Intervention at 4300' 55
Table C-19: Worst Winds without Controller Intervention at 4800' 56
Table C-20: Worst Winds without Controller Intervention at 5300' 57

Executive Summary

In July 2016, the Flight Technologies and Procedures Division (AFS-400) published DOT/FAA/AFS400/2016/R/01, a technical report on the safety of simultaneous independent Established on Required Navigation Performance (RNP) (EoR) operations using track-to-fix (TF) turns, referred to hereafter as TF turn study.[1] It was the first study that could be used to support a change to separation standards throughout the National Airspace System (NAS) utilizing the EoR operational concept, which eliminates the requirement for 3 nautical mile (NM) lateral or 1000 ft vertical separation prior to becoming established on the final approach course for multiple runway operations. This study extends the results of the prior EoR analysis by including procedures designed with radius-to-fix (RF) turns. Selection of an incorrect flight procedure was not included in this study, but has been addressed in a separate technical study.[2]

The primary objective of this study was to assess the mid-air collision risk of simultaneous independent EoR operations using instrument approach procedures with RF leg design by aircraft that may not have vertical guidance. As with existing parallel approach operations, autopilot or flight director is required. Pilot and controller response data to non-normal scenarios conducted during three human-in-the-loop tests for the TF turn study was used for this study. Inputs to the mathematical model used in the TF turn study were adapted to represent non-normal collision risk for EoR operations using RF design.

The analysis indicates that mid-air collision risk is between 10^{-9} and 10^{-10} per operation for simultaneous independent EoR operations to dual parallel runways separated by 3600 ft or greater and to triple parallel runways separated by 3900 ft or greater regardless of whether the turns were designed with TF or RF legs. The analysis and a hardware-in-the-loop simulation revealed some differences between constant bank and varying bank approach procedure designs. While equipment failures are less likely to induce a deviation from course during a constant bank turn, decreased separation from parallel traffic needs to be accounted for in approach procedures designed using RF turns due to the increased likelihood of collision given a deviation from the approach path.

Along with collision risk assessment, Traffic Collision Avoidance System (TCAS) resolution advisories (RAs) and nuisance Final Monitor Aid (FMA) caution alert rates were also assessed. It was determined that all RF EoR operations spaced 4850 ft or greater will experience false FMA caution alerts at a rate lower than 1 in every 1000 operations. By increasing the turn radius of the RF leg, operations at airports with 4000 ft or more of separation can control the probability of encountering false FMA caution alerts. Mitigations to encountering false TCAS RAs include adding and extending the 10° intercept leg, designing the turn-on to the final approach course to occur at an altitude that will reduce the probability of an RA, and staggering the procedure turn-ons by at least 2 NM. Herein, the term procedure stagger is used to identify cases where the final rollout point prior to the final approach course, toward parallel runways, is varied with respect to the runway threshold. Procedure stagger is different from runway stagger.

[1] Flight Technologies and Procedures Division, DOT/FAA/AFS400/2016/R/01, Safety Study on Simultaneous Independent Approaches Using Established on Required Navigation Performance Approach Procedures with Track-to-Fix Design (Federal Aviation Administration, July 2016).

[2] Flight Technologies and Procedures Division, DOT/FAA/AFS400/2016/R/05, Safety Study on the Selection of an Incorrect Established on Required Navigation Performance Instrument Approach Procedure (draft) (Federal Aviation Administration, February 2017).

1 Introduction

Aircraft separation standards currently require a minimum of 1000 ft vertically or 3 NM horizontally between aircraft, until they are established on the final approach course. The EoR concept of operations leverages performance-based navigation to eliminate that requirement.[3] The EoR concept adapts the approach procedure to an area navigation Global Positioning System (RNAV) (GPS) or RNAV (RNP) approach that begins with a segment aligned with the downwind leg. The differences between existing radar vectored interceptions of the final approach course and conceptual EoR operations can be seen in Figure 1-1. The key difference is the shorter and repeatable flight paths required by EoR operations as compared to vectoring aircraft to intercept the final approach course. This results in efficiency gains to the NAS. The first analysis of the EoR concept conducted by AFS-400 used a series of TF legs in order to reduce the barriers to implementation, as not all aircraft are RF equipped. The difference in flight tracks between an EoR approach using fly-by TF legs in place of RF turns is rather small. However, there are some possible safety benefits to using RF turns that may not be readily apparent. When an aircraft is in a stable turning state, it is less likely to result in path deviations as discussed in section 3.1.2. Therefore, approach procedures that require the aircraft to change its bank angle while turning from the downwind to the final approach course can induce higher deviation rates. Instrument approach procedures that only contain constant or increasing bank angles can be designed using RF turns. This study assesses the mid-air collision risk of simultaneous independent EoR operations using instrument approach procedures with RF leg design.

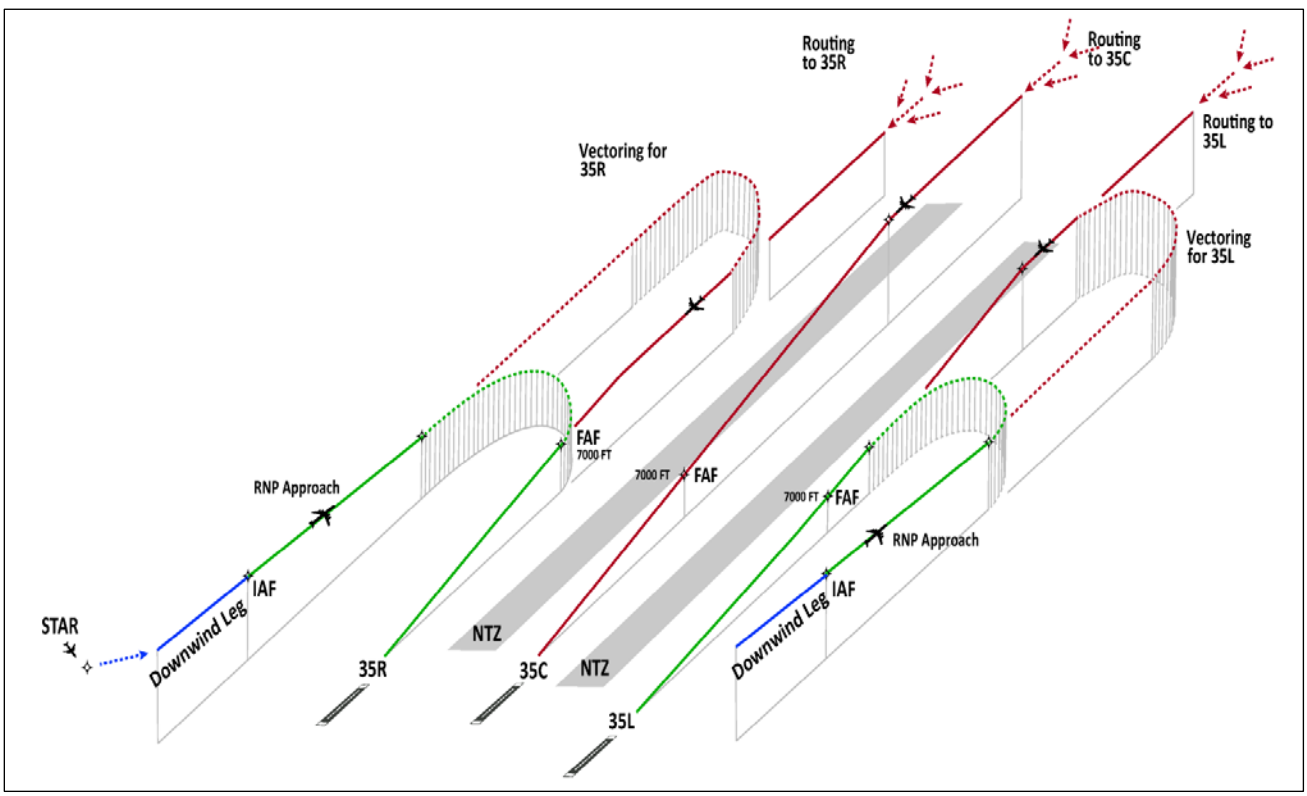

Figure 1-1: EoR Concept

[3] DIGITALiBiz, *FAA Performance Based Navigation Simultaneous Independent Established on RNP Concept of Operation* (Final Version 1.0 draft, 2014).

1.1 Background

The EoR concept was first introduced in February 2011, when the Performance-Based Operations Aviation Rulemaking Committee issued a recommendation to the Federal Aviation Administration (FAA) Associate Administrator for Aviation Safety to consider implementation of EoR.[4] The FAA engaged with Boeing to perform a safety analysis for dependent operations.[5] Additionally, AFS-400 performed a study at Seattle, Washington, on dependent simultaneous operations.[6] Consequently, dependent EoR concept operations have been implemented at the Seattle Terminal Radar Approach Control facility.[7] The FAA has also completed an analysis for RNP authorization required curved path approaches to runways separated by more than 9000 ft.[8] That analysis supported approval of a change to the separation standards to allow simultaneous independent parallel operations between an RNP authorization required curved approach and a straight-in Instrument Landing System (ILS), RNAV with vertical guidance, Ground Based Augmentation System (GBAS) Landing System (GLS), or another RNAV (RNP) approach with an RF leg(s) or an RNAV straight-in to runways spaced more than 9000 ft. Simultaneous approaches utilizing this separation standard have been implemented at Denver International Airport, and other locations are currently being evaluated.[9] The MITRE Center for Advanced Aviation System Development is analyzing the feasibility of the concept and operations as implemented at Seattle and Denver.

The TF turn study concluded that for the runway and approach geometries analyzed, the EoR operations resulted in a collision risk approximately 10^{-9} per operation for dual parallel runway configurations spaced 3600 ft or greater, and for triple parallel runway configurations spaced 3900 ft or greater.[10] EoR operations to runways spaced 3600 ft or more with an FMA and a no transgression zone (NTZ) result in a collision risk on the order of 10^{-9}, while operations to runways spaced more than 9000 ft resulted in a collision risk on the order of 10^{-10} or less without an FMA. Dual EoR operations based on RNAV (GPS) procedures with a 10° intercept of the extended final approach course performed adjacent to a straight-in procedure to one of the runways result in a collision risk on the order of 10^{-9}. Triple EoR operations were analyzed with a 10° intercept on either or both outside runways, and a straight-in approach to the center runway with similar results to those of dual operations. These results apply to GPS based RNAV and RNP aircraft with or without vertical guidance using TF fly-by turn procedure design, and may be combined with ILS or GLS straight-in approaches.

---

[4] PARC RNP Benefits Sub-Team, "RNP Established – Parallel Approach", Prepared by the Performance-Based Operations Aviation Rulemaking Committee (January 10, 2011).

[5] Boeing, *Seattle Greener Skies i2 Established on RNP (EoR) Simultaneous Dependent Closely-Spaced Parallel Approaches National Airspace System (NAS) Modeling and Simulation Report* (SE2020 Task Order 8, Deliverable 19, Version 2, 2014), 136.

[6] Flight Systems Laboratory, *DOT-FAA-AFS-400-89, Established on Required Navigation Performance Human in the Loop Data Collection for Dependent Simultaneous Operations with Runways Spaced 2,500' at Seattle, Washington* (Federal Aviation Administration, May 2014).

[7] Federal Aviation Administration, *Waiver to FAA JO 7110.65 Paragraphs 5-9-6a.1 and 5-9-6b.1, Seattle TRACON Simultaneous Dependent Approaches* (U.S. Department of Transportation, August 21, 2014).

[8] Flight Technologies and Procedures Division, "Memorandum 14-0314-54799, Required Navigation Performance Authorization Required Curved Path Approaches to Widely Spaced Runways" (Federal Aviation Administration, June 24, 2014).

[9] Federal Aviation Administration, *Established on Required Navigation Performance Separation for Simultaneous Independent Approaches to Widely Spaced Parallel Runways without Final Monitors Safety Risk Management Document* (Version 1, October 15, 2015).

[10] Flight Technologies and Procedures Division, *DOT/FAA/AFS400/2016/R/01*.

2 Objectives and Scope

The primary objective of this study was to assess the mid-air collision risk of simultaneous independent EoR operations using instrument approach procedures with RF leg design by aircraft that may not have vertical guidance. The results of this risk analysis intend to provide insight into which parameters have the greatest impact on operational risks. This study also assessed implementation risks such as nuisance alert rates from the TCAS as well as the FMA function in the Standard Terminal Automation Replacement System (STARS). As with existing parallel approach operations, autopilot or flight director is required. This study used controller reactions based on a human-in-the-loop experiment with controller stations simulating an Airport Surveillance Radar 9 with a 4.8 second update rate, a STARS FMA with a high resolution color monitor, visual and aural alerts, and a 3:1 aspect ratio. This study assumed that each final approach course has an established monitor controller with override transmit and receive capabilities on the appropriate control tower frequency during EoR operations.

Although RF leg segments are regularly associated with RNAV (RNP) authorization required approach procedures, it is possible for approach procedures with RF legs to be designed and flown using existing RNAV (GPS) procedure design criteria and the equipage of certain aircraft in the fleet.[11] This study will analyze the least restrictive operational specification with the understanding that improved navigation performance will decrease mid-air collision risk. Therefore, this study applies to any combination of RNAV (GPS) instrument approach procedures to both outboard runways using RF track design with lateral navigation (LNAV), LNAV/vertical navigation (VNAV), localizer performance with vertical guidance (LPV), or localizer performance (LP) line of minima, and to RNAV (RNP) instrument approach procedures using an RF track design. GPS failures are not included in this study, and nominal GPS performance is assumed for both RNAV (RNP) and RNAV (GPS) instrument approach procedures.

We did not include the mid-air collision risk associated with incorrect instrument approach procedure selection in this study. Airspace design can easily mitigate this significant contributor to mid-air collision risk by ensuring that the intended landing runway is easily identifiable to controllers prior to aircraft losing standard separation (a minimum of 1000 ft vertical or a minimum of 3 NM radar separation between aircraft). These and other mitigations were considered in another AFS-400 report.[12]

[11] Federal Aviation Administration, *Order 8260.19G Flight Procedures and Airspace* (U.S. Department of Transportation, July 14, 2015).

[12] Flight Technologies and Procedures Division, *DOT/FAA/AFS400/2016/R/05.*

3 Modeling and Simulation

By applying the results from the human-in-the-loop experiments and using the same techniques described in the TF turn study, results were generated for EoR operations with a RF design. Adaptations of the inputs to the mathematical model, described in section 3.1.1, were necessary to make it representative of the RF design.

3.1 Collision Risk

The EoR concept of operations aims to change a separation standard. This necessitates quantitative analysis on the mid-air collision risk on an operational basis, as efficiency gains to the NAS cannot be to the detriment of aviation safety. A mid-air collision is defined as a catastrophic event and is an important component of the Air Traffic Organization (ATO) Safety Management System process.[13] A simple mathematical model was developed to evaluate the probability of a collision resulting from the loss of separation due to a non-normal event. Due to the inherent infrequency of such non-normal events as well as the assessment of future operational concepts, empirical methods are not feasible to evaluate the collision risk of such operations. In addition, a mathematical model allows the effects of individual parameters on collision risk to be isolated, which is an important and often more informative result than those typically obtained from complex simulations.

3.1.1 Collision Risk Methodology

The TF turn study partitioned the collision risk into two major conditional probabilities: (1) the probability that an aircraft will collide with parallel traffic when all aircraft and aircrews were operating as intended, and (2) the probability that an aircraft will collide with parallel traffic when at least one pilot or aircraft was not operating as intended.[14] Analysis showed that the first case, called normal collision risk, contributed insignificant risk to EoR operations in the runways separated by at least 3600 ft, the minimum permitted for simultaneous independent operations at this time.[15] The normal mid-air collision risk, also referred to as fault-free mid-air collision risk, evaluated in the TF turn study used RF legs as an approximation. Therefore, the normal collision risk model used is more applicable to instrument approach procedures with RF legs than TF legs and normal collision risk does not need to be assessed in this study as it was found to be negligible in comparison. We can consider the total mid-air collision risk to be equal to the non-normal collision risk.

$$P(Collision) = P(\text{Collision}|\text{Normal Ops})\, P(\text{Normal Ops}) + \sum_{\substack{x \in \text{Set of all} \\ \text{Non-Normal States}}} P(\text{Collision}|\text{Non-Normal State x})\, P(\text{Non-Normal State x}) \qquad (1)$$

Similar to the TF non-normal collision risk model, analysis was limited to the most conservative case, where the deviation occurs adjacent to a straight-in approach. In addition, the deviation path was again defined relative to the straight-in path, resulting in the same geometric statistical model beyond the deviation start. The inputs to the mathematical model were modified to represent an RF turn rather than a series of TF turns. The variable definitions and input equations for both the TF and RF models are

[13] Air Traffic Organization, *Safety Management System Manual.*

[14] Flight Technologies and Procedures Division, *DOT/FAA/AFS400/2016/R/01*.

[15] Air Traffic Organization, *Air Traffic Control Order 7110.65W* (U.S. Department of Transportation, 2015).

listed below, followed by a schematic diagram of relevant parameters. This illustrates that the inputs for the RF model are simpler than those of the TF model.

Variables Used in Both the TF and RF Mathematical Models:

$s \coloneqq Groundspeed$

$r_{10} \coloneqq Radius\ of\ 10°\ Turn\ TF\ (fly - by)\ Waypoint$

$r_{50} \coloneqq Radius\ of\ 50°\ Turn\ TF\ (fly - by) Waypoint$

$l \coloneqq Length\ of\ Path\ from\ Glideslope$

$a_G \coloneqq Altitude\ Above\ Glideslope\ Intercept\ at\ Point$

$d_{ILS} \coloneqq Distance\ from\ ILS\ Approach$

$d_G \coloneqq Distance\ from\ Glideslope\ Intercept\ along\ ILS\ Approach$

$T \coloneqq Length\ of\ 10°\ Intercept\ Leg$

$\theta \coloneqq Heading$

$\phi \coloneqq Vertical\ Descent\ Angle\ on\ EoR\ Approach$

$\sigma \coloneqq Parallel\ Runway\ Separation\ Distance$

$R \coloneqq RF\ leg\ Turn\ Radius$

Input Equations for Operations Using the TF Design:

$$r_{10} = \left(\frac{s^2}{(\tan(5°)\ 68625.4)}\right) 6076.115\ ft\ NM^{-1}$$

$$r_{50} = \left(\frac{s^2}{(\tan(25°)\ 68625.4)}\right) 6076.115\ ft\ NM^{-1}$$

$$l = (r_{10}\ 10°) + T + (r_{50}\ (\theta - 10°))$$

$$a_G = \Big((r_{10}\ 10°)\ + T + \big(r_{50}\ (\theta - 10°)\big)\Big) \tan(\phi)$$

$$d_{ILS} = (\sigma + r_{10}) + (r_{10} \cos(170°)) + (T \sin(\ 170\ °)) - (r_{50} \cos(170°)) + (r_{50} \cos(180° - \theta))$$

$$d_G = (r_{10} \sin(170°)) - \big(T cos(170°)\big) - (r_{50} \sin(170°)) + (r_{50} \sin(180° - \theta))$$

Input Equations for Operations Using the RF Design:

$$l = R\ \theta$$

$$a_G = (R\ \theta) \tan(\phi)$$

$$d_{ILS} = \sigma + R - (R \cos(\theta))$$

$$d_G = R \sin(\theta)$$

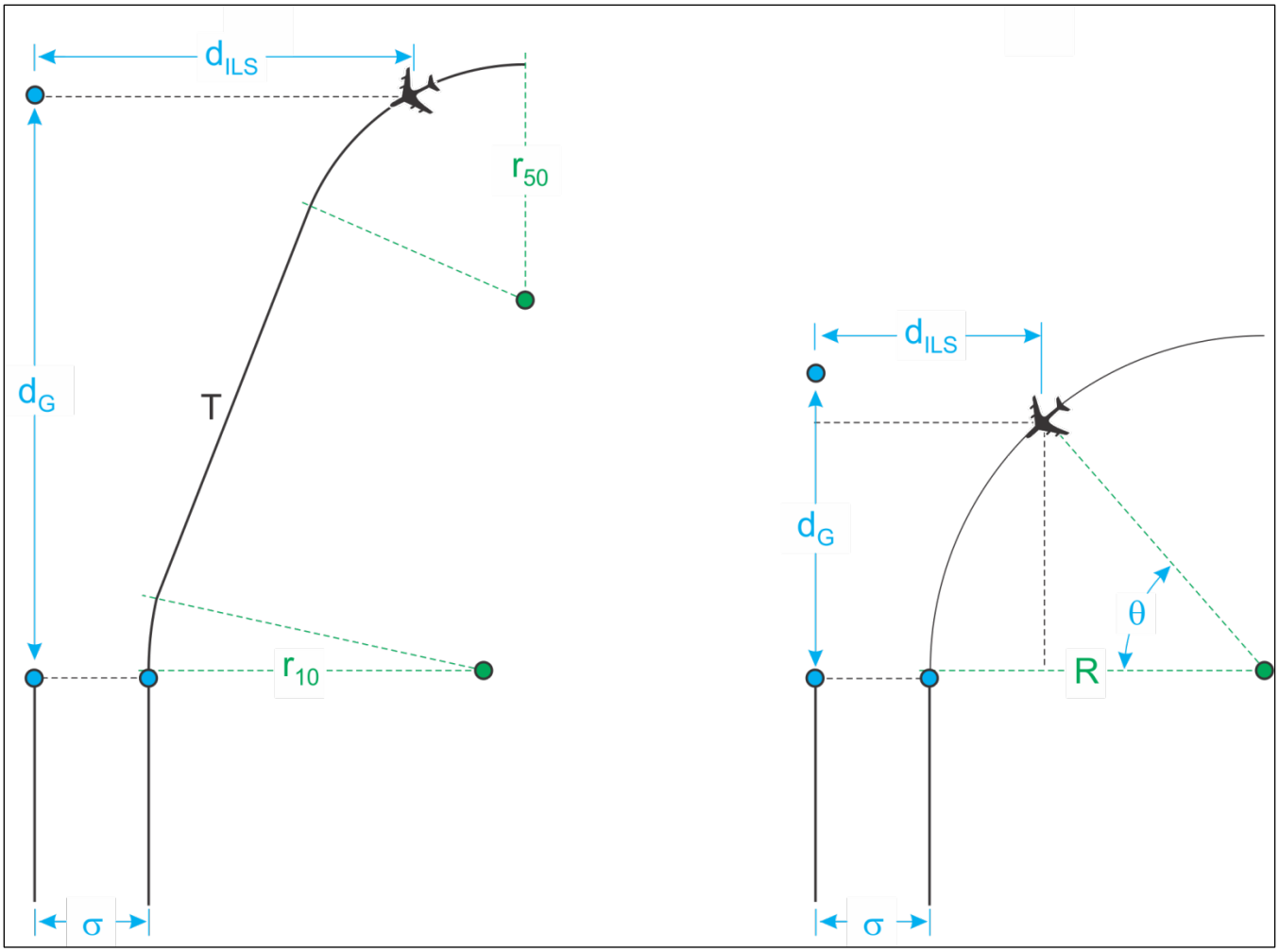

Figure 3-1: TF and RF Mathematical Model Inputs

Runway approach geometries for both dual and triple operations were analyzed at runway separation distances of: 3600, 3900, 4300, 4800, and 5300 ft. In the TF turn study, we strategically calculated the collision risk with varying mitigations. This means that collision risk was calculated with and without accounting for vertical separation. Collision risk was also calculated using both pilot- and controller-initiated corrections. The function for collision risk of an EoR approach using an RF design is parameterized by the following variables:

- Johnson unbounded distribution for the amount of time spent in level flight before correction;
- The standard deviation of the vertical error of each approach path;
- The distance from the other approach laterally when the deviation starts;
- The angle that the deviation travels during the straight segment relative to the other approach path;
- The radius of the correction;
- The groundspeed of the aircraft during the straight flight segment; and
- The mean vertical separation at the time of horizontal overlap.

Some differences to note from the EoR non-normal collision risk model for TF designs are that, for the RF design analysis, the 10° intercept leg is omitted and the deviating aircraft flies a constant radius

RF leg until the start of the deviation. Additionally, the deviation angle relative to the adjacent approach was varied from 0° to 90° in 1° increments rather than a minimum of 10°. This was necessary to correctly model the constant turn associated with the RF turn design.

3.1.2 Collision Risk Input Data

In early 2015, we conducted a large scale human-in-the-loop experiment using 3 full-motion flight simulators and 29 flight crews from various carriers in the airline industry. We also conducted a smaller experiment using 21 certified professional air traffic controllers to collect 38 hours of EoR approach data. During these experiments, test subjects experienced nominal EoR operations, where nothing occurred, and off-nominal EoR operations, in which one of several possible non-normal conditions was triggered. By describing how flight crews and controllers responded to the non-normal conditions using a mathematical model, we quantified their responses to estimate the non-normal collision risk. For the details of these experiments and the data analysis, see the TF turn study.[16] In another AFS-400 safety study regarding the possible selection of an incorrect instrument approach procedure, further work was done to refine the algorithm used to calculate pilot response times associated with evasive commands issued by controllers.[17] The resulting pilot reaction time distribution was used for this study, thus making the RF results less conservative and more representative. Further explanation can be found in appendix B.

Two hardware-in-the-loop simulations were conducted by AFS-400 using both the Airbus A330 and Boeing B737 full-motion flight simulators in order to conservatively quantify a ratio of failures that would result in a path deviation in a constant bank state compared to a varying bank state. The data collected in the hardware-in-the-loop experiments characterize, as the name implies, the response of the hardware (i.e. aircraft systems) to a given failure condition. Although data collected in the TF study was heavily focused on the characterization of human responses (as a human-in-the-loop experiment), the response of the hardware to failure conditions was also captured prior to any human response. This simulation was intended to collect hardware response data in a procedure with a constant bank turn from the downwind leg to the final approach course. Those results are compared here with the TF hardware responses, which are characterized by a varying bank state, to a subset of the same failure conditions.

FAA pilots were used in the hardware-in-the-loop simulations. The pilot crewmembers were given a short briefing on the purpose of the simulation before entering the simulator(s) and were allowed to familiarize themselves with the approach procedure diagram and fly one practice approach each prior to commencing the simulation. These simulations were not intended to be inclusive of all possible failure modes, but they were conducted to gain some insight into the inherent differences from the TF case. The RNAV (RNP) Z approach to runway 16R from the south (IF = VASHN) was flown, and the waypoint PINTR was used as the point at which the failure was introduced in each simulation, see Figure A-1 in appendix A. Both the captain and first officer were given failure conditions individually in the Airbus simulation, but in the Boeing simulation, only the captain received the failures.

Table A-1 in appendix A summarizes the conditions used and observations obtained in the Airbus simulation, and Table A-2 summarizes the analogous information obtained in the Boeing simulation.

[16] Flight Technologies and Procedures Division, *DOT/FAA/AFS400/2016/R/01*.

[17] Flight Technologies and Procedures Division, *DOT/FAA/AFS400/2016/R/05*.

Two failure conditions resulted in a change of bank, but none caused any substantial deviation from course in the Airbus. Only two modes of failure in the Boeing resulted in deviations from course. However, it should be noted that these deviations were inside the RF turn and away from any potential adjacent flight paths, and both deviations were negligible in terms of magnitude. Overall, all equipment failures resulted in distractions to pilots, but 7 out of 8 failure modes during simulated flight guidance failures in both aircraft types shared a common observation: the state of bank/pitch was maintained after the time of the failure with little, if any, deviation from course. These are depicted by the gray lines in Figure 3-2. In two particular scenarios, the aircraft rolled to 0° of bank. These two are plotted in red, and they were both associated with the same failure condition, RNP loss of navigation mode. In summary, we observed that the aircraft maintained the established state of bank following equipment failures in most cases. In approach procedures designed with constant or decreasing bank states, this resulted in failures that closely approximated the intended track or turned to the inside of the turn in many cases. However, in varying bank approaches, the equipment failures could occur just prior to rolling into a bank (in wings-level flight), resulting in more deviations towards the adjacent traffic.

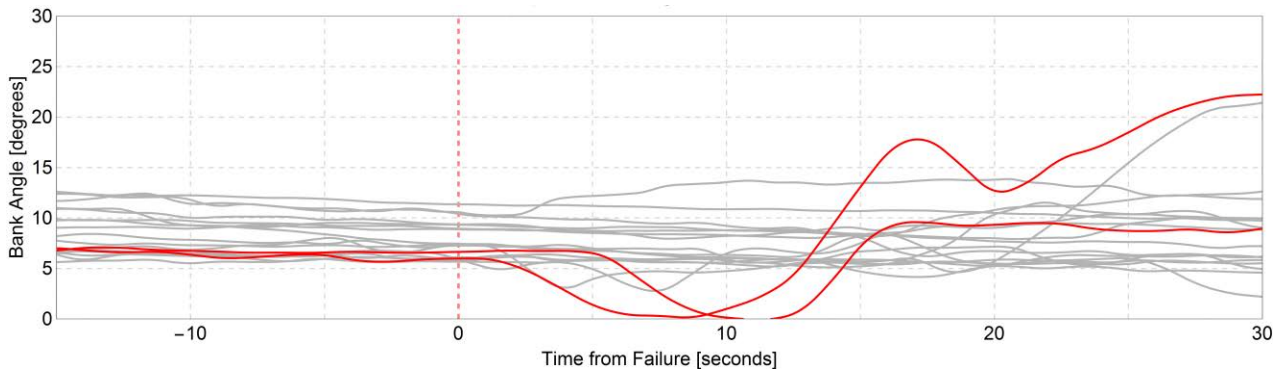

Figure 3-2: Plot of Bank Angle Responses Relative to Failure Initiation with RF legs

The results from the RF hardware-in-the-loop simulation suggest that an EoR procedure that uses a constant bank design has a lower probability of entering non-normal flight conditions as a result of aircraft equipment failure as compared to a procedure with a varying bank design. Due to the qualitative nature of the hardware-in-the-loop simulation observations, it is difficult to quantify the ratio of non-normal state inducing failures between EoR procedures using constant bank and variable bank designs. The qualitative results above indicate that this ratio is certainly less than one-half given the same set of failure conditions. Therefore, in an effort to more representatively model mid-air collision risk, we introduced a ratio for the probability of being in a non-normal state between constant bank and varying bank EoR procedures. Realistically, this ratio is no more than one and likely one-half or lower, but refining this value is beyond the scope of this study, as it would require extensive human-in-the-loop experimentation and analysis.

An additional component of the collision risk model used, historical wind distribution data, is explained here. Instrument approach procedures are designed to provide a nominal path that can be flown at a maximum groundspeed. These procedures incorporate a conversion from the maximum allowable indicated airspeed to true airspeed based on altitude, and a further conversion from the true airspeed to

groundspeed based on a wind formula that scales with altitude.[18] The formula used in procedure design is very conservative, and while it provides a safe upper bound for operational groundspeeds, it is not representative of groundspeeds that are typically flown. For this reason, 99th quantile historical wind data was obtained from MITRE Center for Advanced Aviation System Development for sites within the NAS that collect historical wind data. The historical winds were used to calculate groundspeed weighted by wind speed probabilities, effectively replacing the overly conservative groundspeeds calculated by the instrument approach design formula described above.

Data at each site contained a variable amount of AGL altitudes with each altitude corresponding to a probability mass function of wind speeds in knots. The cumulative distribution function of each probability mass function was used to select two wind speed distributions from altitudes less than 10,000 ft AGL using a simple metric: the difference between the 99th quantile wind speed and the median wind speed. Using this metric, the distribution with the minimum metric value was selected and used as a worst-case wind distribution, depicted in red below in Figure 3-3. Likewise, a wind speed distribution with the metric value equal to the median of all metric values was selected to represent a typical wind distribution. These two selected probability mass functions of wind speeds, depicted in the top panel of Figure 3-3, were contextualized as groundspeeds relative to the 99th quantile wind speed, as seen in the bottom panel in Figure 3-3. In other words, the worst winds yielded the highest probability mass for when the flown groundspeed was the same as the designed maximum groundspeed, and the median winds yielded a more representative probability of an aircraft traveling at the maximum procedure design groundspeed. It is important to note, using the worst wind distribution to weight groundspeeds is still a more representative approach compared to using no weighting method on groundspeed, which would mean all aircraft always execute these operations at the maximum groundspeed calculated for procedure design.

[18] Federal Aviation Administration, *Order 8260.58A United States Standard for Performance Based Navigation (PBN) Instrument Procedure Design* (U.S. Department of Transportation, March 14, 2016), 1-13.

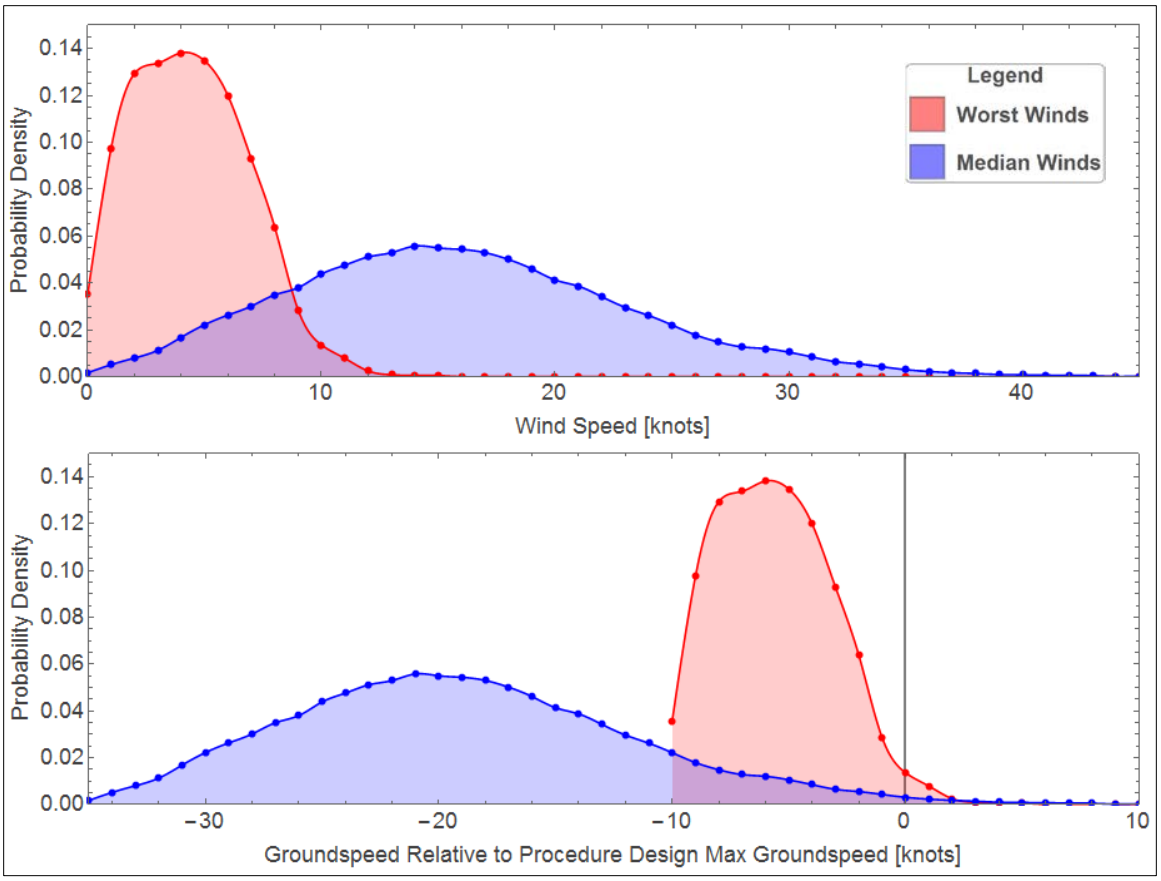

Figure 3-3: Historical Wind Distributions

The resulting probability mass functions of groundspeed relative to the maximum groundspeed defined by the procedure design were used to appropriately weight collision risk by applying the following equation to the model outputs:

$$P\left(Collision \middle| S_{\Gamma,R}\right) = \sum_{v \in V} P\left(Collision \middle| S_{\Gamma-v,R}\right) * P(v) \qquad (2)$$

where S is the operational scenario with specific values for Γ and R, which represent the design groundspeed and turn radius respectively. Relative wind speed is depicted as ν, and V represents the set of empirical relative wind velocities.

The distributions shown in the lower panel of Figure 3-3 were organized into bins of five knots in order to match the designed groundspeed input to the model. Thus, $P(v)$ in the equation above represents the sum of all ν for each bin of either the worst or median wind distribution. The bin containing zero knot winds spanned from zero to four knots slower than the designed speeds, with the possibility of encountering wind velocities greater than the design speeds. This effectively weights each bin toward the more conservative case. Referring back to the second panel of Figure 3-3, it is clear that the median wind distribution, shown in blue, has more probability mass at groundspeeds less than the designed maximum groundspeed for any given procedure. In contrast, the worst-case wind distribution, shown in red, has a higher probability mass at greater relative wind speeds, meaning it is more probable that

aircraft would travel with a groundspeed much closer to the designed maximum allowable based on the wind conditions. As one would expect, the higher the probability an aircraft is traveling slower than the designed ground speed, the lower the collision risk. In fact, this can be seen in the collision risk results below, when comparing between the different wind probability mass functions used. In other words, using the median distribution, shown in blue, places more probability on aircraft traveling slower than the maximum allowable designed groundspeed. Thus, the collision risk is lower using representative ground speeds instead of designed ground speeds. It is important to note, the worst wind results were included to demonstrate an upper bound, while the median, or typical, wind results are much more representative of reality and not overly conservative.

3.1.3 Collision Risk Results

Figure 3-4 through 3-6 illustrate a series of contour plots depicting the mid-air collision risk of an independent EoR RF operation without controller intervention. In the case of Figure 3-4 through 3-6, "without controller intervention" simply means that for the modelled failure conditions, only the pilot recovery initiation time was used to estimate collision risk. The risk is plotted as a function of turn radius and procedure design groundspeed. Each column corresponds to the runway separation distance noted in the column header, while each row corresponds to the wind distribution used to appropriately weight the probability of encountering wind speeds lower than the historical winds used in procedure design. The legends in Figure 3-4 through 3-9 indicate all white regions represent relatively low levels of collision risk for both dual and triple EoR RF operations, and any region under a pink contour represent low collision risk for only dual EoR RF operations. Regions under red contours represent high levels of collision risk in any case, while dark gray contours represent high-risk conditions of a greater severity. Bank angles are also shown with lines of different style and color. Since procedures are not designed with a maximum bank angle greater than 25°, the region of interest for each subplot is everything to the left of the 25° bank line.[19] Figure 3-5, which conservatively applies an bank changing ratio of one-half, which best applies to approach procedures designed with a constant bank, illustrates that without taking credit for controller intervention under the non-normal circumstances modeled, dual EoR RF operations exhibit low levels of collision risk down to 3600 ft of runway separation and triple EoR RF operations exhibit low levels of collision risk at 4300 ft of runway separation or greater with a worst historical wind distribution, or 3900 ft or greater with a median wind distribution. The median wind results align with Closely Spaced Parallel Operations (CSPO) analyses for dual and triple simultaneous independent runway operations as well as the TF turn analysis results.

The collision risk values displayed in the heat maps below have been weighted with both the worst and median wind distributions and displayed separately for comparison. In any case, the worst winds did not reduce collision risk by a noticeable amount, while the median winds did. Figure 3-4 through 3-9 illustrate how a specified maximum bank angle would keep the level of risk on the side of lower values for the specified bank angle curve. See appendix C for tabulated RF design mid-air collision risk values.

[19] Federal Aviation Administration, *Order 8260.58A* 1-13, 1-14.

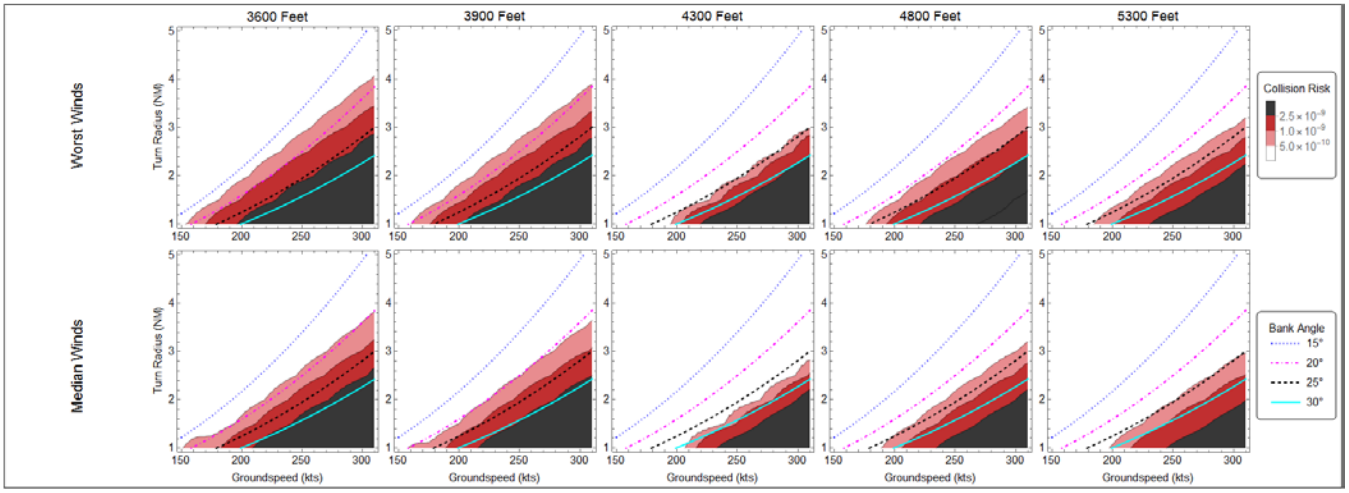

Figure 3-4: EoR RF Design Mid-Air Collision Risk without Controller Intervention and Bank Changing Ratio equal to 1

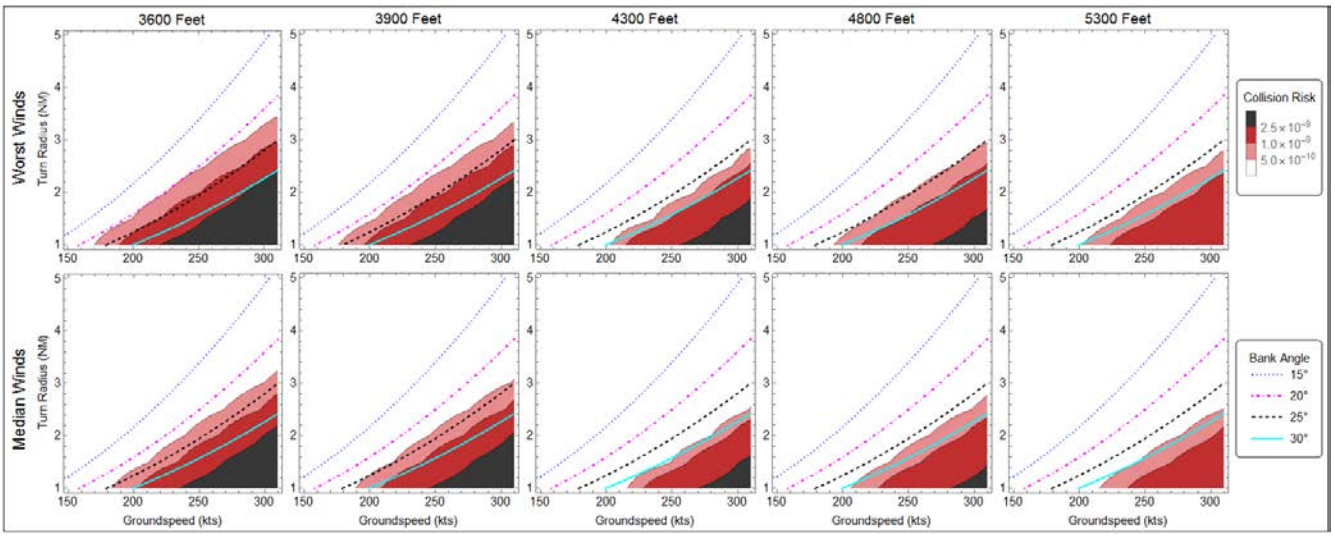

Figure 3-5: EoR RF Design Mid-Air Collision Risk without Controller Intervention and Bank Changing Ratio equal to 0.5

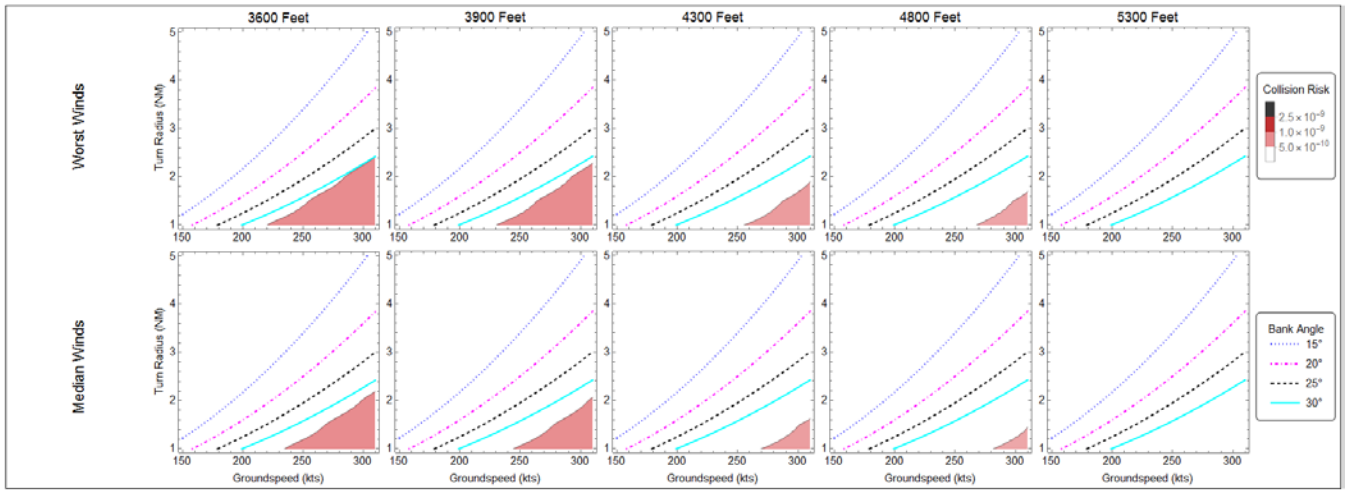

Figure 3-6: EoR RF Design Mid-Air Collision Risk without Controller Intervention and Bank Changing Ratio equal to 0.1

Similarly, Figures 3-7 through 3-9 also display a series of mid-air collision risk contour maps. However, the collision risk calculated in these figures uses controller intervention as the primary means of mitigation. Including the reaction of a final monitor unsurprisingly lowers the risk across all the subplots. Specifically, it is clear that the level of midair collision risk for both dual and triple operations are on the order of 10^{-9} at 3600 ft (the minimum runway spacing allowed for independent simultaneous operations for runways that are not offset) when credit is taken for controller intervention. However, CSPO triple runway operations restrict the straight-in portion of the final approach procedure to 3900 ft. Therefore, EoR triple operations are currently limited to 3900 ft to align CSPO and EoR safety analyses. See appendix C for tabulated RF design mid-air collision risk values.

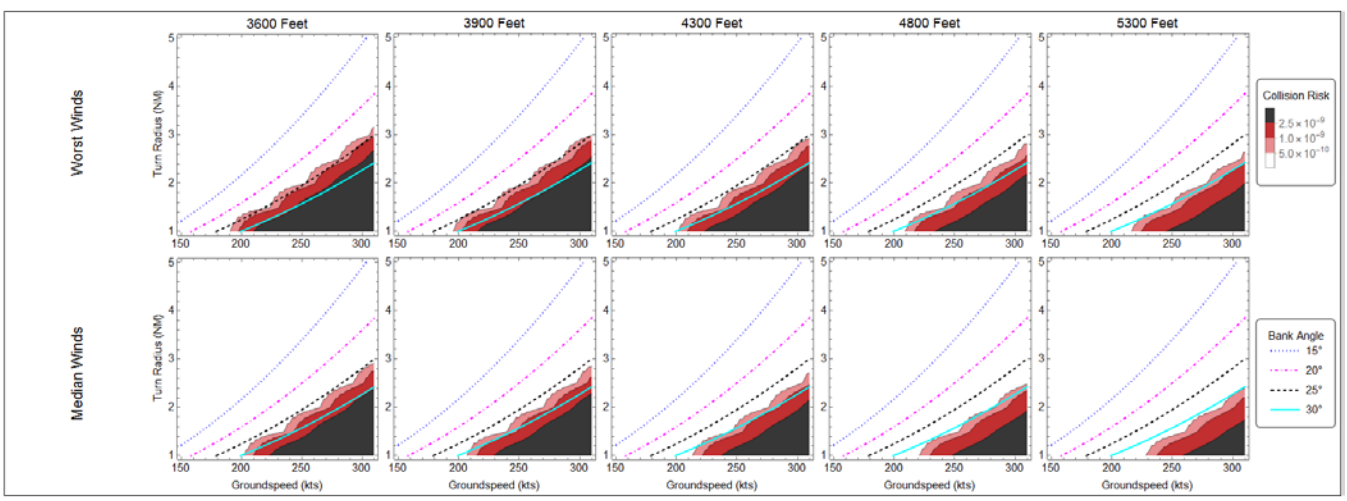

Figure 3-7: EoR RF Design Mid-Air Collision Risk with Controller Intervention and Bank Changing Ratio equal to 1

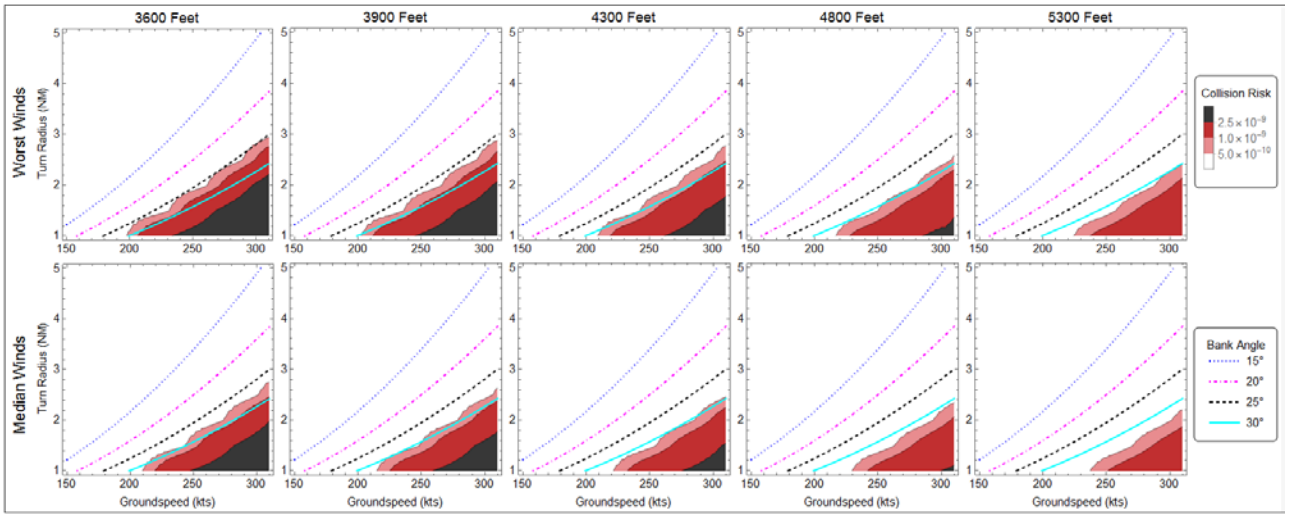

Figure 3-8: EoR RF Design Mid-Air Collision Risk with Controller Intervention and Bank Changing Ratio equal to 0.5

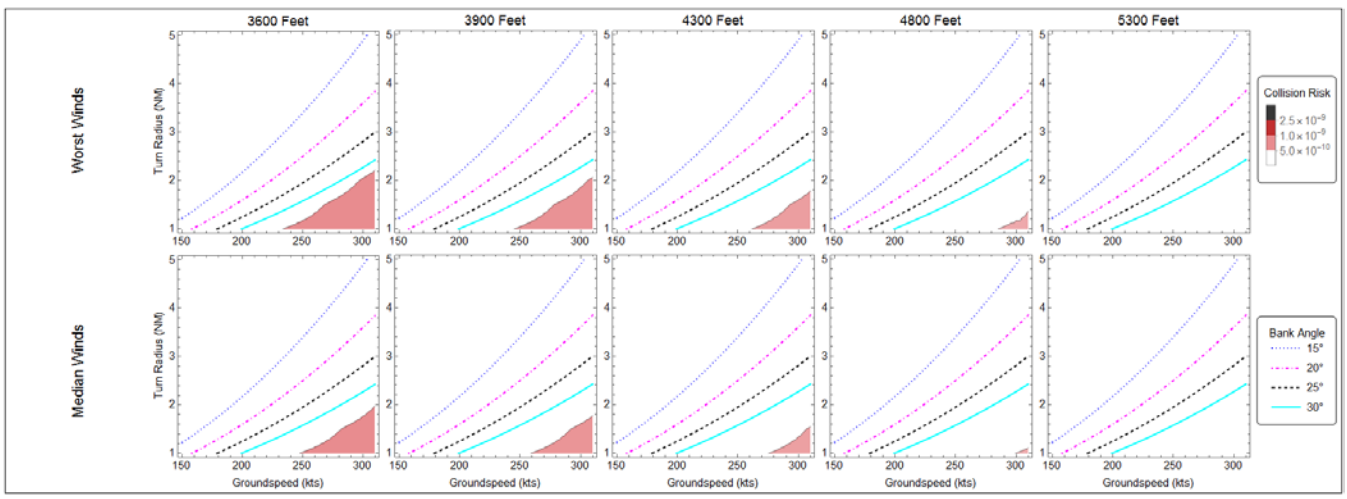

Figure 3-9: EoR RF Design Mid-Air Collision Risk with Controller Intervention and RF-to-TF Bank Changing Ratio equal to 0.1

3.2 Implementation Risks

From a collision risk perspective, the results show that RF operations demonstrate a comparable level of risk to the analogous TF results for all standard instrument approach procedures, but other implementation impacts remain to be considered. Perhaps the most obvious implementation risk is an anticipated increase in the rate of nuisance FMA caution alerts compared to the TF turn study. An additional implementation risk considered was the rate of nuisance TCAS RAs.

3.2.1 Final Monitor Aid Caution Alerts

The FMA is a tool used by Terminal Radar Approach Control controllers assigned to each approach, called final monitors, to provide additional detection and alerting of deviations for simultaneous independent CSPO. The FMA defines a 2000 ft wide region between the extended runway centerlines of parallel runways called the NTZ. The FMA displays the radar position of each target aircraft along with

its call sign and aircraft type, a 10 second prediction of the future location of the target aircraft, each runway and the approach course leading to it, and the NTZ for each runway pair. During TF turn study testing of EoR operations to parallel runways separated by 9000 ft or less, the use of an FMA and an NTZ was assumed.

The primary cause of false caution alerts is the 10 second prediction of the target aircraft entering the NTZ. This is because the predicted aircraft location is calculated by an algorithm that does not account for turning since it was designed for use with straight-in approaches. Instead, the aircraft is predicted to continue tangentially from its current location at its current velocity. Consequently, any operation requiring a turn onto the extended runway centerline poses a risk of false alarms, primarily dependent on: aircraft position, groundspeed, runway spacing, and magnitude of turn. Additionally, an aspect ratio of 4:1 is typically used by controllers monitoring parallel approach operations at runway separation distances of 4300 ft or less, which significantly distorts turning approaches and could negatively impact reaction times. However, an aspect ratio of 3:1 was used by controllers during the TF turn study because it allowed controllers to observe the entire downwind leg while continuing to magnify cross track errors on final. When the 10 second predictor line segment intersects the NTZ, an FMA caution alert is issued causing the deviating target and data block to flash yellow and an audible indication. Figure 3-10 illustrates the overall geometry of an FMA-predicted overshoot based on a constant radius turn flown at a constant velocity. The length of v is the distance projected to be flown by the aircraft in 10 seconds using the instantaneous groundspeed. From Figure 3-10, x represents the amount of overshoot.

$$x = \sqrt{R^2 + v^2} - R \tag{3}$$

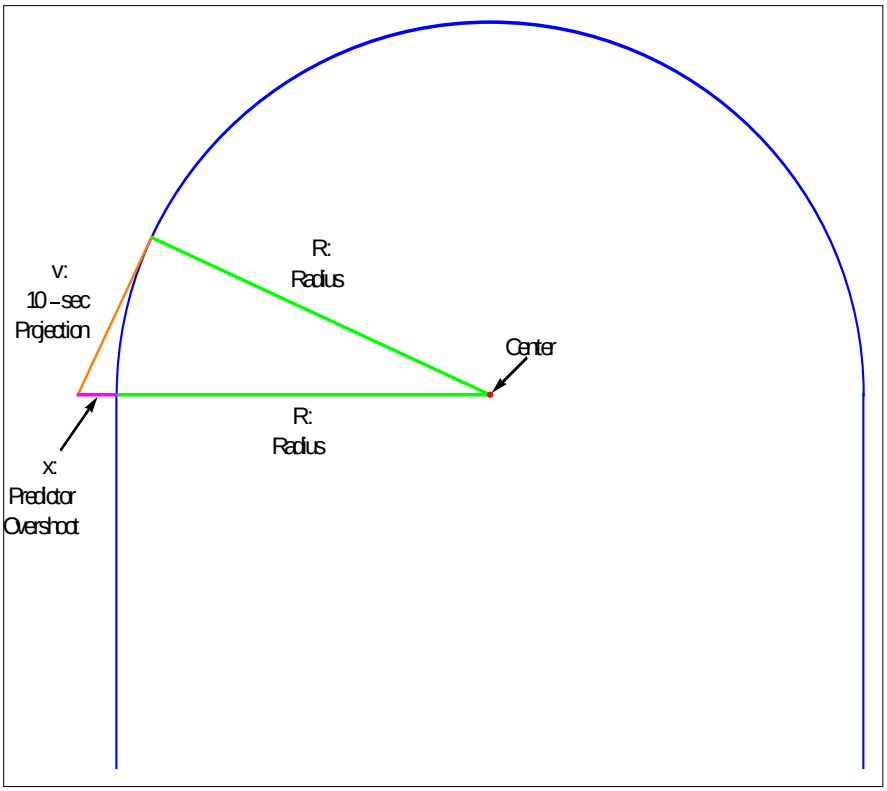

Figure 3-10: FMA 10 Second Predictor Overshoot Geometry

The model used to quantify the expected FMA nuisance alert rate for EoR operations utilizing RF turns is effectively a simplified version of the FMA caution alert rate model used in the TF turn study. Additional functions were composed with this model in order to convert it into a generic function that calculates the nuisance caution alert rate based on the RF turn procedure design. The full function composition diagram is depicted in Figure 3-11. Ultimately, the calculation of the radius was replaced with a direct input of the radius. Specifically, the function (defined as β) taking groundspeed, heading change, Flight Management System bank angle, and fleet mix as input parameters was replaced with direct groundspeed and turn radius inputs. Refer to appendix K in the TF turn study for a more detailed contrast between the two models.[20]

[20] Flight Systems Laboratory, *DOT/FAA/AFS400/2016/R/01*.

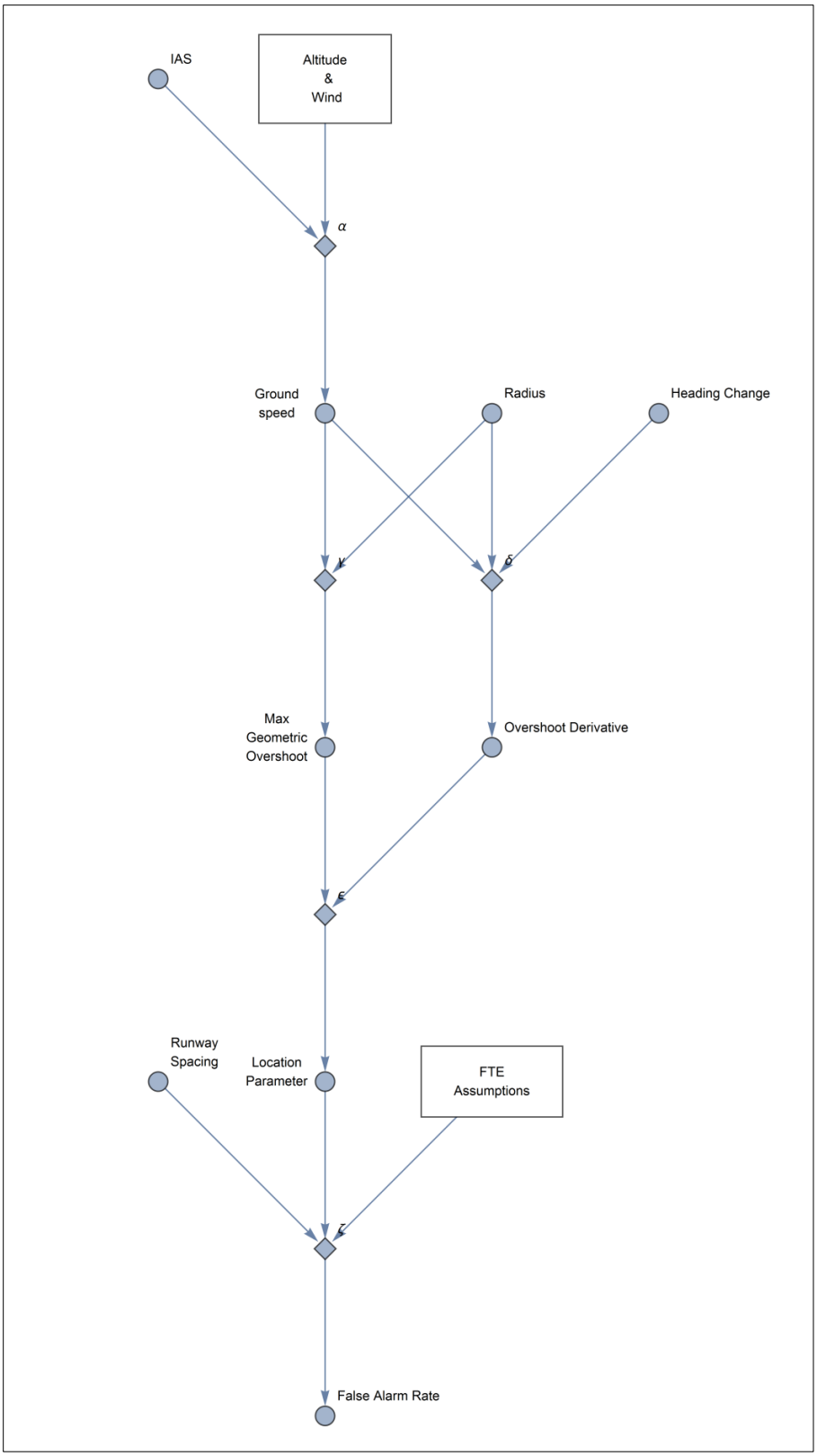

Figure 3-11: FMA Caution Alert Rate Function Composition Diagram

Figure 3-12 shows that tighter turn radii and closer runways increase the risk or rate of nuisance alerts. For example, an approach with a turn radius of 1.8 NM with a parallel approach just 3600 ft away has a 25% chance of experiencing a false FMA caution alert, yet any approach with at least 4850 ft of runway separation would encounter a false alert at the rate of 1 in every 1000 operations performed. Figure 3-12 illustrates the effectiveness of increasing the turn radius for a given runway separation as a mitigation strategy against false FMA caution alerts. Alternatively, in instances where the runway separation is such that increasing the turn radius of the RF leg is insufficient to reduce nuisance alerts to a level acceptable by air traffic, an extra waypoint could be inserted before the final roll out point so that a turn onto the extended runway centerline occurs after the RF turn. Nuisance alerts can be minimized and managed efficiently by adding a shallow intercept (up to 20°) of the final approach course prior to the final roll out point, either as a TF or larger radius RF leg, and increasing the length of this leg.[21] The only relevant parameter in this mitigation strategy is the distance between the RF turn and the final roll out point, because increasing the intercept leg length offsets the entire procedure flight path (defined as procedure stagger). Thus, this strategy could be used to reduce the probability of encountering false alerts for approach procedures using either TF fly-by turn or RF turn designs for both FMA caution alerts and TCAS RAs.

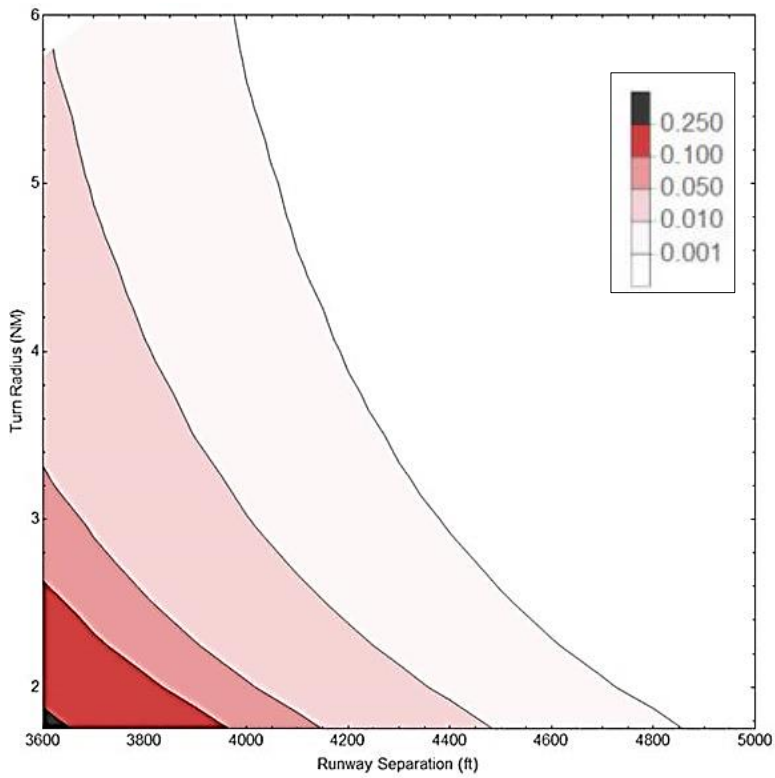

Figure 3-12: Established on RNP RF Design – Nuisance FMA Caution Alert Rate

[21] Flight Systems Laboratory, *DOT/FAA/AFS400/2016/R/01.*

3.2.2 Traffic Collision Avoidance System Resolution Advisories

Another implementation risk considered was the rate of false RAs issued by TCAS. TCAS is the aircraft system analog to the ground-based FMA system, and, similarly, it is designed to provide additional detection and reduced incidence of mid-air collision. Two types of TCAS alerts are possible: traffic advisories, and RAs. Traffic advisories indicate a potential hazard and do not require any maneuver from the aircrew. When an RA is issued, however, the aircrew is expected to respond immediately to the aural command which may require re-sequencing of the evading aircraft. RA rates greater than 3% may significantly reduce expected capacity gains at airports that support independent simultaneous operations.[22] Ultimately, false RAs increase track miles, negating the benefits of EoR and adversely affecting collision risk. For these reasons, nuisance RA rates were quantified in the TF turn study.[23] The RA mitigation strategies investigated in the TF turn study included: increasing leg length of 10° intercept, adding runway stagger, reducing the aircraft altitude AGL at turn on, and increasing runway separation.

It was noted that there was a negligible difference between the TF and RF designs in terms of the rate of occurrence of nuisance RAs. Therefore, the same mitigations apply for both designs. Adding a TF leg between RF legs that turn from the downwind to the final approach course or using a larger turn radius for an RF leg that intercepts the final approach course will separate the apex portion of the turn from the parallel traffic and effectively control nuisance RA rates. Increasing the length of the TF leg or the turn radius of the final RF segment would increase the effectiveness of the mitigation. Furthermore, results indicated that if the turn-on occurred when the aircraft was below 2350 ft AGL (sensitivity level 3 or below) the rate of TCAS RAs would be reduced. Similarly, when two EoR operations are in progress, TCAS RAs are particularly likely, due to the high closure rate. In this case, extending the final rollout point of one procedure past the adjacent final roll out point by at least 2 NM was identified to be effective for reducing nuisance TCAS RAs.

---

[22] Flight Systems Laboratory, *DOT-FAA-AFS-450-69, Simultaneous Independent Close Parallel Approaches – High Update Radar Not Required* (Federal Aviation Administration, September 2011).

[23] Flight Technologies and Procedures Division, *DOT/FAA/AFS400/2016/R/01.*

4 Key Findings and Conclusions

The analysis indicates that mid-air collision risk is between 10^{-9} and 10^{-10} per operation for simultaneous independent RF turn procedures to dual parallel runways separated by 3600 ft or greater and to triple parallel runways separated by 3900 ft or greater. In either case, a controller is assumed to be the primary mitigation of mid-air collision. These results apply to any combination of RNAV (GPS) instrument approach procedures to both outboard runways using RF track design with LNAV, LNAV/VNAV, LPV, or LP line of minima, and to RNAV (RNP) instrument approach procedures using an RF track design. The RNAV (GPS) instrument approach procedures may be performed adjacent to ILS, LOC, GLS, RNAV (GPS), or RNAV (RNP) approach procedures during the EoR operation. These results would support RF turn procedures performed adjacent to TF turn procedures. During triple runway operations, collision risk results would be the same in the event that instrument approach procedures approved to operate in a closely spaced parallel environment were used for the center runway.

Both TF and RF designs have similar collision risk results because the differences between flight tracks of the two designs are relatively small. While equipment failures are less likely to induce a deviation from course during approach procedures designed with constant or increasing bank angles, decreased separation from the parallel traffic in approach procedures with a constant RF turn increases the likelihood of collision given a deviation from the approach path. Therefore, instrument approach procedures designed with RF legs should not include straight flight segments or increased required bank angles during the turn to final (i.e. increasing the size of the RF turn radius during the turn to final introduces less risk than decreasing the size of the RF turn radius during the turn to final).

Limiting maximum designed bank angle appears to be the most effective means of managing the level of collision risk for EoR operations using the RF design. This is because maximum bank angle leverages both turn radius and groundspeed simultaneously to affect the collision risk. Increased runway separation also improves the effectiveness of the above parameters at minimizing risk.

For both the TF Turn and this study, we assumed the use of an FMA and an NTZ for EoR operations to parallel runways separated by 9000 ft or less. EoR operations to runways spaced more than 9000 ft (widely spaced) exhibit a collision risk on the order of 10^{-10} without controller intervention, suggesting that operations without the use of an FMA may be acceptable given that other simultaneous operations do not require final monitors outside of 9000 ft runway spacing.

The implementation considerations include TCAS and FMA nuisance alerts. Nuisance FMA caution alerts are more likely with an RF approach procedure design. EoR operations with RF legs to runways spaced 4850 ft or less may generate unacceptable rates of nuisance FMA caution alerts. These nuisance alert rates can be reduced at runways spaced less than 4850 ft by incorporating an intercept of the final approach with a larger turn radius or using a straight leg to separate all but the last portion of the turn from the NTZ. There is no observable difference between nuisance TCAS RA alerts in approach procedures with RF legs versus TF legs. Nuisance TCAS RAs can be mitigated with the same strategies suggested for TF approach procedures: an added straight segment prior to interception of the final approach course to separate the turn from the adjacent traffic (similar to the mitigation for FMA alerts), staggering the procedure turn-ons by at least 2 NM, or ensuring that the last 50° of the turn occurs below 2350 ft AGL (in sensitivity level 3 or lower).

This study focused on the risk of mid-air collision. Operational considerations due to FMA and TCAS were included to consider their impact on the implementation of this operation. No other potential hazards, such as controlled flight into terrain, wake vortex encounter, GPS-related failures, or incorrect flight procedure selection were evaluated.

References

Air Traffic Organization. *Air Traffic Control, Order 7110.65*. Federal Aviation Administration. 2015.

Air Traffic Organization. *Safety Management System Manual*. Federal Aviation Administration. July 2016.

ATC Simulation Team. *DOT/FAA/CT-92/16,I, Evaluation of Triple Simultaneous Parallel ILS Approaches Spaced 4300 Feet Apart, Final Monitor Aid with Simulated Radar 4.8 Second Update Rate.* FAA Technical Center, Federal Aviation Administration. November 1993.

Boeing. *Seattle Greener Skies i2 Established on RNP (EoR) Simultaneous Dependent Closely-Spaced Parallel Approaches National Airspace System (NAS) Modeling and Simulation Report.* SE2020 Task Order 8, Deliverable 19 Version 2. March 31, 2014. p. 136.

DIGITALiBiz. *FAA Performance Based Navigation Simultaneous Independent Established on RNP Concept of Operations*. Final Version 1.0 (draft). August 22, 2014.

Federal Aviation Administration. Established on Required Navigation Performance Separation for Simultaneous Independent Approaches to Widely Spaced Parallel Runways without Final Monitors Safety Risk Management Document. Version 1. October 15, 2015.

Federal Aviation Administration. Order 8260.58A United States Standard for Performance Based Navigation (PBN) Instrument Procedure Design. U.S. Department of Transportation. March 14, 2016. p. 1-13, 1-14.

Federal Aviation Administration. Order 8260.19G Flight Procedures and Airspace. U.S. Department of Transportation. July 14, 2015.

Federal Aviation Administration. "Request for Waiver to FAA Order JO 7110.65, Simultaneous Independent Approaches to Widely Spaced Parallel Runways without Final Monitors, for Denver Airport Traffic Control Tower (DEN ATCT) and Denver Terminal Radar Approach Control (D01 TRACON), your request dated November 19, 2014." March 11, 2015.

Federal Aviation Administration. *Waiver to FAA JO 7110.65 Paragraphs 5-9-6a.1 and 5-9-6b.1, Seattle TRACON Simultaneous Dependent Approaches*. U.S. Department of Transportation. August 21, 2014.

Flight Systems Laboratory. *DOT-FAA-AFS-450-67, Report on Pilot Response Times from the March 2010 Human in the Loop Data Collection Effort.* Flight Technologies and Procedures Division, Federal Aviation Administration. June 2011.

Flight Systems Laboratory. *DOT-FAA-AFS-450-69, Simultaneous Independent Close Parallel Approaches – High Update Radar Not Required.* Federal Aviation Administration. September 2011.

Flight Systems Laboratory. *DOT-FAA-AFS-400-89, Established on Required Navigation Performance Human in the Loop Data Collection for Dependent Simultaneous Operations with Runways Spaced 2,500' at Seattle, Washington.* Federal Aviation Administration. May 2014.

Flight Technologies and Procedures Division. *DOT/FAA/AFS400/2016/R/01, Safety Study on Simultaneous Independent Approaches Using Established on Required Navigation Performance Approach Procedures with Track-to-Fix Design.* Federal Aviation Administration. July 2016.

Flight Technologies and Procedures Division. *DOT/FAA/AFS400/2016/R/05, Safety Study on the Selection of an Incorrect Established on Required Navigation Performance Instrument Approach Procedure (draft).* Federal Aviation Administration. February 2017.

Flight Technologies and Procedures Division. *DOT/FAA/AFS400/2017/W/18, Ramping Satellite Clock Failures in the Global Positioning System during Simultaneous Independent Operations to Parallel Runways (draft).* Federal Aviation Administration. 2017.

Flight Technologies and Procedures Division. "Memorandum 14-0314-54799, Required Navigation Performance Authorization Required Curved Path Approaches to Widely Spaced Runways." Federal Aviation Administration. June 24, 2014.

Ozmore, Richard E. and Sherri L. Morrow. *DOT/FAA/CT-96/2, Evaluation of Dual Simultaneous Instrument Landing System Approaches to Runways Spaced 3000 Feet Apart with One Localizer Offset Using a Precision Runway Monitor System*. William J. Hughes Technical Center, Federal Aviation Administration. September 1996.

Performance-based Operations Aviation Rule Making Committee, RNP Benefits Sub-Team. "RNP Established – Parallel Approach." Federal Aviation Administration. January 10, 2011.

Appendix A: Equipment Failure Hardware-in-the-Loop Simulation Conditions

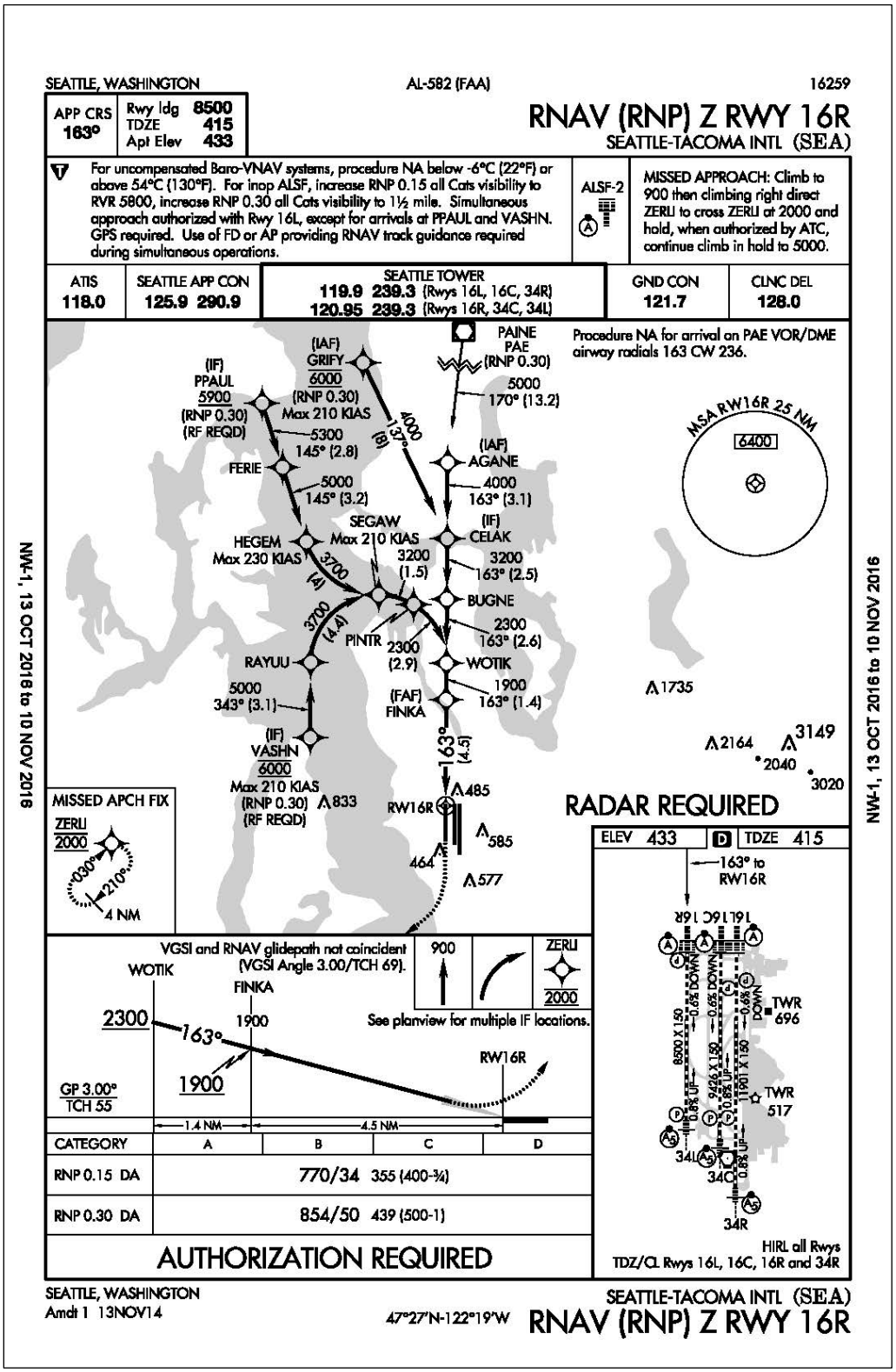

Figure A-1: Approach Plate

Table A-1: Airbus A330 RF Flight Guidance Failure Observations

Failure	Auto Pilot	Position	Location	Indications	Crew Actions	Deviation
Display Unit Failure	Off	Captain	PINTR	Lost Data	Transfer	None
FMC Failure	Off	First Officer	PINTR	Lost Data	Transfer	None
Auto Pilot Failure	On	Captain	PINTR	Lost Autopilot	Kept Flying	None
Display Unit Failure	On	First Officer	PINTR	Invalid Data	Transfer	None
FMC Failure	Off	Captain	PINTR	Lost Vertical	Transfer	None
RNP loss of Nav Mode	On	First Officer	PINTR	Lost Autopilot	Transfer, AP1	None
Controller Directed Breakout	On	Captain	PINTR	Normal	TOGA to Managed Nav	None
Display Unit Failure	Off	First Officer	PINTR	Invalid Data	Transfer	None
FCU Fault	On	Captain	PINTR	Lost Data	Transfer	None
FM GFC Fault	Off	First Officer	PINTR	Lost Data	Transfer	None
FM Fault	On	Captain	PINTR	Lost Data	Transfer	None
ALT Law 1 Flap Position Lost	On	First Officer	PINTR	Autopilot disconnect, Flight Director unreliable	Took Over Manually	Mild, would have discontinued
RNP loss of Nav Mode	On	First Officer	PINTR	Autopilot disconnect, then tracks to heading	Took Over Manually	Mild
RNP loss of Nav Mode	On	Captain	PINTR	Autopilot disconnect, then tracks to heading	Took Over Manually	Mild, rolled out, corrected inside turn
ALT Law 1 Flap Position Lost	On	Captain	PINTR	Autopilot disconnect, Flight Director unreliable	Took Over Manually	None, would have discontinued approach

Table A-2: Boeing B737 RF Flight Guidance Failure Observations

Failure	Auto Pilot	Position	Location	Indications	Crew Actions	Deviation
Display Unit Failure	Off	Captain	PINTR	Lost MD, PFD to Good Screen	Transfer	None
Autopilot Failure	On	Captain	PINTR	Lost Autopilot, Maintained State	Kept Flying	None
Flight Director Failure	Off	Captain	PINTR	Lost Flight Director, Maintained State	Transfer	None
FMC Failure	On	Captain	PINTR	Lost Flight Director and Auto Thrust	Transfer	Mild Inside
Pitot Tube Block	On	Captain	PINTR	Airspeed Differential	Transfer	None
FCC Failure	On	Captain	PINTR	Autopilot Disengaged, Flight Director Failed	Transfer	Mild Inside

Appendix B: Pilot Reaction Data from TF Turn Human-in-the-Loop Experiment

The following information was collected in a pilot human-in-the-loop experiment conducted from January 12 through January 30, 2015.

The runs selected for determination of pilot response times to execute an evasion were those where the controller issued a breakout instruction to the evading aircraft, and the flight crew did not make visual contact with the deviating aircraft during the approach. There were 18 test runs that met these criteria.

In previous CSPO studies, the pilot response time for executing an evasion was calculated from "the instant the controller pressed the Push To Talk (PTT) switch, until the pilot made an input to either the roll or throttle control."[24] The roll control input was used to simulate the turn initiation. In the EoR TF HITL experiment, however, the aircraft was on the 10° intercept leg in a quartering crosswind, either in a bank or about to bank in order to transition to the final approach course. This made it impossible to apply the CSPO algorithm. In the EoR TF study, therefore, we used an algorithm based on previous work for the Multiple Parallel Approach Program which determined pilot response using the change in heading from the final approach course.[25, 26] However, due to the position of the aircraft at the time of the evasion command, we determined that these reactions were extremely conservative. For this study, we calculated the pilot response with a technique used in later studies in the Multiple Parallel Approach Program, which used the bank angle of the aircraft.[27]

For this study, the pilot response time for evasion was the time elapsed from the controller pressing the push-to-talk button to the time the aircraft corrected by achieving a bank angle of 7.5° for the B737 or 12.5° for the A330. These values were selected to be certain the evaluated bank angle was the result of pilot compliance with the breakout instruction, and not due to bank angles commanded during nominal flight of the approach. Once the maximum was identified, the point in time prior to the maximum bank angle where the target bank angle was achieved was identified as the time for aircraft correction.

In all but one evaluated case, the target bank angle was determined to be the first occurrence of the bank angle following the breakout instruction. Figure B-1 depicts a representative example.

---

[24] Flight Systems Laboratory. *DOT-FAA-AFS-450-67, Report on Pilot Response Times from the March 2010 Human in the Loop Data Collection Effort* (Flight Technologies and Procedures Division, Federal Aviation Administration, June 2011).

[25] Flight Technologies and Procedures Division, *DOT/FAA/AFS400/2016/R/01*.

[26] ATC Simulation Team. *DOT/FAA/CT-92/16, I, Evaluation of Triple Simultaneous Parallel ILS Approaches Spaced 4300 Feet Apart, Final Monitor Aid with Simulated Radar 4.8 Second Update Rate* (FAA Technical Center, Federal Aviation Administration, November 1993).

[27] Ozmore, Richard E. and Sherri L. Morrow. *DOT/FAA/CT-96/2, Evaluation of Dual Simultaneous Instrument Landing System Approaches to Runways Spaced 3000 Feet Apart with One Localizer Offset Using a Precision Runway Monitor System* (William J. Hughes Technical Center, Federal Aviation Administration, September 1996).

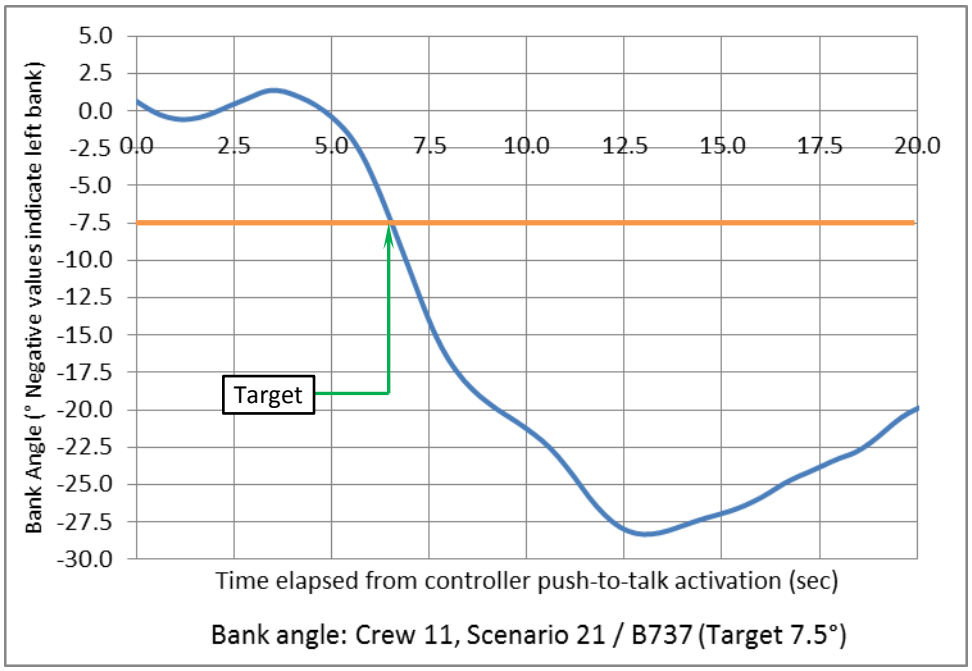

Figure B-1: Representative Bank Angle after Controller Instruction

In one instance, the test aircraft initially achieved the target bank angle, but rolled back to wings-level before initiating the turn for the controller instruction compliance. In this case, the latest incident of target bank angle prior to maximum bank was utilized as the point for reaction time determination. From a review of flight track data for this particular test, it would appear likely the turn shortly after the controller initiated the breakout instruction was a correction back to the approach path after a slight overshoot during a turn. Figure B-2 depicts the bank angle data for this flight.

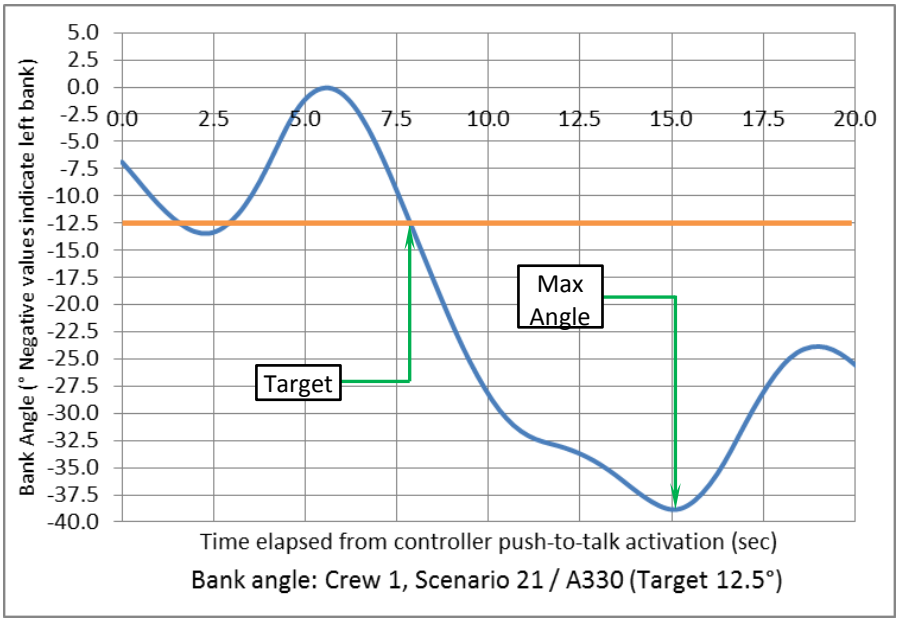

Figure B-2: Bank Angle after Controller Instruction with Turn Prior to Target Angle

Summary of Results

The summary of results for the 18 test scenarios evaluated to determine pilot reaction time is shown in table B-1.

Table B-1: Time from Controller Breakout Instruction to Achieve Target Bank Angle

Crew	Scenario	Aircraft	Elapsed Time (sec)
1	21	A330	7.919
5	21	A330	20.789
8	9	A330	7.721
8	21	A330	5.742
8	22	A330	10.098
9	21	A330	10.889
11	21	B737	6.599
13	21	B737	8.999
14	9	B737	12.198
15	9	B737	5.000
16	21	B737	5.200
17	9	B737	11.398
17	21	B737	9.199
17	22	B737	6.399
18	9	B737	6.399
20	9	B737	5.999
20	21	B737	3.999
20	22	B737	7.199

Appendix C: EoR RF Design Tabulated Mid-Air Collision Risk

This appendix contains the model outputs used to generate Figure 3-5 and Figure 3-8. They assume a bank changing non-normal state ratio of 0.5. To derive the model outputs for a ratio of 1, multiply any value in the table by 2. To derive the model outputs for a ratio of 0.1, multiply any value in the table by 0.2.

Table C-1: Median Winds at 3600’

Turn Radius

Groundspeed	1 NM	1.5 NM	2 NM	2.5NM	3 NM	3.5 NM	4 NM	4.5 NM	5 NM
150 kts	2.49E-12	1.49E-13	2.1E-14	4.54E-15	1.29E-15	4.41E-16	1.73E-16	7.53E-17	3.56E-17
155 kts	4.33E-12	2.41E-13	3.3E-14	7.02E-15	1.97E-15	6.71E-16	2.62E-16	1.14E-16	5.38E-17
160 kts	6.94E-12	3.61E-13	4.77E-14	1E-14	2.78E-15	9.42E-16	3.66E-16	1.59E-16	7.49E-17
165 kts	9.59E-12	4.67E-13	6.01E-14	1.24E-14	3.42E-15	1.15E-15	4.47E-16	1.94E-16	9.11E-17
170 kts	1.27E-11	5.18E-13	6.52E-14	1.33E-14	3.66E-15	1.23E-15	4.75E-16	2.06E-16	9.66E-17
175 kts	1.42E-11	5.64E-13	7.01E-14	1.42E-14	3.9E-15	1.31E-15	5.05E-16	2.18E-16	1.03E-16
180 kts	1.99E-11	7.45E-13	9.05E-14	1.82E-14	4.95E-15	1.65E-15	6.37E-16	2.75E-16	1.29E-16
185 kts	3.72E-11	1.22E-12	1.42E-13	2.78E-14	7.48E-15	2.48E-15	9.5E-16	4.08E-16	1.91E-16
190 kts	6.78E-11	2E-12	2.21E-13	4.23E-14	1.12E-14	3.68E-15	1.4E-15	6.01E-16	2.81E-16
195 kts	1.19E-10	3.29E-12	3.43E-13	6.39E-14	1.67E-14	5.42E-15	2.06E-15	8.77E-16	4.09E-16
200 kts	2.03E-10	5.47E-12	5.3E-13	9.59E-14	2.46E-14	7.92E-15	2.99E-15	1.27E-15	5.89E-16
205 kts	3.3E-10	9.32E-12	8.16E-13	1.43E-13	3.61E-14	1.15E-14	4.31E-15	1.82E-15	8.43E-16
210 kts	5.11E-10	1.62E-11	1.25E-12	2.13E-13	5.27E-14	1.66E-14	6.17E-15	2.59E-15	1.2E-15
215 kts	7.49E-10	2.89E-11	1.93E-12	3.15E-13	7.64E-14	2.38E-14	8.77E-15	3.66E-15	1.69E-15
220 kts	1.04E-09	5.16E-11	2.96E-12	4.66E-13	1.1E-13	3.39E-14	1.24E-14	5.14E-15	2.36E-15
225 kts	1.35E-09	8.96E-11	4.56E-12	6.86E-13	1.59E-13	4.8E-14	1.74E-14	7.18E-15	3.28E-15
230 kts	1.67E-09	1.5E-10	7.11E-12	1.01E-12	2.27E-13	6.77E-14	2.43E-14	9.97E-15	4.53E-15
235 kts	1.95E-09	2.42E-10	1.14E-11	1.48E-12	3.25E-13	9.52E-14	3.38E-14	1.38E-14	6.22E-15
240 kts	2.2E-09	3.77E-10	1.87E-11	2.17E-12	4.63E-13	1.33E-13	4.68E-14	1.89E-14	8.5E-15
245 kts	2.41E-09	5.62E-10	3.17E-11	3.19E-12	6.58E-13	1.86E-13	6.45E-14	2.59E-14	1.16E-14
250 kts	2.59E-09	7.97E-10	5.47E-11	4.69E-12	9.34E-13	2.59E-13	8.86E-14	3.52E-14	1.57E-14
255 kts	2.76E-09	1.07E-09	9.31E-11	6.95E-12	1.33E-12	3.59E-13	1.21E-13	4.78E-14	2.11E-14
260 kts	2.9E-09	1.36E-09	1.54E-10	1.05E-11	1.88E-12	4.98E-13	1.66E-13	6.47E-14	2.83E-14
265 kts	3.04E-09	1.65E-09	2.45E-10	1.63E-11	2.66E-12	6.88E-13	2.26E-13	8.71E-14	3.79E-14
270 kts	3.16E-09	1.93E-09	3.76E-10	2.62E-11	3.78E-12	9.51E-13	3.07E-13	1.17E-13	5.05E-14
275 kts	3.27E-09	2.18E-09	5.53E-10	4.34E-11	5.37E-12	1.31E-12	4.16E-13	1.57E-13	6.71E-14
280 kts	3.37E-09	2.42E-09	7.75E-10	7.28E-11	7.69E-12	1.81E-12	5.63E-13	2.1E-13	8.9E-14
285 kts	3.46E-09	2.64E-09	1.03E-09	1.2E-10	1.12E-11	2.5E-12	7.61E-13	2.8E-13	1.18E-13
290 kts	3.54E-09	2.84E-09	1.32E-09	1.94E-10	1.67E-11	3.45E-12	1.03E-12	3.73E-13	1.55E-13
295 kts	3.62E-09	3.02E-09	1.61E-09	3.02E-10	2.59E-11	4.76E-12	1.39E-12	4.96E-13	2.04E-13
300 kts	3.68E-09	3.19E-09	1.91E-09	4.53E-10	4.16E-11	6.57E-12	1.87E-12	6.56E-13	2.67E-13
305 kts	3.74E-09	3.34E-09	2.19E-09	6.5E-10	6.83E-11	9.08E-12	2.5E-12	8.66E-13	3.49E-13
310 kts	3.78E-09	3.48E-09	2.46E-09	8.97E-10	1.14E-10	1.29E-11	3.38E-12	1.15E-12	4.57E-13

Table C-2: Median Winds at 3900’

Turn Radius

Groundspeed	1 NM	1.5 NM	2 NM	2.5NM	3 NM	3.5 NM	4 NM	4.5 NM	5 NM
150 kts	1.38E-12	8.65E-14	1.24E-14	2.72E-15	7.72E-16	2.64E-16	1.03E-16	4.47E-17	2.11E-17
155 kts	2.41E-12	1.41E-13	1.96E-14	4.22E-15	1.19E-15	4.03E-16	1.57E-16	6.81E-17	3.21E-17
160 kts	3.86E-12	2.11E-13	2.85E-14	6.03E-15	1.68E-15	5.69E-16	2.21E-16	9.54E-17	4.49E-17
165 kts	5.33E-12	2.74E-13	3.6E-14	7.5E-15	2.08E-15	6.98E-16	2.7E-16	1.16E-16	5.48E-17
170 kts	6.25E-12	3.04E-13	3.91E-14	8.08E-15	2.22E-15	7.45E-16	2.88E-16	1.24E-16	5.82E-17
175 kts	7.65E-12	3.32E-13	4.21E-14	8.64E-15	2.37E-15	7.93E-16	3.06E-16	1.32E-16	6.18E-17
180 kts	1.06E-11	4.39E-13	5.45E-14	1.11E-14	3.01E-15	1E-15	3.87E-16	1.66E-16	7.78E-17
185 kts	2.01E-11	7.21E-13	8.56E-14	1.7E-14	4.57E-15	1.51E-15	5.79E-16	2.48E-16	1.16E-16
190 kts	3.77E-11	1.18E-12	1.34E-13	2.59E-14	6.88E-15	2.26E-15	8.59E-16	3.67E-16	1.71E-16
195 kts	6.88E-11	1.94E-12	2.08E-13	3.93E-14	1.03E-14	3.34E-15	1.26E-15	5.37E-16	2.5E-16
200 kts	1.21E-10	3.21E-12	3.23E-13	5.92E-14	1.52E-14	4.9E-15	1.84E-15	7.8E-16	3.61E-16
205 kts	2.05E-10	5.36E-12	4.98E-13	8.87E-14	2.24E-14	7.13E-15	2.67E-15	1.12E-15	5.19E-16
210 kts	3.3E-10	9.19E-12	7.68E-13	1.32E-13	3.28E-14	1.03E-14	3.83E-15	1.6E-15	7.39E-16
215 kts	5.06E-10	1.62E-11	1.18E-12	1.96E-13	4.77E-14	1.48E-14	5.46E-15	2.28E-15	1.04E-15
220 kts	7.32E-10	2.91E-11	1.82E-12	2.91E-13	6.91E-14	2.12E-14	7.74E-15	3.21E-15	1.47E-15
225 kts	9.98E-10	5.22E-11	2.8E-12	4.29E-13	9.96E-14	3.01E-14	1.09E-14	4.49E-15	2.04E-15
230 kts	1.28E-09	9.1E-11	4.34E-12	6.32E-13	1.43E-13	4.26E-14	1.53E-14	6.25E-15	2.83E-15
235 kts	1.56E-09	1.53E-10	6.79E-12	9.31E-13	2.05E-13	6.01E-14	2.13E-14	8.66E-15	3.9E-15
240 kts	1.81E-09	2.45E-10	1.09E-11	1.37E-12	2.93E-13	8.43E-14	2.96E-14	1.19E-14	5.35E-15
245 kts	2.03E-09	3.79E-10	1.81E-11	2.01E-12	4.18E-13	1.18E-13	4.09E-14	1.64E-14	7.29E-15
250 kts	2.21E-09	5.58E-10	3.11E-11	2.96E-12	5.94E-13	1.65E-13	5.63E-14	2.23E-14	9.89E-15
255 kts	2.38E-09	7.8E-10	5.42E-11	4.37E-12	8.45E-13	2.29E-13	7.73E-14	3.04E-14	1.34E-14
260 kts	2.53E-09	1.03E-09	9.34E-11	6.5E-12	1.2E-12	3.18E-13	1.06E-13	4.12E-14	1.8E-14
265 kts	2.67E-09	1.29E-09	1.55E-10	9.8E-12	1.71E-12	4.41E-13	1.44E-13	5.56E-14	2.41E-14
270 kts	2.79E-09	1.55E-09	2.48E-10	1.52E-11	2.43E-12	6.1E-13	1.97E-13	7.49E-14	3.22E-14
275 kts	2.91E-09	1.79E-09	3.77E-10	2.45E-11	3.46E-12	8.45E-13	2.67E-13	1.01E-13	4.29E-14
280 kts	3.01E-09	2.02E-09	5.48E-10	4.11E-11	4.94E-12	1.17E-12	3.62E-13	1.35E-13	5.7E-14
285 kts	3.1E-09	2.23E-09	7.56E-10	7.03E-11	7.1E-12	1.61E-12	4.91E-13	1.8E-13	7.55E-14
290 kts	3.19E-09	2.43E-09	9.95E-10	1.19E-10	1.04E-11	2.23E-12	6.65E-13	2.4E-13	9.98E-14
295 kts	3.27E-09	2.61E-09	1.25E-09	1.94E-10	1.56E-11	3.09E-12	8.99E-13	3.2E-13	1.32E-13
300 kts	3.34E-09	2.78E-09	1.52E-09	3.02E-10	2.41E-11	4.27E-12	1.21E-12	4.25E-13	1.73E-13
305 kts	3.4E-09	2.93E-09	1.79E-09	4.51E-10	3.89E-11	5.91E-12	1.63E-12	5.62E-13	2.26E-13
310 kts	3.44E-09	3.07E-09	2.05E-09	6.45E-10	6.62E-11	8.31E-12	2.21E-12	7.47E-13	2.96E-13

Table C-3: Median Winds at 4300’

Turn Radius

Groundspeed	1 NM	1.5 NM	2 NM	2.5NM	3 NM	3.5 NM	4 NM	4.5 NM	5 NM
150 kts	6.56E-13	4.37E-14	6.44E-15	1.43E-15	4.08E-16	1.4E-16	5.44E-17	2.35E-17	1.11E-17
155 kts	1.14E-12	7.16E-14	1.02E-14	2.23E-15	6.32E-16	2.15E-16	8.34E-17	3.6E-17	1.69E-17
160 kts	1.84E-12	1.08E-13	1.49E-14	3.21E-15	8.99E-16	3.04E-16	1.18E-16	5.07E-17	2.38E-17
165 kts	2.53E-12	1.4E-13	1.89E-14	4.01E-15	1.11E-15	3.75E-16	1.45E-16	6.22E-17	2.91E-17
170 kts	2.95E-12	1.56E-13	2.06E-14	4.32E-15	1.2E-15	4.01E-16	1.54E-16	6.63E-17	3.1E-17
175 kts	3.37E-12	1.7E-13	2.22E-14	4.63E-15	1.28E-15	4.27E-16	1.64E-16	7.05E-17	3.29E-17
180 kts	4.84E-12	2.25E-13	2.87E-14	5.94E-15	1.63E-15	5.42E-16	2.08E-16	8.92E-17	4.16E-17
185 kts	9.12E-12	3.71E-13	4.53E-14	9.18E-15	2.48E-15	8.2E-16	3.14E-16	1.34E-16	6.22E-17
190 kts	1.74E-11	6.1E-13	7.12E-14	1.41E-14	3.75E-15	1.23E-15	4.68E-16	1.99E-16	9.23E-17
195 kts	3.28E-11	1E-12	1.11E-13	2.14E-14	5.62E-15	1.83E-15	6.91E-16	2.93E-16	1.35E-16
200 kts	6.02E-11	1.65E-12	1.73E-13	3.23E-14	8.37E-15	2.69E-15	1.01E-15	4.27E-16	1.97E-16
205 kts	1.06E-10	2.72E-12	2.67E-13	4.86E-14	1.24E-14	3.94E-15	1.47E-15	6.17E-16	2.84E-16
210 kts	1.8E-10	4.57E-12	4.13E-13	7.28E-14	1.82E-14	5.72E-15	2.12E-15	8.86E-16	4.06E-16
215 kts	2.91E-10	7.86E-12	6.38E-13	1.08E-13	2.65E-14	8.26E-15	3.04E-15	1.26E-15	5.77E-16
220 kts	4.46E-10	1.39E-11	9.83E-13	1.61E-13	3.85E-14	1.18E-14	4.32E-15	1.78E-15	8.13E-16
225 kts	6.45E-10	2.52E-11	1.52E-12	2.38E-13	5.58E-14	1.69E-14	6.11E-15	2.51E-15	1.14E-15
230 kts	8.8E-10	4.57E-11	2.34E-12	3.52E-13	8.04E-14	2.4E-14	8.59E-15	3.51E-15	1.58E-15
235 kts	1.13E-09	8.05E-11	3.64E-12	5.19E-13	1.15E-13	3.39E-14	1.2E-14	4.87E-15	2.19E-15
240 kts	1.37E-09	1.36E-10	5.7E-12	7.65E-13	1.65E-13	4.77E-14	1.67E-14	6.73E-15	3.01E-15
245 kts	1.59E-09	2.2E-10	9.11E-12	1.13E-12	2.36E-13	6.7E-14	2.32E-14	9.26E-15	4.11E-15
250 kts	1.78E-09	3.39E-10	1.51E-11	1.66E-12	3.37E-13	9.37E-14	3.2E-14	1.27E-14	5.6E-15
255 kts	1.95E-09	4.99E-10	2.59E-11	2.46E-12	4.81E-13	1.31E-13	4.41E-14	1.73E-14	7.59E-15
260 kts	2.11E-09	6.93E-10	4.57E-11	3.65E-12	6.85E-13	1.82E-13	6.05E-14	2.35E-14	1.02E-14
265 kts	2.25E-09	9.11E-10	8.05E-11	5.44E-12	9.76E-13	2.53E-13	8.28E-14	3.18E-14	1.38E-14
270 kts	2.37E-09	1.13E-09	1.37E-10	8.22E-12	1.39E-12	3.51E-13	1.13E-13	4.3E-14	1.85E-14
275 kts	2.49E-09	1.36E-09	2.21E-10	1.27E-11	1.98E-12	4.87E-13	1.54E-13	5.78E-14	2.46E-14
280 kts	2.6E-09	1.57E-09	3.37E-10	2.05E-11	2.84E-12	6.75E-13	2.09E-13	7.77E-14	3.28E-14
285 kts	2.69E-09	1.77E-09	4.88E-10	3.42E-11	4.08E-12	9.35E-13	2.84E-13	1.04E-13	4.36E-14
290 kts	2.78E-09	1.96E-09	6.72E-10	5.91E-11	5.89E-12	1.3E-12	3.86E-13	1.39E-13	5.77E-14
295 kts	2.86E-09	2.14E-09	8.82E-10	1.02E-10	8.64E-12	1.8E-12	5.23E-13	1.86E-13	7.62E-14
300 kts	2.93E-09	2.3E-09	1.11E-09	1.69E-10	1.28E-11	2.49E-12	7.06E-13	2.47E-13	1E-13
305 kts	2.99E-09	2.45E-09	1.35E-09	2.68E-10	1.95E-11	3.45E-12	9.52E-13	3.28E-13	1.31E-13
310 kts	3.04E-09	2.59E-09	1.58E-09	4.05E-10	3.22E-11	4.83E-12	1.29E-12	4.37E-13	1.73E-13

Table C-4: Median Winds at 4800’

Turn Radius

Groundspeed	1 NM	1.5 NM	2 NM	2.5NM	3 NM	3.5 NM	4 NM	4.5 NM	5 NM
150 kts	2.73E-13	1.97E-14	2.99E-15	6.79E-16	1.96E-16	6.69E-17	2.61E-17	1.13E-17	5.26E-18
155 kts	4.76E-13	3.23E-14	4.77E-15	1.07E-15	3.05E-16	1.04E-16	4.02E-17	1.74E-17	8.09E-18
160 kts	7.63E-13	4.89E-14	7E-15	1.54E-15	4.36E-16	1.48E-16	5.71E-17	2.46E-17	1.15E-17
165 kts	1.05E-12	6.37E-14	8.89E-15	1.93E-15	5.42E-16	1.83E-16	7.05E-17	3.03E-17	1.41E-17
170 kts	1.22E-12	7.1E-14	9.71E-15	2.09E-15	5.83E-16	1.96E-16	7.55E-17	3.24E-17	1.5E-17
175 kts	1.38E-12	7.75E-14	1.05E-14	2.24E-15	6.24E-16	2.09E-16	8.04E-17	3.44E-17	1.6E-17
180 kts	1.93E-12	1.03E-13	1.36E-14	2.89E-15	7.97E-16	2.66E-16	1.02E-16	4.37E-17	2.03E-17
185 kts	3.58E-12	1.7E-13	2.16E-14	4.48E-15	1.22E-15	4.05E-16	1.55E-16	6.6E-17	3.06E-17
190 kts	6.73E-12	2.8E-13	3.4E-14	6.9E-15	1.86E-15	6.11E-16	2.32E-16	9.86E-17	4.56E-17
195 kts	1.28E-11	4.6E-13	5.33E-14	1.06E-14	2.8E-15	9.13E-16	3.45E-16	1.46E-16	6.73E-17
200 kts	2.44E-11	7.57E-13	8.31E-14	1.6E-14	4.19E-15	1.35E-15	5.08E-16	2.14E-16	9.84E-17
205 kts	4.55E-11	1.25E-12	1.29E-13	2.42E-14	6.22E-15	1.99E-15	7.41E-16	3.11E-16	1.43E-16
210 kts	8.16E-11	2.05E-12	2E-13	3.63E-14	9.17E-15	2.9E-15	1.07E-15	4.48E-16	2.05E-16
215 kts	1.4E-10	3.43E-12	3.1E-13	5.42E-14	1.34E-14	4.2E-15	1.54E-15	6.41E-16	2.92E-16
220 kts	2.28E-10	5.82E-12	4.78E-13	8.08E-14	1.96E-14	6.05E-15	2.21E-15	9.11E-16	4.14E-16
225 kts	3.54E-10	1.02E-11	7.39E-13	1.2E-13	2.85E-14	8.66E-15	3.13E-15	1.29E-15	5.82E-16
230 kts	5.19E-10	1.84E-11	1.14E-12	1.77E-13	4.12E-14	1.23E-14	4.42E-15	1.8E-15	8.12E-16
235 kts	7.15E-10	3.38E-11	1.77E-12	2.62E-13	5.93E-14	1.75E-14	6.21E-15	2.52E-15	1.13E-15
240 kts	9.29E-10	6.14E-11	2.76E-12	3.88E-13	8.52E-14	2.47E-14	8.68E-15	3.49E-15	1.55E-15
245 kts	1.14E-09	1.07E-10	4.33E-12	5.72E-13	1.22E-13	3.48E-14	1.21E-14	4.82E-15	2.13E-15
250 kts	1.33E-09	1.76E-10	6.9E-12	8.46E-13	1.75E-13	4.88E-14	1.67E-14	6.62E-15	2.92E-15
255 kts	1.5E-09	2.75E-10	1.13E-11	1.25E-12	2.49E-13	6.83E-14	2.31E-14	9.05E-15	3.97E-15
260 kts	1.66E-09	4.06E-10	1.93E-11	1.86E-12	3.56E-13	9.53E-14	3.17E-14	1.23E-14	5.37E-15
265 kts	1.8E-09	5.67E-10	3.4E-11	2.77E-12	5.08E-13	1.33E-13	4.35E-14	1.68E-14	7.24E-15
270 kts	1.93E-09	7.47E-10	6.07E-11	4.15E-12	7.26E-13	1.85E-13	5.96E-14	2.27E-14	9.73E-15
275 kts	2.05E-09	9.35E-10	1.06E-10	6.28E-12	1.04E-12	2.57E-13	8.14E-14	3.06E-14	1.3E-14
280 kts	2.16E-09	1.12E-09	1.75E-10	9.71E-12	1.49E-12	3.57E-13	1.11E-13	4.12E-14	1.74E-14
285 kts	2.26E-09	1.31E-09	2.71E-10	1.54E-11	2.14E-12	4.95E-13	1.51E-13	5.54E-14	2.31E-14
290 kts	2.35E-09	1.49E-09	3.96E-10	2.56E-11	3.08E-12	6.89E-13	2.05E-13	7.42E-14	3.07E-14
295 kts	2.44E-09	1.66E-09	5.49E-10	4.38E-11	4.49E-12	9.58E-13	2.79E-13	9.93E-14	4.07E-14
300 kts	2.51E-09	1.82E-09	7.24E-10	7.55E-11	6.56E-12	1.33E-12	3.78E-13	1.32E-13	5.36E-14
305 kts	2.57E-09	1.96E-09	9.15E-10	1.28E-10	9.73E-12	1.84E-12	5.1E-13	1.76E-13	7.04E-14
310 kts	2.62E-09	2.1E-09	1.12E-09	2.11E-10	1.52E-11	2.58E-12	6.94E-13	2.35E-13	9.28E-14

Table C-5: Median Winds at 5300’

Turn Radius

Groundspeed	1 NM	1.5 NM	2 NM	2.5NM	3 NM	3.5 NM	4 NM	4.5 NM	5 NM
150 kts	1.2E-13	9.3E-15	1.46E-15	3.39E-16	9.87E-17	3.39E-17	1.33E-17	5.73E-18	2.67E-18
155 kts	2.09E-13	1.54E-14	2.34E-15	5.36E-16	1.55E-16	5.29E-17	2.06E-17	8.87E-18	4.13E-18
160 kts	3.34E-13	2.33E-14	3.45E-15	7.79E-16	2.23E-16	7.58E-17	2.94E-17	1.26E-17	5.87E-18
165 kts	4.6E-13	3.05E-14	4.4E-15	9.81E-16	2.78E-16	9.42E-17	3.64E-17	1.56E-17	7.25E-18
170 kts	5.34E-13	3.4E-14	4.82E-15	1.06E-15	3E-16	1.01E-16	3.91E-17	1.67E-17	7.76E-18
175 kts	5.99E-13	3.71E-14	5.2E-15	1.14E-15	3.21E-16	1.08E-16	4.17E-17	1.78E-17	8.27E-18
180 kts	8.28E-13	4.93E-14	6.78E-15	1.47E-15	4.12E-16	1.38E-16	5.31E-17	2.27E-17	1.05E-17
185 kts	1.49E-12	8.17E-14	1.08E-14	2.3E-15	6.35E-16	2.11E-16	8.09E-17	3.44E-17	1.59E-17
190 kts	2.72E-12	1.35E-13	1.71E-14	3.55E-15	9.7E-16	3.2E-16	1.22E-16	5.17E-17	2.39E-17
195 kts	5.09E-12	2.22E-13	2.68E-14	5.46E-15	1.47E-15	4.81E-16	1.82E-16	7.69E-17	3.54E-17
200 kts	9.68E-12	3.65E-13	4.2E-14	8.31E-15	2.2E-15	7.16E-16	2.69E-16	1.13E-16	5.2E-17
205 kts	1.86E-11	6E-13	6.54E-14	1.26E-14	3.29E-15	1.06E-15	3.95E-16	1.65E-16	7.58E-17
210 kts	3.52E-11	9.89E-13	1.02E-13	1.9E-14	4.87E-15	1.55E-15	5.74E-16	2.4E-16	1.09E-16
215 kts	6.43E-11	1.63E-12	1.57E-13	2.84E-14	7.16E-15	2.25E-15	8.29E-16	3.44E-16	1.57E-16
220 kts	1.12E-10	2.72E-12	2.43E-13	4.24E-14	1.05E-14	3.25E-15	1.19E-15	4.91E-16	2.22E-16
225 kts	1.84E-10	4.62E-12	3.76E-13	6.31E-14	1.53E-14	4.67E-15	1.69E-15	6.96E-16	3.14E-16
230 kts	2.89E-10	8.06E-12	5.83E-13	9.36E-14	2.21E-14	6.68E-15	2.4E-15	9.79E-16	4.4E-16
235 kts	4.27E-10	1.45E-11	9.04E-13	1.39E-13	3.19E-14	9.5E-15	3.38E-15	1.37E-15	6.13E-16
240 kts	5.94E-10	2.67E-11	1.41E-12	2.05E-13	4.6E-14	1.35E-14	4.74E-15	1.91E-15	8.48E-16
245 kts	7.77E-10	4.89E-11	2.2E-12	3.03E-13	6.6E-14	1.9E-14	6.61E-15	2.64E-15	1.17E-15
250 kts	9.6E-10	8.65E-11	3.45E-12	4.48E-13	9.46E-14	2.67E-14	9.18E-15	3.64E-15	1.6E-15
255 kts	1.13E-09	1.45E-10	5.5E-12	6.64E-13	1.35E-13	3.74E-14	1.27E-14	4.99E-15	2.18E-15
260 kts	1.29E-09	2.29E-10	8.96E-12	9.85E-13	1.94E-13	5.23E-14	1.75E-14	6.82E-15	2.96E-15
265 kts	1.43E-09	3.39E-10	1.51E-11	1.47E-12	2.77E-13	7.31E-14	2.41E-14	9.28E-15	4.01E-15
270 kts	1.56E-09	4.75E-10	2.64E-11	2.19E-12	3.96E-13	1.02E-13	3.3E-14	1.26E-14	5.4E-15
275 kts	1.68E-09	6.28E-10	4.7E-11	3.31E-12	5.66E-13	1.42E-13	4.52E-14	1.7E-14	7.24E-15
280 kts	1.8E-09	7.89E-10	8.3E-11	5.04E-12	8.12E-13	1.97E-13	6.17E-14	2.3E-14	9.69E-15
285 kts	1.9E-09	9.54E-10	1.4E-10	7.83E-12	1.17E-12	2.74E-13	8.42E-14	3.09E-14	1.29E-14
290 kts	2E-09	1.12E-09	2.22E-10	1.25E-11	1.68E-12	3.82E-13	1.15E-13	4.15E-14	1.72E-14
295 kts	2.08E-09	1.28E-09	3.29E-10	2.06E-11	2.44E-12	5.32E-13	1.56E-13	5.57E-14	2.28E-14
300 kts	2.16E-09	1.43E-09	4.58E-10	3.46E-11	3.55E-12	7.38E-13	2.11E-13	7.43E-14	3.01E-14
305 kts	2.23E-09	1.57E-09	6.07E-10	5.91E-11	5.19E-12	1.02E-12	2.86E-13	9.88E-14	3.96E-14
310 kts	2.29E-09	1.7E-09	7.73E-10	1.02E-10	7.92E-12	1.44E-12	3.9E-13	1.32E-13	5.23E-14

Table C-6: Median Winds with No Controller Intervention at 3600’

Turn Radius

Groundspeed	1 NM	1.5 NM	2 NM	2.5NM	3 NM	3.5 NM	4 NM	4.5 NM	5 NM
150 kts	2.35E-10	5.43E-11	1.32E-11	4.57E-12	1.81E-12	7.91E-13	3.76E-13	1.91E-13	1.02E-13
155 kts	2.96E-10	7.49E-11	1.74E-11	6.11E-12	2.44E-12	1.08E-12	5.17E-13	2.64E-13	1.43E-13
160 kts	3.52E-10	9.37E-11	2.16E-11	7.64E-12	3.08E-12	1.37E-12	6.61E-13	3.41E-13	1.85E-13
165 kts	3.81E-10	1.05E-10	2.61E-11	8.57E-12	3.47E-12	1.56E-12	7.53E-13	3.9E-13	2.12E-13
170 kts	3.83E-10	1.06E-10	2.69E-11	8.71E-12	3.54E-12	1.59E-12	7.71E-13	4E-13	2.18E-13
175 kts	3.94E-10	1.1E-10	2.81E-11	9.04E-12	3.67E-12	1.65E-12	8.03E-13	4.17E-13	2.27E-13
180 kts	4.48E-10	1.29E-10	3.37E-11	1.07E-11	4.34E-12	1.96E-12	9.57E-13	4.99E-13	2.73E-13
185 kts	5.49E-10	1.66E-10	4.65E-11	1.4E-11	5.72E-12	2.61E-12	1.28E-12	6.72E-13	3.7E-13
190 kts	6.65E-10	2.1E-10	6.31E-11	1.84E-11	7.44E-12	3.42E-12	1.69E-12	8.95E-13	4.96E-13
195 kts	7.95E-10	2.62E-10	8.38E-11	2.43E-11	9.59E-12	4.43E-12	2.21E-12	1.18E-12	6.57E-13
200 kts	9.42E-10	3.22E-10	1.08E-10	3.24E-11	1.23E-11	5.69E-12	2.86E-12	1.53E-12	8.6E-13
205 kts	1.11E-09	3.92E-10	1.38E-10	4.33E-11	1.56E-11	7.22E-12	3.66E-12	1.97E-12	1.11E-12
210 kts	1.3E-09	4.72E-10	1.72E-10	5.74E-11	1.99E-11	9.09E-12	4.64E-12	2.51E-12	1.43E-12
215 kts	1.51E-09	5.63E-10	2.12E-10	7.46E-11	2.56E-11	1.14E-11	5.82E-12	3.17E-12	1.81E-12
220 kts	1.75E-09	6.65E-10	2.59E-10	9.48E-11	3.32E-11	1.41E-11	7.24E-12	3.97E-12	2.28E-12
225 kts	2.01E-09	7.79E-10	3.14E-10	1.18E-10	4.31E-11	1.76E-11	8.94E-12	4.93E-12	2.85E-12
230 kts	2.27E-09	9.06E-10	3.75E-10	1.44E-10	5.55E-11	2.2E-11	1.1E-11	6.06E-12	3.53E-12
235 kts	2.51E-09	1.05E-09	4.45E-10	1.75E-10	7.05E-11	2.78E-11	1.34E-11	7.41E-12	4.33E-12
240 kts	2.73E-09	1.21E-09	5.22E-10	2.09E-10	8.77E-11	3.53E-11	1.63E-11	8.99E-12	5.29E-12
245 kts	2.91E-09	1.4E-09	6.06E-10	2.49E-10	1.07E-10	4.47E-11	2E-11	1.08E-11	6.4E-12
250 kts	3.06E-09	1.62E-09	6.98E-10	2.94E-10	1.29E-10	5.6E-11	2.48E-11	1.3E-11	7.69E-12
255 kts	3.2E-09	1.85E-09	7.99E-10	3.44E-10	1.53E-10	6.94E-11	3.08E-11	1.56E-11	9.19E-12
260 kts	3.33E-09	2.09E-09	9.1E-10	3.99E-10	1.8E-10	8.45E-11	3.82E-11	1.89E-11	1.09E-11
265 kts	3.45E-09	2.34E-09	1.03E-09	4.58E-10	2.11E-10	1.01E-10	4.7E-11	2.3E-11	1.3E-11
270 kts	3.55E-09	2.58E-09	1.18E-09	5.22E-10	2.45E-10	1.2E-10	5.76E-11	2.81E-11	1.54E-11
275 kts	3.64E-09	2.81E-09	1.34E-09	5.89E-10	2.83E-10	1.4E-10	7E-11	3.44E-11	1.83E-11
280 kts	3.73E-09	3.02E-09	1.54E-09	6.62E-10	3.24E-10	1.63E-10	8.37E-11	4.16E-11	2.21E-11
285 kts	3.8E-09	3.21E-09	1.77E-09	7.44E-10	3.68E-10	1.88E-10	9.88E-11	5.01E-11	2.67E-11
290 kts	3.87E-09	3.39E-09	2.03E-09	8.4E-10	4.14E-10	2.16E-10	1.15E-10	6.01E-11	3.21E-11
295 kts	3.93E-09	3.56E-09	2.3E-09	9.58E-10	4.63E-10	2.46E-10	1.33E-10	7.18E-11	3.83E-11
300 kts	3.98E-09	3.7E-09	2.58E-09	1.11E-09	5.15E-10	2.78E-10	1.53E-10	8.47E-11	4.52E-11
305 kts	4.02E-09	3.84E-09	2.85E-09	1.29E-09	5.73E-10	3.11E-10	1.74E-10	9.85E-11	5.33E-11
310 kts	4.05E-09	3.97E-09	3.1E-09	1.52E-09	6.42E-10	3.47E-10	1.97E-10	1.13E-10	6.3E-11

Table C-7: Median Winds with No Controller Intervention at 3900’

Turn Radius

Groundspeed	1 NM	1.5 NM	2 NM	2.5NM	3 NM	3.5 NM	4 NM	4.5 NM	5 NM
150 kts	1.74E-10	3.44E-11	9.43E-12	3.22E-12	1.25E-12	5.39E-13	2.52E-13	1.26E-13	6.66E-14
155 kts	2.23E-10	5.05E-11	1.26E-11	4.37E-12	1.71E-12	7.43E-13	3.51E-13	1.76E-13	9.41E-14
160 kts	2.69E-10	6.61E-11	1.58E-11	5.51E-12	2.18E-12	9.54E-13	4.53E-13	2.29E-13	1.23E-13
165 kts	2.93E-10	7.46E-11	1.77E-11	6.22E-12	2.47E-12	1.09E-12	5.19E-13	2.64E-13	1.42E-13
170 kts	2.94E-10	7.56E-11	1.85E-11	6.34E-12	2.53E-12	1.11E-12	5.33E-13	2.72E-13	1.47E-13
175 kts	3.03E-10	7.87E-11	1.94E-11	6.58E-12	2.63E-12	1.16E-12	5.56E-13	2.84E-13	1.53E-13
180 kts	3.46E-10	9.4E-11	2.31E-11	7.78E-12	3.12E-12	1.39E-12	6.66E-13	3.41E-13	1.85E-13
185 kts	4.28E-10	1.24E-10	3.16E-11	1.03E-11	4.16E-12	1.86E-12	9E-13	4.65E-13	2.53E-13
190 kts	5.23E-10	1.6E-10	4.33E-11	1.34E-11	5.46E-12	2.46E-12	1.2E-12	6.25E-13	3.42E-13
195 kts	6.31E-10	2.02E-10	5.9E-11	1.75E-11	7.09E-12	3.23E-12	1.59E-12	8.3E-13	4.57E-13
200 kts	7.54E-10	2.51E-10	7.89E-11	2.27E-11	9.12E-12	4.18E-12	2.07E-12	1.09E-12	6.04E-13
205 kts	8.93E-10	3.09E-10	1.03E-10	2.98E-11	1.16E-11	5.35E-12	2.67E-12	1.42E-12	7.9E-13
210 kts	1.05E-09	3.75E-10	1.32E-10	3.95E-11	1.47E-11	6.79E-12	3.41E-12	1.82E-12	1.02E-12
215 kts	1.23E-09	4.5E-10	1.65E-10	5.24E-11	1.85E-11	8.54E-12	4.32E-12	2.32E-12	1.31E-12
220 kts	1.43E-09	5.35E-10	2.04E-10	6.86E-11	2.34E-11	1.06E-11	5.42E-12	2.92E-12	1.66E-12
225 kts	1.66E-09	6.31E-10	2.49E-10	8.82E-11	2.98E-11	1.32E-11	6.73E-12	3.66E-12	2.09E-12
230 kts	1.9E-09	7.39E-10	3E-10	1.11E-10	3.83E-11	1.62E-11	8.3E-12	4.53E-12	2.6E-12
235 kts	2.13E-09	8.6E-10	3.59E-10	1.36E-10	4.93E-11	2E-11	1.02E-11	5.58E-12	3.22E-12
240 kts	2.34E-09	9.97E-10	4.24E-10	1.66E-10	6.31E-11	2.48E-11	1.23E-11	6.82E-12	3.96E-12
245 kts	2.52E-09	1.15E-09	4.96E-10	1.98E-10	7.94E-11	3.1E-11	1.49E-11	8.28E-12	4.83E-12
250 kts	2.68E-09	1.33E-09	5.76E-10	2.36E-10	9.8E-11	3.89E-11	1.8E-11	9.97E-12	5.84E-12
255 kts	2.82E-09	1.53E-09	6.62E-10	2.78E-10	1.19E-10	4.88E-11	2.17E-11	1.19E-11	7.03E-12
260 kts	2.95E-09	1.74E-09	7.56E-10	3.24E-10	1.42E-10	6.09E-11	2.65E-11	1.42E-11	8.4E-12
265 kts	3.07E-09	1.96E-09	8.59E-10	3.76E-10	1.67E-10	7.51E-11	3.26E-11	1.69E-11	9.99E-12
270 kts	3.18E-09	2.18E-09	9.75E-10	4.31E-10	1.96E-10	9.12E-11	4.03E-11	2.02E-11	1.18E-11
275 kts	3.27E-09	2.39E-09	1.11E-09	4.91E-10	2.28E-10	1.09E-10	4.94E-11	2.43E-11	1.39E-11
280 kts	3.36E-09	2.6E-09	1.27E-09	5.55E-10	2.62E-10	1.28E-10	6.02E-11	2.94E-11	1.63E-11
285 kts	3.44E-09	2.79E-09	1.46E-09	6.24E-10	3E-10	1.49E-10	7.27E-11	3.56E-11	1.92E-11
290 kts	3.51E-09	2.97E-09	1.68E-09	7.02E-10	3.41E-10	1.72E-10	8.68E-11	4.28E-11	2.28E-11
295 kts	3.58E-09	3.13E-09	1.92E-09	7.95E-10	3.85E-10	1.97E-10	1.02E-10	5.11E-11	2.73E-11
300 kts	3.63E-09	3.28E-09	2.18E-09	9.09E-10	4.31E-10	2.24E-10	1.19E-10	6.07E-11	3.26E-11
305 kts	3.67E-09	3.41E-09	2.43E-09	1.06E-09	4.8E-10	2.53E-10	1.37E-10	7.2E-11	3.86E-11
310 kts	3.69E-09	3.54E-09	2.67E-09	1.24E-09	5.36E-10	2.85E-10	1.56E-10	8.48E-11	4.52E-11

Table C-8: Median Winds with No Controller Intervention at 4300’

Turn Radius

Groundspeed	1 NM	1.5 NM	2 NM	2.5NM	3 NM	3.5 NM	4 NM	4.5 NM	5 NM
150 kts	6.01E-13	5.63E-15	1.51E-16	8.1E-18	6.84E-19	7.99E-20	1.19E-20	2.15E-21	4.51E-22
155 kts	1.42E-12	1.39E-14	3.75E-16	2.02E-17	1.72E-18	2.02E-19	3.04E-20	5.52E-21	1.17E-21
160 kts	2.88E-12	3E-14	8.16E-16	4.41E-17	3.78E-18	4.48E-19	6.77E-20	1.24E-20	2.64E-21
165 kts	4.72E-12	5.29E-14	1.45E-15	7.88E-17	6.78E-18	8.08E-19	1.23E-19	2.27E-20	4.86E-21
170 kts	6.49E-12	7.35E-14	2.04E-15	1.11E-16	9.59E-18	1.15E-18	1.76E-19	3.26E-20	7.03E-21
175 kts	7.81E-12	9.17E-14	2.57E-15	1.41E-16	1.22E-17	1.47E-18	2.25E-19	4.19E-20	9.08E-21
180 kts	1.14E-11	1.43E-13	4.05E-15	2.23E-16	1.94E-17	2.33E-18	3.6E-19	6.72E-20	1.46E-20
185 kts	2.3E-11	3.12E-13	9.06E-15	5.01E-16	4.37E-17	5.3E-18	8.21E-19	1.54E-19	3.37E-20
190 kts	4.38E-11	6.61E-13	1.98E-14	1.1E-15	9.65E-17	1.17E-17	1.83E-18	3.45E-19	7.58E-20
195 kts	7.86E-11	1.37E-12	4.21E-14	2.36E-15	2.08E-16	2.54E-17	3.98E-18	7.54E-19	1.66E-19
200 kts	1.33E-10	2.77E-12	8.75E-14	4.97E-15	4.4E-16	5.4E-17	8.47E-18	1.61E-18	3.58E-19
205 kts	2.13E-10	5.54E-12	1.78E-13	1.02E-14	9.09E-16	1.12E-16	1.77E-17	3.38E-18	7.52E-19
210 kts	3.23E-10	1.09E-11	3.52E-13	2.06E-14	1.84E-15	2.28E-16	3.61E-17	6.93E-18	1.55E-18
215 kts	4.68E-10	2.09E-11	6.81E-13	4.06E-14	3.67E-15	4.56E-16	7.25E-17	1.4E-17	3.14E-18
220 kts	6.49E-10	3.87E-11	1.29E-12	7.87E-14	7.16E-15	8.95E-16	1.43E-16	2.76E-17	6.22E-18
225 kts	8.61E-10	6.79E-11	2.38E-12	1.49E-13	1.37E-14	1.73E-15	2.76E-16	5.36E-17	1.21E-17
230 kts	1.1E-09	1.12E-10	4.34E-12	2.78E-13	2.59E-14	3.27E-15	5.26E-16	1.03E-16	2.33E-17
235 kts	1.34E-09	1.76E-10	7.85E-12	5.07E-13	4.8E-14	6.1E-15	9.86E-16	1.93E-16	4.39E-17
240 kts	1.57E-09	2.63E-10	1.41E-11	9.08E-13	8.74E-14	1.12E-14	1.82E-15	3.57E-16	8.16E-17
245 kts	1.78E-09	3.78E-10	2.53E-11	1.59E-12	1.57E-13	2.03E-14	3.31E-15	6.52E-16	1.49E-16
250 kts	1.96E-09	5.25E-10	4.43E-11	2.73E-12	2.76E-13	3.61E-14	5.92E-15	1.17E-15	2.7E-16
255 kts	2.12E-09	7.01E-10	7.45E-11	4.61E-12	4.77E-13	6.33E-14	1.05E-14	2.08E-15	4.8E-16
260 kts	2.27E-09	9.01E-10	1.19E-10	7.68E-12	8.12E-13	1.09E-13	1.82E-14	3.64E-15	8.44E-16
265 kts	2.4E-09	1.11E-09	1.81E-10	1.28E-11	1.36E-12	1.86E-13	3.13E-14	6.29E-15	1.46E-15
270 kts	2.52E-09	1.33E-09	2.63E-10	2.12E-11	2.23E-12	3.12E-13	5.31E-14	1.07E-14	2.51E-15
275 kts	2.63E-09	1.55E-09	3.68E-10	3.52E-11	3.6E-12	5.17E-13	8.88E-14	1.81E-14	4.24E-15
280 kts	2.73E-09	1.75E-09	5E-10	5.76E-11	5.71E-12	8.41E-13	1.47E-13	3.01E-14	7.1E-15
285 kts	2.82E-09	1.95E-09	6.6E-10	9.11E-11	8.95E-12	1.35E-12	2.39E-13	4.94E-14	1.17E-14
290 kts	2.9E-09	2.14E-09	8.47E-10	1.38E-10	1.4E-11	2.13E-12	3.84E-13	8.03E-14	1.92E-14
295 kts	2.97E-09	2.31E-09	1.06E-09	2.02E-10	2.18E-11	3.3E-12	6.09E-13	1.29E-13	3.1E-14
300 kts	3.04E-09	2.47E-09	1.28E-09	2.87E-10	3.4E-11	5E-12	9.46E-13	2.02E-13	4.91E-14
305 kts	3.09E-09	2.61E-09	1.52E-09	3.98E-10	5.3E-11	7.45E-12	1.45E-12	3.14E-13	7.66E-14
310 kts	3.13E-09	2.75E-09	1.76E-09	5.43E-10	8.2E-11	1.1E-11	2.2E-12	4.87E-13	1.2E-13

Table C-9: Median Winds with No Controller Intervention at 4800’

Turn Radius

Groundspeed	1 NM	1.5 NM	2 NM	2.5NM	3 NM	3.5 NM	4 NM	4.5 NM	5 NM
150 kts	7.03E-11	1.2E-11	3.54E-12	1.2E-12	4.47E-13	1.84E-13	8.29E-14	4E-14	2.04E-14
155 kts	9.46E-11	1.62E-11	4.88E-12	1.67E-12	6.3E-13	2.62E-13	1.19E-13	5.78E-14	2.96E-14
160 kts	1.18E-10	2.04E-11	6.25E-12	2.17E-12	8.22E-13	3.45E-13	1.57E-13	7.7E-14	3.97E-14
165 kts	1.31E-10	2.4E-11	7.12E-12	2.49E-12	9.49E-13	4E-13	1.84E-13	9.03E-14	4.68E-14
170 kts	1.33E-10	2.54E-11	7.28E-12	2.55E-12	9.78E-13	4.14E-13	1.9E-13	9.36E-14	4.86E-14
175 kts	1.38E-10	2.7E-11	7.58E-12	2.66E-12	1.02E-12	4.32E-13	1.99E-13	9.81E-14	5.1E-14
180 kts	1.61E-10	3.25E-11	9.03E-12	3.2E-12	1.23E-12	5.24E-13	2.42E-13	1.2E-13	6.25E-14
185 kts	2.07E-10	4.62E-11	1.21E-11	4.33E-12	1.68E-12	7.22E-13	3.36E-13	1.67E-13	8.8E-14
190 kts	2.61E-10	6.49E-11	1.6E-11	5.79E-12	2.27E-12	9.83E-13	4.61E-13	2.31E-13	1.22E-13
195 kts	3.25E-10	8.9E-11	2.11E-11	7.65E-12	3.03E-12	1.32E-12	6.24E-13	3.14E-13	1.67E-13
200 kts	3.99E-10	1.18E-10	2.78E-11	9.99E-12	3.99E-12	1.75E-12	8.34E-13	4.23E-13	2.26E-13
205 kts	4.82E-10	1.52E-10	3.71E-11	1.29E-11	5.2E-12	2.3E-12	1.1E-12	5.62E-13	3.03E-13
210 kts	5.77E-10	1.91E-10	5.01E-11	1.65E-11	6.7E-12	2.99E-12	1.44E-12	7.4E-13	4.01E-13
215 kts	6.83E-10	2.36E-10	6.78E-11	2.09E-11	8.55E-12	3.84E-12	1.86E-12	9.63E-13	5.25E-13
220 kts	8.05E-10	2.88E-10	9.03E-11	2.64E-11	1.08E-11	4.89E-12	2.39E-12	1.24E-12	6.8E-13
225 kts	9.43E-10	3.47E-10	1.17E-10	3.33E-11	1.35E-11	6.17E-12	3.03E-12	1.59E-12	8.74E-13
230 kts	1.1E-09	4.14E-10	1.48E-10	4.26E-11	1.68E-11	7.72E-12	3.82E-12	2.01E-12	1.11E-12
235 kts	1.27E-09	4.89E-10	1.84E-10	5.51E-11	2.07E-11	9.58E-12	4.77E-12	2.52E-12	1.4E-12
240 kts	1.45E-09	5.72E-10	2.24E-10	7.16E-11	2.54E-11	1.18E-11	5.91E-12	3.15E-12	1.76E-12
245 kts	1.63E-09	6.65E-10	2.7E-10	9.21E-11	3.12E-11	1.44E-11	7.27E-12	3.89E-12	2.18E-12
250 kts	1.79E-09	7.7E-10	3.2E-10	1.16E-10	3.83E-11	1.75E-11	8.87E-12	4.77E-12	2.69E-12
255 kts	1.93E-09	8.85E-10	3.76E-10	1.43E-10	4.75E-11	2.11E-11	1.07E-11	5.82E-12	3.3E-12
260 kts	2.05E-09	1.01E-09	4.35E-10	1.72E-10	5.93E-11	2.53E-11	1.29E-11	7.04E-12	4.02E-12
265 kts	2.17E-09	1.15E-09	4.98E-10	2.05E-10	7.4E-11	3.03E-11	1.55E-11	8.47E-12	4.86E-12
270 kts	2.28E-09	1.3E-09	5.66E-10	2.41E-10	9.19E-11	3.63E-11	1.84E-11	1.01E-11	5.84E-12
275 kts	2.38E-09	1.46E-09	6.4E-10	2.79E-10	1.13E-10	4.37E-11	2.18E-11	1.21E-11	6.98E-12
280 kts	2.47E-09	1.63E-09	7.23E-10	3.21E-10	1.36E-10	5.3E-11	2.57E-11	1.43E-11	8.29E-12
285 kts	2.56E-09	1.79E-09	8.22E-10	3.66E-10	1.6E-10	6.44E-11	3.02E-11	1.68E-11	9.8E-12
290 kts	2.64E-09	1.95E-09	9.42E-10	4.14E-10	1.86E-10	7.78E-11	3.56E-11	1.96E-11	1.15E-11
295 kts	2.71E-09	2.1E-09	1.09E-09	4.67E-10	2.15E-10	9.36E-11	4.22E-11	2.29E-11	1.35E-11
300 kts	2.76E-09	2.23E-09	1.25E-09	5.28E-10	2.45E-10	1.12E-10	5.02E-11	2.65E-11	1.57E-11
305 kts	2.79E-09	2.35E-09	1.43E-09	6.01E-10	2.77E-10	1.31E-10	5.95E-11	3.08E-11	1.82E-11
310 kts	2.82E-09	2.46E-09	1.63E-09	6.96E-10	3.12E-10	1.52E-10	7.01E-11	3.58E-11	2.1E-11

Table C-10: Median Winds with No Controller Intervention at 5300’

Turn Radius

Groundspeed	1 NM	1.5 NM	2 NM	2.5NM	3 NM	3.5 NM	4 NM	4.5 NM	5 NM
150 kts	3.59E-11	7.28E-12	2.1E-12	7.09E-13	2.61E-13	1.06E-13	4.7E-14	2.23E-14	1.12E-14
155 kts	5.68E-11	9.99E-12	2.94E-12	1E-12	3.73E-13	1.53E-13	6.83E-14	3.27E-14	1.65E-14
160 kts	7.29E-11	1.27E-11	3.81E-12	1.32E-12	4.93E-13	2.04E-13	9.16E-14	4.41E-14	2.24E-14
165 kts	8.19E-11	1.45E-11	4.38E-12	1.53E-12	5.75E-13	2.39E-13	1.08E-13	5.21E-14	2.66E-14
170 kts	8.31E-11	1.48E-11	4.5E-12	1.58E-12	5.95E-13	2.48E-13	1.12E-13	5.43E-14	2.78E-14
175 kts	8.68E-11	1.57E-11	4.69E-12	1.65E-12	6.22E-13	2.6E-13	1.18E-13	5.7E-14	2.92E-14
180 kts	1.04E-10	1.89E-11	5.64E-12	1.99E-12	7.57E-13	3.17E-13	1.44E-13	7.01E-14	3.6E-14
185 kts	1.37E-10	2.63E-11	7.64E-12	2.74E-12	1.05E-12	4.43E-13	2.03E-13	9.92E-14	5.14E-14
190 kts	1.77E-10	3.69E-11	1.02E-11	3.71E-12	1.43E-12	6.1E-13	2.81E-13	1.39E-13	7.22E-14
195 kts	2.25E-10	5.21E-11	1.35E-11	4.96E-12	1.94E-12	8.3E-13	3.85E-13	1.91E-13	1E-13
200 kts	2.8E-10	7.27E-11	1.76E-11	6.56E-12	2.58E-12	1.12E-12	5.21E-13	2.6E-13	1.37E-13
205 kts	3.45E-10	9.84E-11	2.28E-11	8.57E-12	3.41E-12	1.48E-12	6.97E-13	3.5E-13	1.85E-13
210 kts	4.19E-10	1.29E-10	2.97E-11	1.11E-11	4.44E-12	1.95E-12	9.21E-13	4.65E-13	2.48E-13
215 kts	5.02E-10	1.64E-10	3.9E-11	1.41E-11	5.73E-12	2.53E-12	1.21E-12	6.13E-13	3.28E-13
220 kts	5.96E-10	2.04E-10	5.2E-11	1.79E-11	7.33E-12	3.26E-12	1.56E-12	7.99E-13	4.3E-13
225 kts	7.03E-10	2.5E-10	6.98E-11	2.25E-11	9.28E-12	4.15E-12	2.01E-12	1.03E-12	5.58E-13
230 kts	8.24E-10	3.02E-10	9.27E-11	2.8E-11	1.16E-11	5.25E-12	2.55E-12	1.32E-12	7.17E-13
235 kts	9.61E-10	3.61E-10	1.2E-10	3.47E-11	1.45E-11	6.58E-12	3.22E-12	1.67E-12	9.14E-13
240 kts	1.11E-09	4.27E-10	1.52E-10	4.32E-11	1.79E-11	8.18E-12	4.02E-12	2.1E-12	1.16E-12
245 kts	1.27E-09	5.01E-10	1.87E-10	5.43E-11	2.19E-11	1.01E-11	4.99E-12	2.62E-12	1.45E-12
250 kts	1.42E-09	5.82E-10	2.26E-10	6.93E-11	2.66E-11	1.24E-11	6.15E-12	3.25E-12	1.81E-12
255 kts	1.56E-09	6.72E-10	2.7E-10	8.87E-11	3.22E-11	1.5E-11	7.52E-12	4E-12	2.23E-12
260 kts	1.68E-09	7.7E-10	3.17E-10	1.12E-10	3.88E-11	1.81E-11	9.14E-12	4.88E-12	2.74E-12
265 kts	1.8E-09	8.77E-10	3.67E-10	1.39E-10	4.67E-11	2.18E-11	1.1E-11	5.93E-12	3.34E-12
270 kts	1.91E-09	9.93E-10	4.2E-10	1.68E-10	5.65E-11	2.6E-11	1.32E-11	7.15E-12	4.05E-12
275 kts	2E-09	1.12E-09	4.77E-10	1.99E-10	6.9E-11	3.08E-11	1.58E-11	8.57E-12	4.88E-12
280 kts	2.09E-09	1.26E-09	5.39E-10	2.33E-10	8.47E-11	3.65E-11	1.87E-11	1.02E-11	5.84E-12
285 kts	2.17E-09	1.4E-09	6.1E-10	2.69E-10	1.04E-10	4.3E-11	2.21E-11	1.21E-11	6.96E-12
290 kts	2.24E-09	1.54E-09	6.96E-10	3.07E-10	1.26E-10	5.08E-11	2.59E-11	1.43E-11	8.24E-12
295 kts	2.31E-09	1.68E-09	8E-10	3.49E-10	1.49E-10	6.03E-11	3.03E-11	1.68E-11	9.72E-12
300 kts	2.37E-09	1.81E-09	9.24E-10	3.95E-10	1.75E-10	7.15E-11	3.52E-11	1.96E-11	1.14E-11
305 kts	2.41E-09	1.93E-09	1.07E-09	4.48E-10	2.01E-10	8.43E-11	4.08E-11	2.27E-11	1.33E-11
310 kts	2.45E-09	2.04E-09	1.23E-09	5.13E-10	2.29E-10	9.88E-11	4.74E-11	2.63E-11	1.55E-11

Table C-11: Worst Winds at 3600’

Turn Radius

Groundspeed	1 NM	1.5 NM	2 NM	2.5NM	3 NM	3.5 NM	4 NM	4.5 NM	5 NM
150 kts	2.49E-12	1.49E-13	2.1E-14	4.54E-15	1.29E-15	4.41E-16	1.73E-16	7.52E-17	3.56E-17
155 kts	3.22E-12	1.86E-13	2.57E-14	5.52E-15	1.56E-15	5.32E-16	2.08E-16	9.06E-17	4.28E-17
160 kts	5.57E-12	2.99E-13	4.01E-14	8.47E-15	2.37E-15	8.03E-16	3.13E-16	1.36E-16	6.41E-17
165 kts	1E-11	4.94E-13	6.39E-14	1.32E-14	3.66E-15	1.23E-15	4.78E-16	2.07E-16	9.74E-17
170 kts	1.97E-11	8.13E-13	1.01E-13	2.04E-14	5.58E-15	1.87E-15	7.21E-16	3.11E-16	1.46E-16
175 kts	3.96E-11	1.33E-12	1.58E-13	3.13E-14	8.45E-15	2.8E-15	1.08E-15	4.63E-16	2.17E-16
180 kts	7.29E-11	2.18E-12	2.47E-13	4.76E-14	1.27E-14	4.17E-15	1.59E-15	6.83E-16	3.19E-16
185 kts	1.31E-10	3.56E-12	3.82E-13	7.2E-14	1.89E-14	6.14E-15	2.33E-15	9.97E-16	4.65E-16
190 kts	2.31E-10	5.81E-12	5.91E-13	1.08E-13	2.78E-14	8.98E-15	3.39E-15	1.44E-15	6.7E-16
195 kts	3.9E-10	9.48E-12	9.1E-13	1.61E-13	4.08E-14	1.3E-14	4.89E-15	2.07E-15	9.58E-16
200 kts	6.18E-10	1.56E-11	1.4E-12	2.4E-13	5.95E-14	1.88E-14	7E-15	2.94E-15	1.36E-15
205 kts	9.13E-10	2.94E-11	2.14E-12	3.55E-13	8.64E-14	2.69E-14	9.95E-15	4.16E-15	1.91E-15
210 kts	1.25E-09	5.77E-11	3.29E-12	5.24E-13	1.25E-13	3.84E-14	1.4E-14	5.84E-15	2.68E-15
215 kts	1.61E-09	1.01E-10	5.04E-12	7.71E-13	1.79E-13	5.44E-14	1.97E-14	8.15E-15	3.72E-15
220 kts	1.93E-09	1.69E-10	7.73E-12	1.13E-12	2.57E-13	7.67E-14	2.76E-14	1.13E-14	5.14E-15
225 kts	2.16E-09	2.79E-10	1.19E-11	1.66E-12	3.67E-13	1.08E-13	3.83E-14	1.56E-14	7.05E-15
230 kts	2.37E-09	4.45E-10	1.84E-11	2.44E-12	5.22E-13	1.51E-13	5.3E-14	2.14E-14	9.64E-15
235 kts	2.56E-09	6.77E-10	3.23E-11	3.57E-12	7.42E-13	2.1E-13	7.3E-14	2.93E-14	1.31E-14
240 kts	2.73E-09	9.71E-10	6.06E-11	5.24E-12	1.05E-12	2.92E-13	1E-13	3.99E-14	1.77E-14
245 kts	2.88E-09	1.29E-09	1.05E-10	7.69E-12	1.49E-12	4.06E-13	1.37E-13	5.41E-14	2.38E-14
250 kts	3.01E-09	1.59E-09	1.75E-10	1.13E-11	2.12E-12	5.62E-13	1.87E-13	7.31E-14	3.2E-14
255 kts	3.13E-09	1.86E-09	2.85E-10	1.68E-11	3E-12	7.77E-13	2.55E-13	9.84E-14	4.28E-14
260 kts	3.24E-09	2.13E-09	4.47E-10	2.65E-11	4.25E-12	1.07E-12	3.46E-13	1.32E-13	5.7E-14
265 kts	3.35E-09	2.37E-09	6.68E-10	4.63E-11	6.02E-12	1.48E-12	4.69E-13	1.77E-13	7.57E-14
270 kts	3.44E-09	2.59E-09	9.33E-10	8.11E-11	8.55E-12	2.04E-12	6.35E-13	2.36E-13	1E-13
275 kts	3.53E-09	2.8E-09	1.22E-09	1.35E-10	1.22E-11	2.81E-12	8.58E-13	3.15E-13	1.33E-13
280 kts	3.61E-09	2.99E-09	1.52E-09	2.22E-10	1.75E-11	3.88E-12	1.16E-12	4.2E-13	1.75E-13
285 kts	3.68E-09	3.15E-09	1.83E-09	3.55E-10	2.59E-11	5.35E-12	1.56E-12	5.58E-13	2.3E-13
290 kts	3.74E-09	3.31E-09	2.13E-09	5.41E-10	4.35E-11	7.4E-12	2.11E-12	7.42E-13	3.02E-13
295 kts	3.79E-09	3.45E-09	2.41E-09	7.82E-10	7.83E-11	1.03E-11	2.85E-12	9.84E-13	3.96E-13
300 kts	3.8E-09	3.59E-09	2.66E-09	1.07E-09	1.31E-10	1.44E-11	3.84E-12	1.3E-12	5.18E-13
305 kts	3.79E-09	3.7E-09	2.89E-09	1.39E-09	2.14E-10	2.04E-11	5.16E-12	1.72E-12	6.75E-13
310 kts	3.84E-09	3.81E-09	3.1E-09	1.72E-09	3.44E-10	3.09E-11	6.99E-12	2.28E-12	8.82E-13

Table C-12: Worst Winds at 3900’

Turn Radius

Groundspeed	1 NM	1.5 NM	2 NM	2.5NM	3 NM	3.5 NM	4 NM	4.5 NM	5 NM
150 kts	1.38E-12	8.65E-14	1.24E-14	2.72E-15	7.72E-16	2.64E-16	1.03E-16	4.47E-17	2.11E-17
155 kts	1.79E-12	1.08E-13	1.53E-14	3.31E-15	9.37E-16	3.19E-16	1.25E-16	5.4E-17	2.55E-17
160 kts	3.1E-12	1.75E-13	2.39E-14	5.1E-15	1.43E-15	4.84E-16	1.88E-16	8.14E-17	3.84E-17
165 kts	5.55E-12	2.9E-13	3.83E-14	8E-15	2.22E-15	7.45E-16	2.89E-16	1.25E-16	5.86E-17
170 kts	1E-11	4.79E-13	6.06E-14	1.24E-14	3.4E-15	1.14E-15	4.38E-16	1.88E-16	8.83E-17
175 kts	1.99E-11	7.87E-13	9.54E-14	1.91E-14	5.17E-15	1.71E-15	6.56E-16	2.81E-16	1.32E-16
180 kts	4.02E-11	1.29E-12	1.49E-13	2.92E-14	7.78E-15	2.56E-15	9.75E-16	4.16E-16	1.94E-16
185 kts	7.41E-11	2.11E-12	2.32E-13	4.42E-14	1.16E-14	3.78E-15	1.43E-15	6.1E-16	2.84E-16
190 kts	1.34E-10	3.45E-12	3.6E-13	6.67E-14	1.72E-14	5.55E-15	2.09E-15	8.86E-16	4.11E-16
195 kts	2.36E-10	5.65E-12	5.55E-13	9.98E-14	2.53E-14	8.08E-15	3.03E-15	1.28E-15	5.9E-16
200 kts	3.93E-10	9.27E-12	8.55E-13	1.49E-13	3.71E-14	1.17E-14	4.35E-15	1.82E-15	8.4E-16
205 kts	6.14E-10	1.54E-11	1.32E-12	2.21E-13	5.39E-14	1.68E-14	6.2E-15	2.58E-15	1.19E-15
210 kts	8.92E-10	2.94E-11	2.02E-12	3.27E-13	7.81E-14	2.4E-14	8.78E-15	3.64E-15	1.66E-15
215 kts	1.21E-09	5.86E-11	3.11E-12	4.83E-13	1.13E-13	3.41E-14	1.24E-14	5.09E-15	2.32E-15
220 kts	1.52E-09	1.03E-10	4.78E-12	7.11E-13	1.62E-13	4.83E-14	1.73E-14	7.09E-15	3.21E-15
225 kts	1.78E-09	1.73E-10	7.36E-12	1.05E-12	2.32E-13	6.8E-14	2.41E-14	9.81E-15	4.43E-15
230 kts	1.99E-09	2.85E-10	1.14E-11	1.54E-12	3.31E-13	9.54E-14	3.35E-14	1.35E-14	6.06E-15
235 kts	2.18E-09	4.51E-10	1.78E-11	2.26E-12	4.71E-13	1.33E-13	4.63E-14	1.85E-14	8.26E-15
240 kts	2.35E-09	6.78E-10	3.1E-11	3.32E-12	6.7E-13	1.86E-13	6.37E-14	2.53E-14	1.12E-14
245 kts	2.5E-09	9.5E-10	5.91E-11	4.88E-12	9.52E-13	2.59E-13	8.74E-14	3.44E-14	1.51E-14
250 kts	2.64E-09	1.23E-09	1.06E-10	7.2E-12	1.35E-12	3.59E-13	1.2E-13	4.65E-14	2.03E-14
255 kts	2.77E-09	1.48E-09	1.79E-10	1.07E-11	1.92E-12	4.97E-13	1.63E-13	6.28E-14	2.72E-14
260 kts	2.89E-09	1.73E-09	2.92E-10	1.59E-11	2.73E-12	6.89E-13	2.22E-13	8.45E-14	3.64E-14
265 kts	2.99E-09	1.97E-09	4.53E-10	2.41E-11	3.88E-12	9.52E-13	3.01E-13	1.13E-13	4.84E-14
270 kts	3.09E-09	2.19E-09	6.6E-10	4.17E-11	5.52E-12	1.32E-12	4.09E-13	1.52E-13	6.43E-14
275 kts	3.17E-09	2.39E-09	9.02E-10	7.8E-11	7.89E-12	1.82E-12	5.54E-13	2.03E-13	8.51E-14
280 kts	3.25E-09	2.57E-09	1.17E-09	1.35E-10	1.13E-11	2.52E-12	7.49E-13	2.71E-13	1.12E-13
285 kts	3.33E-09	2.74E-09	1.44E-09	2.26E-10	1.65E-11	3.48E-12	1.01E-12	3.61E-13	1.48E-13
290 kts	3.39E-09	2.9E-09	1.72E-09	3.59E-10	2.46E-11	4.82E-12	1.37E-12	4.81E-13	1.95E-13
295 kts	3.45E-09	3.04E-09	1.99E-09	5.43E-10	4.06E-11	6.7E-12	1.85E-12	6.39E-13	2.56E-13
300 kts	3.47E-09	3.17E-09	2.24E-09	7.76E-10	7.37E-11	9.37E-12	2.51E-12	8.48E-13	3.36E-13
305 kts	3.47E-09	3.3E-09	2.47E-09	1.05E-09	1.29E-10	1.32E-11	3.38E-12	1.12E-12	4.39E-13
310 kts	3.52E-09	3.41E-09	2.67E-09	1.35E-09	2.18E-10	1.91E-11	4.58E-12	1.49E-12	5.75E-13

Table C-13: Worst Winds at 4300’

Turn Radius

Groundspeed	1 NM	1.5 NM	2 NM	2.5NM	3 NM	3.5 NM	4 NM	4.5 NM	5 NM
150 kts	6.55E-13	4.37E-14	6.43E-15	1.43E-15	4.08E-16	1.4E-16	5.44E-17	2.35E-17	1.11E-17
155 kts	8.5E-13	5.48E-14	7.93E-15	1.75E-15	4.97E-16	1.69E-16	6.59E-17	2.85E-17	1.34E-17
160 kts	1.47E-12	8.9E-14	1.25E-14	2.71E-15	7.62E-16	2.58E-16	1E-16	4.32E-17	2.02E-17
165 kts	2.64E-12	1.48E-13	2.01E-14	4.27E-15	1.19E-15	4E-16	1.54E-16	6.64E-17	3.11E-17
170 kts	4.73E-12	2.45E-13	3.2E-14	6.66E-15	1.83E-15	6.13E-16	2.36E-16	1.01E-16	4.71E-17
175 kts	8.53E-12	4.04E-13	5.05E-14	1.03E-14	2.8E-15	9.28E-16	3.55E-16	1.52E-16	7.06E-17
180 kts	1.7E-11	6.64E-13	7.93E-14	1.58E-14	4.24E-15	1.39E-15	5.3E-16	2.26E-16	1.05E-16
185 kts	3.47E-11	1.09E-12	1.24E-13	2.41E-14	6.35E-15	2.07E-15	7.84E-16	3.32E-16	1.54E-16
190 kts	6.5E-11	1.79E-12	1.92E-13	3.64E-14	9.45E-15	3.05E-15	1.15E-15	4.85E-16	2.24E-16
195 kts	1.18E-10	2.93E-12	2.98E-13	5.47E-14	1.4E-14	4.46E-15	1.67E-15	7.01E-16	3.23E-16
200 kts	2.08E-10	4.81E-12	4.6E-13	8.19E-14	2.05E-14	6.48E-15	2.41E-15	1.01E-15	4.62E-16
205 kts	3.46E-10	7.92E-12	7.09E-13	1.22E-13	3E-14	9.36E-15	3.45E-15	1.43E-15	6.55E-16
210 kts	5.41E-10	1.32E-11	1.09E-12	1.81E-13	4.36E-14	1.34E-14	4.9E-15	2.03E-15	9.23E-16
215 kts	7.87E-10	2.5E-11	1.68E-12	2.68E-13	6.3E-14	1.91E-14	6.93E-15	2.85E-15	1.29E-15
220 kts	1.07E-09	5.05E-11	2.6E-12	3.95E-13	9.08E-14	2.72E-14	9.73E-15	3.98E-15	1.8E-15
225 kts	1.34E-09	9.11E-11	4.01E-12	5.83E-13	1.3E-13	3.84E-14	1.36E-14	5.52E-15	2.48E-15
230 kts	1.56E-09	1.55E-10	6.21E-12	8.58E-13	1.87E-13	5.4E-14	1.89E-14	7.63E-15	3.41E-15
235 kts	1.74E-09	2.56E-10	9.65E-12	1.26E-12	2.67E-13	7.57E-14	2.63E-14	1.05E-14	4.66E-15
240 kts	1.91E-09	4.06E-10	1.51E-11	1.86E-12	3.8E-13	1.06E-13	3.62E-14	1.44E-14	6.34E-15
245 kts	2.08E-09	6.09E-10	2.47E-11	2.75E-12	5.42E-13	1.48E-13	4.99E-14	1.96E-14	8.59E-15
250 kts	2.22E-09	8.45E-10	4.68E-11	4.06E-12	7.71E-13	2.05E-13	6.84E-14	2.66E-14	1.16E-14
255 kts	2.35E-09	1.07E-09	9.17E-11	6.03E-12	1.1E-12	2.85E-13	9.35E-14	3.6E-14	1.56E-14
260 kts	2.47E-09	1.3E-09	1.6E-10	8.97E-12	1.56E-12	3.96E-13	1.27E-13	4.85E-14	2.08E-14
265 kts	2.57E-09	1.52E-09	2.62E-10	1.35E-11	2.23E-12	5.49E-13	1.74E-13	6.53E-14	2.78E-14
270 kts	2.67E-09	1.73E-09	4.07E-10	2.06E-11	3.18E-12	7.6E-13	2.36E-13	8.77E-14	3.7E-14
275 kts	2.77E-09	1.92E-09	5.9E-10	3.35E-11	4.55E-12	1.05E-12	3.21E-13	1.17E-13	4.91E-14
280 kts	2.85E-09	2.1E-09	7.98E-10	6.15E-11	6.54E-12	1.46E-12	4.35E-13	1.57E-13	6.5E-14
285 kts	2.92E-09	2.27E-09	1.03E-09	1.16E-10	9.47E-12	2.03E-12	5.9E-13	2.1E-13	8.59E-14
290 kts	2.99E-09	2.42E-09	1.28E-09	2.01E-10	1.39E-11	2.82E-12	7.99E-13	2.79E-13	1.13E-13
295 kts	3.05E-09	2.56E-09	1.53E-09	3.23E-10	2.1E-11	3.92E-12	1.08E-12	3.72E-13	1.49E-13
300 kts	3.07E-09	2.69E-09	1.76E-09	4.9E-10	3.32E-11	5.48E-12	1.47E-12	4.96E-13	1.96E-13
305 kts	3.07E-09	2.82E-09	1.98E-09	6.98E-10	5.68E-11	7.67E-12	1.99E-12	6.58E-13	2.56E-13
310 kts	3.12E-09	2.93E-09	2.18E-09	9.44E-10	1.07E-10	1.09E-11	2.7E-12	8.76E-13	3.37E-13

Table C-14: Worst Winds at 4800’

Turn Radius

Groundspeed	1 NM	1.5 NM	2 NM	2.5NM	3 NM	3.5 NM	4 NM	4.5 NM	5 NM
150 kts	2.72E-13	1.96E-14	2.98E-15	6.79E-16	1.95E-16	6.68E-17	2.61E-17	1.13E-17	5.26E-18
155 kts	3.53E-13	2.47E-14	3.69E-15	8.33E-16	2.39E-16	8.14E-17	3.17E-17	1.37E-17	6.38E-18
160 kts	6.13E-13	4.03E-14	5.85E-15	1.3E-15	3.68E-16	1.25E-16	4.85E-17	2.09E-17	9.73E-18
165 kts	1.1E-12	6.74E-14	9.45E-15	2.06E-15	5.78E-16	1.95E-16	7.53E-17	3.23E-17	1.51E-17
170 kts	1.97E-12	1.12E-13	1.51E-14	3.23E-15	8.97E-16	3E-16	1.16E-16	4.95E-17	2.3E-17
175 kts	3.52E-12	1.85E-13	2.4E-14	5.03E-15	1.38E-15	4.58E-16	1.75E-16	7.48E-17	3.47E-17
180 kts	6.32E-12	3.05E-13	3.79E-14	7.75E-15	2.1E-15	6.91E-16	2.63E-16	1.12E-16	5.18E-17
185 kts	1.23E-11	5.01E-13	5.94E-14	1.19E-14	3.16E-15	1.03E-15	3.91E-16	1.65E-16	7.64E-17
190 kts	2.51E-11	8.22E-13	9.26E-14	1.8E-14	4.73E-15	1.53E-15	5.76E-16	2.43E-16	1.12E-16
195 kts	4.9E-11	1.35E-12	1.44E-13	2.72E-14	7.03E-15	2.25E-15	8.41E-16	3.53E-16	1.62E-16
200 kts	9.04E-11	2.22E-12	2.23E-13	4.08E-14	1.04E-14	3.29E-15	1.22E-15	5.09E-16	2.33E-16
205 kts	1.6E-10	3.66E-12	3.44E-13	6.1E-14	1.52E-14	4.76E-15	1.75E-15	7.28E-16	3.32E-16
210 kts	2.7E-10	6.04E-12	5.31E-13	9.08E-14	2.22E-14	6.85E-15	2.5E-15	1.03E-15	4.7E-16
215 kts	4.29E-10	1E-11	8.2E-13	1.35E-13	3.22E-14	9.81E-15	3.55E-15	1.46E-15	6.61E-16
220 kts	6.34E-10	1.69E-11	1.27E-12	1.99E-13	4.65E-14	1.4E-14	5.01E-15	2.05E-15	9.22E-16
225 kts	8.73E-10	3.42E-11	1.96E-12	2.95E-13	6.7E-14	1.98E-14	7.04E-15	2.85E-15	1.28E-15
230 kts	1.11E-09	7.05E-11	3.04E-12	4.35E-13	9.61E-14	2.8E-14	9.83E-15	3.96E-15	1.76E-15
235 kts	1.3E-09	1.23E-10	4.73E-12	6.41E-13	1.38E-13	3.94E-14	1.37E-14	5.46E-15	2.42E-15
240 kts	1.47E-09	2.06E-10	7.4E-12	9.47E-13	1.97E-13	5.52E-14	1.89E-14	7.49E-15	3.3E-15
245 kts	1.63E-09	3.3E-10	1.16E-11	1.4E-12	2.81E-13	7.71E-14	2.61E-14	1.02E-14	4.49E-15
250 kts	1.77E-09	4.98E-10	1.87E-11	2.07E-12	4.01E-13	1.08E-13	3.59E-14	1.4E-14	6.07E-15
255 kts	1.9E-09	6.89E-10	3.28E-11	3.08E-12	5.72E-13	1.5E-13	4.92E-14	1.89E-14	8.19E-15
260 kts	2.03E-09	8.79E-10	6.54E-11	4.59E-12	8.16E-13	2.08E-13	6.73E-14	2.56E-14	1.1E-14
265 kts	2.14E-09	1.07E-09	1.25E-10	6.88E-12	1.17E-12	2.89E-13	9.19E-14	3.46E-14	1.47E-14
270 kts	2.24E-09	1.26E-09	2.1E-10	1.04E-11	1.67E-12	4.02E-13	1.25E-13	4.65E-14	1.96E-14
275 kts	2.33E-09	1.45E-09	3.29E-10	1.6E-11	2.39E-12	5.58E-13	1.7E-13	6.25E-14	2.61E-14
280 kts	2.42E-09	1.62E-09	4.77E-10	2.55E-11	3.44E-12	7.75E-13	2.32E-13	8.37E-14	3.46E-14
285 kts	2.5E-09	1.78E-09	6.52E-10	4.36E-11	4.98E-12	1.08E-12	3.15E-13	1.12E-13	4.58E-14
290 kts	2.57E-09	1.93E-09	8.51E-10	8.17E-11	7.25E-12	1.5E-12	4.28E-13	1.5E-13	6.06E-14
295 kts	2.63E-09	2.07E-09	1.06E-09	1.53E-10	1.07E-11	2.1E-12	5.81E-13	2E-13	8E-14
300 kts	2.66E-09	2.2E-09	1.27E-09	2.58E-10	1.64E-11	2.93E-12	7.9E-13	2.67E-13	1.05E-13
305 kts	2.66E-09	2.31E-09	1.47E-09	3.97E-10	2.61E-11	4.1E-12	1.07E-12	3.54E-13	1.38E-13
310 kts	2.71E-09	2.42E-09	1.66E-09	5.75E-10	4.44E-11	5.81E-12	1.46E-12	4.72E-13	1.81E-13

Table C-15: Worst Winds at 5300’

Turn Radius

Groundspeed	1 NM	1.5 NM	2 NM	2.5NM	3 NM	3.5 NM	4 NM	4.5 NM	5 NM
150 kts	1.19E-13	9.3E-15	1.46E-15	3.39E-16	9.87E-17	3.39E-17	1.33E-17	5.72E-18	2.67E-18
155 kts	1.55E-13	1.17E-14	1.81E-15	4.17E-16	1.21E-16	4.15E-17	1.62E-17	6.97E-18	3.25E-18
160 kts	2.69E-13	1.92E-14	2.88E-15	6.54E-16	1.88E-16	6.4E-17	2.49E-17	1.07E-17	4.98E-18
165 kts	4.81E-13	3.22E-14	4.68E-15	1.04E-15	2.97E-16	1E-16	3.89E-17	1.67E-17	7.75E-18
170 kts	8.59E-13	5.37E-14	7.52E-15	1.65E-15	4.63E-16	1.56E-16	6E-17	2.56E-17	1.19E-17
175 kts	1.53E-12	8.9E-14	1.2E-14	2.58E-15	7.15E-16	2.39E-16	9.15E-17	3.9E-17	1.81E-17
180 kts	2.74E-12	1.47E-13	1.9E-14	3.99E-15	1.09E-15	3.62E-16	1.38E-16	5.86E-17	2.71E-17
185 kts	4.89E-12	2.42E-13	2.99E-14	6.13E-15	1.66E-15	5.44E-16	2.06E-16	8.72E-17	4.02E-17
190 kts	8.84E-12	3.97E-13	4.68E-14	9.35E-15	2.49E-15	8.1E-16	3.05E-16	1.29E-16	5.91E-17
195 kts	1.81E-11	6.51E-13	7.28E-14	1.42E-14	3.71E-15	1.2E-15	4.48E-16	1.88E-16	8.61E-17
200 kts	3.81E-11	1.07E-12	1.13E-13	2.13E-14	5.5E-15	1.75E-15	6.51E-16	2.72E-16	1.24E-16
205 kts	7.12E-11	1.76E-12	1.75E-13	3.2E-14	8.09E-15	2.55E-15	9.41E-16	3.91E-16	1.78E-16
210 kts	1.27E-10	2.91E-12	2.7E-13	4.77E-14	1.18E-14	3.68E-15	1.35E-15	5.57E-16	2.53E-16
215 kts	2.17E-10	4.82E-12	4.18E-13	7.09E-14	1.72E-14	5.29E-15	1.92E-15	7.9E-16	3.56E-16
220 kts	3.49E-10	8.03E-12	6.46E-13	1.05E-13	2.5E-14	7.57E-15	2.72E-15	1.11E-15	4.99E-16
225 kts	5.23E-10	1.36E-11	9.99E-13	1.56E-13	3.61E-14	1.08E-14	3.83E-15	1.55E-15	6.95E-16
230 kts	7.27E-10	2.6E-11	1.55E-12	2.3E-13	5.19E-14	1.52E-14	5.37E-15	2.16E-15	9.62E-16
235 kts	9.26E-10	5.38E-11	2.41E-12	3.39E-13	7.45E-14	2.15E-14	7.48E-15	2.99E-15	1.32E-15
240 kts	1.1E-09	1E-10	3.78E-12	5.02E-13	1.07E-13	3.02E-14	1.04E-14	4.12E-15	1.81E-15
245 kts	1.25E-09	1.71E-10	5.94E-12	7.42E-13	1.53E-13	4.23E-14	1.44E-14	5.65E-15	2.47E-15
250 kts	1.4E-09	2.76E-10	9.42E-12	1.1E-12	2.18E-13	5.91E-14	1.98E-14	7.71E-15	3.36E-15
255 kts	1.53E-09	4.17E-10	1.51E-11	1.63E-12	3.11E-13	8.25E-14	2.72E-14	1.05E-14	4.53E-15
260 kts	1.66E-09	5.76E-10	2.51E-11	2.44E-12	4.45E-13	1.15E-13	3.73E-14	1.42E-14	6.1E-15
265 kts	1.77E-09	7.38E-10	4.73E-11	3.65E-12	6.36E-13	1.6E-13	5.1E-14	1.92E-14	8.18E-15
270 kts	1.88E-09	9.05E-10	9.56E-11	5.51E-12	9.11E-13	2.22E-13	6.96E-14	2.59E-14	1.09E-14
275 kts	1.98E-09	1.07E-09	1.71E-10	8.4E-12	1.31E-12	3.09E-13	9.49E-14	3.49E-14	1.46E-14
280 kts	2.07E-09	1.24E-09	2.72E-10	1.31E-11	1.88E-12	4.3E-13	1.29E-13	4.68E-14	1.94E-14
285 kts	2.15E-09	1.39E-09	3.96E-10	2.11E-11	2.72E-12	5.99E-13	1.76E-13	6.28E-14	2.57E-14
290 kts	2.22E-09	1.54E-09	5.46E-10	3.56E-11	3.96E-12	8.35E-13	2.39E-13	8.41E-14	3.41E-14
295 kts	2.29E-09	1.67E-09	7.16E-10	6.38E-11	5.81E-12	1.17E-12	3.26E-13	1.12E-13	4.5E-14
300 kts	2.33E-09	1.79E-09	8.96E-10	1.17E-10	8.7E-12	1.64E-12	4.43E-13	1.5E-13	5.94E-14
305 kts	2.35E-09	1.9E-09	1.08E-09	2.04E-10	1.34E-11	2.29E-12	6.01E-13	2E-13	7.79E-14
310 kts	2.38E-09	2.01E-09	1.25E-09	3.3E-10	2.19E-11	3.23E-12	8.21E-13	2.67E-13	1.03E-13

Table C-16: Worst Winds without Controller Intervention at 3600’

Turn Radius

Groundspeed	1 NM	1.5 NM	2 NM	2.5NM	3 NM	3.5 NM	4 NM	4.5 NM	5 NM
150 kts	2.35E-10	5.43E-11	1.32E-11	4.57E-12	1.8E-12	7.91E-13	3.76E-13	1.91E-13	1.02E-13
155 kts	2.59E-10	6.24E-11	1.48E-11	5.18E-12	2.06E-12	9.05E-13	4.32E-13	2.2E-13	1.18E-13
160 kts	3.25E-10	8.44E-11	1.95E-11	6.88E-12	2.76E-12	1.23E-12	5.89E-13	3.02E-13	1.63E-13
165 kts	4.07E-10	1.13E-10	2.7E-11	9.18E-12	3.72E-12	1.67E-12	8.08E-13	4.18E-13	2.28E-13
170 kts	5.03E-10	1.48E-10	3.86E-11	1.21E-11	4.95E-12	2.24E-12	1.09E-12	5.7E-13	3.12E-13
175 kts	6.15E-10	1.89E-10	5.39E-11	1.57E-11	6.51E-12	2.97E-12	1.46E-12	7.67E-13	4.23E-13
180 kts	7.42E-10	2.37E-10	7.38E-11	2.02E-11	8.44E-12	3.89E-12	1.93E-12	1.02E-12	5.66E-13
185 kts	8.8E-10	2.94E-10	9.66E-11	2.69E-11	1.08E-11	5.03E-12	2.51E-12	1.34E-12	7.47E-13
190 kts	1.03E-09	3.6E-10	1.23E-10	3.68E-11	1.37E-11	6.43E-12	3.24E-12	1.74E-12	9.76E-13
195 kts	1.21E-09	4.36E-10	1.56E-10	4.94E-11	1.73E-11	8.14E-12	4.13E-12	2.23E-12	1.26E-12
200 kts	1.41E-09	5.25E-10	1.94E-10	6.68E-11	2.18E-11	1.02E-11	5.22E-12	2.83E-12	1.61E-12
205 kts	1.65E-09	6.23E-10	2.38E-10	8.58E-11	2.85E-11	1.27E-11	6.54E-12	3.57E-12	2.04E-12
210 kts	1.93E-09	7.32E-10	2.89E-10	1.08E-10	3.74E-11	1.56E-11	8.11E-12	4.45E-12	2.57E-12
215 kts	2.22E-09	8.53E-10	3.49E-10	1.32E-10	4.86E-11	1.91E-11	9.98E-12	5.51E-12	3.19E-12
220 kts	2.49E-09	9.86E-10	4.16E-10	1.61E-10	6.39E-11	2.41E-11	1.22E-11	6.77E-12	3.94E-12
225 kts	2.7E-09	1.14E-09	4.91E-10	1.94E-10	8.07E-11	3.15E-11	1.47E-11	8.25E-12	4.83E-12
230 kts	2.87E-09	1.32E-09	5.73E-10	2.32E-10	9.9E-11	3.96E-11	1.77E-11	9.98E-12	5.88E-12
235 kts	3.03E-09	1.53E-09	6.63E-10	2.74E-10	1.19E-10	5E-11	2.18E-11	1.2E-11	7.1E-12
240 kts	3.18E-09	1.77E-09	7.59E-10	3.23E-10	1.42E-10	6.41E-11	2.77E-11	1.43E-11	8.51E-12
245 kts	3.31E-09	2.02E-09	8.63E-10	3.78E-10	1.68E-10	7.84E-11	3.48E-11	1.7E-11	1.01E-11
250 kts	3.43E-09	2.27E-09	9.79E-10	4.37E-10	1.98E-10	9.44E-11	4.22E-11	2.04E-11	1.2E-11
255 kts	3.53E-09	2.52E-09	1.11E-09	4.99E-10	2.31E-10	1.12E-10	5.2E-11	2.54E-11	1.42E-11
260 kts	3.62E-09	2.76E-09	1.26E-09	5.64E-10	2.69E-10	1.32E-10	6.54E-11	3.18E-11	1.66E-11
265 kts	3.71E-09	2.98E-09	1.44E-09	6.33E-10	3.09E-10	1.54E-10	7.87E-11	3.84E-11	1.98E-11
270 kts	3.79E-09	3.17E-09	1.67E-09	7.07E-10	3.52E-10	1.78E-10	9.25E-11	4.54E-11	2.44E-11
275 kts	3.86E-09	3.36E-09	1.93E-09	7.92E-10	3.97E-10	2.05E-10	1.09E-10	5.5E-11	3.01E-11
280 kts	3.92E-09	3.52E-09	2.22E-09	8.91E-10	4.45E-10	2.35E-10	1.26E-10	6.75E-11	3.58E-11
285 kts	3.98E-09	3.67E-09	2.51E-09	1.02E-09	4.95E-10	2.67E-10	1.45E-10	8.01E-11	4.18E-11
290 kts	4.04E-09	3.81E-09	2.79E-09	1.19E-09	5.48E-10	3E-10	1.66E-10	9.33E-11	4.88E-11
295 kts	4.07E-09	3.94E-09	3.05E-09	1.41E-09	6.07E-10	3.34E-10	1.89E-10	1.08E-10	5.88E-11
300 kts	4.06E-09	4.06E-09	3.28E-09	1.68E-09	6.79E-10	3.72E-10	2.14E-10	1.24E-10	7.02E-11
305 kts	4.03E-09	4.16E-09	3.49E-09	1.99E-09	7.7E-10	4.11E-10	2.39E-10	1.41E-10	8.18E-11
310 kts	4.07E-09	4.25E-09	3.69E-09	2.3E-09	8.97E-10	4.53E-10	2.67E-10	1.58E-10	9.46E-11

Table C-17: Worst Winds without Controller Intervention at 3900’

Turn Radius

Groundspeed	1 NM	1.5 NM	2 NM	2.5NM	3 NM	3.5 NM	4 NM	4.5 NM	5 NM
150 kts	1.74E-10	3.44E-11	9.43E-12	3.22E-12	1.25E-12	5.39E-13	2.52E-13	1.26E-13	6.66E-14
155 kts	1.94E-10	4.07E-11	1.07E-11	3.68E-12	1.43E-12	6.2E-13	2.91E-13	1.46E-13	7.75E-14
160 kts	2.46E-10	5.83E-11	1.42E-11	4.93E-12	1.94E-12	8.48E-13	4.01E-13	2.03E-13	1.08E-13
165 kts	3.13E-10	8.13E-11	1.89E-11	6.67E-12	2.65E-12	1.17E-12	5.57E-13	2.84E-13	1.53E-13
170 kts	3.91E-10	1.09E-10	2.55E-11	8.88E-12	3.57E-12	1.58E-12	7.62E-13	3.91E-13	2.12E-13
175 kts	4.81E-10	1.42E-10	3.53E-11	1.17E-11	4.74E-12	2.12E-12	1.03E-12	5.31E-13	2.89E-13
180 kts	5.84E-10	1.82E-10	4.96E-11	1.51E-11	6.21E-12	2.81E-12	1.37E-12	7.13E-13	3.91E-13
185 kts	7.01E-10	2.28E-10	6.9E-11	1.94E-11	8.05E-12	3.66E-12	1.8E-12	9.45E-13	5.21E-13
190 kts	8.33E-10	2.83E-10	9.17E-11	2.49E-11	1.03E-11	4.73E-12	2.35E-12	1.24E-12	6.87E-13
195 kts	9.81E-10	3.45E-10	1.18E-10	3.3E-11	1.31E-11	6.05E-12	3.02E-12	1.6E-12	8.96E-13
200 kts	1.15E-09	4.17E-10	1.49E-10	4.49E-11	1.64E-11	7.65E-12	3.85E-12	2.06E-12	1.16E-12
205 kts	1.34E-09	4.99E-10	1.86E-10	6E-11	2.04E-11	9.59E-12	4.86E-12	2.61E-12	1.48E-12
210 kts	1.57E-09	5.91E-10	2.28E-10	7.97E-11	2.56E-11	1.19E-11	6.08E-12	3.29E-12	1.87E-12
215 kts	1.83E-09	6.94E-10	2.78E-10	1.01E-10	3.31E-11	1.47E-11	7.54E-12	4.1E-12	2.35E-12
220 kts	2.09E-09	8.07E-10	3.34E-10	1.25E-10	4.3E-11	1.79E-11	9.27E-12	5.07E-12	2.92E-12
225 kts	2.32E-09	9.35E-10	3.97E-10	1.53E-10	5.56E-11	2.18E-11	1.13E-11	6.23E-12	3.6E-12
230 kts	2.49E-09	1.08E-09	4.67E-10	1.84E-10	7.28E-11	2.71E-11	1.37E-11	7.59E-12	4.41E-12
235 kts	2.65E-09	1.26E-09	5.46E-10	2.19E-10	9.04E-11	3.48E-11	1.65E-11	9.19E-12	5.37E-12
240 kts	2.79E-09	1.46E-09	6.3E-10	2.6E-10	1.1E-10	4.35E-11	1.97E-11	1.1E-11	6.48E-12
245 kts	2.93E-09	1.67E-09	7.2E-10	3.05E-10	1.32E-10	5.44E-11	2.34E-11	1.32E-11	7.77E-12
250 kts	3.05E-09	1.89E-09	8.16E-10	3.55E-10	1.56E-10	6.93E-11	2.89E-11	1.56E-11	9.27E-12
255 kts	3.16E-09	2.11E-09	9.22E-10	4.11E-10	1.84E-10	8.52E-11	3.7E-11	1.85E-11	1.1E-11
260 kts	3.26E-09	2.34E-09	1.04E-09	4.7E-10	2.15E-10	1.02E-10	4.48E-11	2.17E-11	1.3E-11
265 kts	3.34E-09	2.55E-09	1.19E-09	5.32E-10	2.48E-10	1.2E-10	5.46E-11	2.64E-11	1.52E-11
270 kts	3.43E-09	2.75E-09	1.37E-09	5.97E-10	2.85E-10	1.4E-10	6.75E-11	3.33E-11	1.77E-11
275 kts	3.5E-09	2.93E-09	1.59E-09	6.66E-10	3.26E-10	1.63E-10	8.14E-11	3.98E-11	2.06E-11
280 kts	3.57E-09	3.1E-09	1.84E-09	7.44E-10	3.71E-10	1.87E-10	9.66E-11	4.69E-11	2.46E-11
285 kts	3.62E-09	3.24E-09	2.1E-09	8.41E-10	4.16E-10	2.14E-10	1.12E-10	5.55E-11	3.06E-11
290 kts	3.67E-09	3.38E-09	2.37E-09	9.71E-10	4.61E-10	2.42E-10	1.3E-10	6.73E-11	3.67E-11
295 kts	3.71E-09	3.51E-09	2.62E-09	1.14E-09	5.1E-10	2.74E-10	1.49E-10	8.04E-11	4.25E-11
300 kts	3.7E-09	3.63E-09	2.85E-09	1.37E-09	5.68E-10	3.08E-10	1.7E-10	9.35E-11	4.9E-11
305 kts	3.68E-09	3.74E-09	3.07E-09	1.63E-09	6.37E-10	3.41E-10	1.92E-10	1.08E-10	5.68E-11
310 kts	3.72E-09	3.84E-09	3.26E-09	1.92E-09	7.31E-10	3.77E-10	2.15E-10	1.24E-10	6.78E-11

Table C-18: Worst Winds without Controller Intervention at 4300’

Turn Radius

Groundspeed	1 NM	1.5 NM	2 NM	2.5NM	3 NM	3.5 NM	4 NM	4.5 NM	5 NM
150 kts	5.98E-13	5.6E-15	1.5E-16	8.04E-18	6.79E-19	7.93E-20	1.18E-20	2.13E-21	4.47E-22
155 kts	9.24E-13	8.91E-15	2.4E-16	1.29E-17	1.09E-18	1.28E-19	1.92E-20	3.48E-21	7.36E-22
160 kts	2.1E-12	2.14E-14	5.79E-16	3.13E-17	2.67E-18	3.16E-19	4.76E-20	8.69E-21	1.85E-21
165 kts	4.76E-12	5.2E-14	1.42E-15	7.71E-17	6.63E-18	7.89E-19	1.2E-19	2.2E-20	4.72E-21
170 kts	1.07E-11	1.23E-13	3.39E-15	1.85E-16	1.59E-17	1.91E-18	2.92E-19	5.41E-20	1.17E-20
175 kts	2.38E-11	2.79E-13	7.83E-15	4.29E-16	3.72E-17	4.49E-18	6.9E-19	1.29E-19	2.79E-20
180 kts	4.85E-11	6.16E-13	1.76E-14	9.72E-16	8.47E-17	1.03E-17	1.59E-18	2.97E-19	6.49E-20
185 kts	8.97E-11	1.31E-12	3.86E-14	2.14E-15	1.88E-16	2.28E-17	3.55E-18	6.69E-19	1.47E-19
190 kts	1.56E-10	2.7E-12	8.26E-14	4.62E-15	4.06E-16	4.96E-17	7.76E-18	1.47E-18	3.24E-19
195 kts	2.53E-10	5.35E-12	1.72E-13	9.71E-15	8.59E-16	1.05E-16	1.65E-17	3.15E-18	6.98E-19
200 kts	3.86E-10	1.03E-11	3.49E-13	2E-14	1.78E-15	2.19E-16	3.45E-17	6.59E-18	1.47E-18
205 kts	5.57E-10	2.11E-11	6.91E-13	4.02E-14	3.6E-15	4.45E-16	7.05E-17	1.35E-17	3.03E-18
210 kts	7.67E-10	4.39E-11	1.33E-12	7.93E-14	7.14E-15	8.88E-16	1.41E-16	2.72E-17	6.11E-18
215 kts	1.01E-09	7.99E-11	2.51E-12	1.53E-13	1.39E-14	1.74E-15	2.77E-16	5.36E-17	1.21E-17
220 kts	1.28E-09	1.32E-10	4.57E-12	2.89E-13	2.66E-14	3.34E-15	5.35E-16	1.04E-16	2.35E-17
225 kts	1.54E-09	2.07E-10	8.11E-12	5.36E-13	4.99E-14	6.31E-15	1.01E-15	1.98E-16	4.49E-17
230 kts	1.75E-09	3.09E-10	1.4E-11	9.73E-13	9.2E-14	1.17E-14	1.89E-15	3.7E-16	8.45E-17
235 kts	1.93E-09	4.45E-10	2.63E-11	1.73E-12	1.67E-13	2.14E-14	3.48E-15	6.83E-16	1.56E-16
240 kts	2.09E-09	6.2E-10	5.09E-11	3E-12	2.97E-13	3.85E-14	6.28E-15	1.24E-15	2.84E-16
245 kts	2.24E-09	8.29E-10	8.83E-11	5.1E-12	5.19E-13	6.81E-14	1.12E-14	2.22E-15	5.11E-16
250 kts	2.37E-09	1.05E-09	1.41E-10	8.44E-12	8.92E-13	1.19E-13	1.96E-14	3.91E-15	9.04E-16
255 kts	2.49E-09	1.27E-09	2.13E-10	1.36E-11	1.51E-12	2.04E-13	3.4E-14	6.8E-15	1.58E-15
260 kts	2.6E-09	1.49E-09	3.08E-10	2.19E-11	2.49E-12	3.44E-13	5.8E-14	1.17E-14	2.72E-15
265 kts	2.71E-09	1.7E-09	4.31E-10	3.84E-11	4.05E-12	5.73E-13	9.77E-14	1.98E-14	4.63E-15
270 kts	2.8E-09	1.91E-09	5.84E-10	6.84E-11	6.46E-12	9.39E-13	1.62E-13	3.31E-14	7.79E-15
275 kts	2.88E-09	2.1E-09	7.63E-10	1.08E-10	1.01E-11	1.51E-12	2.66E-13	5.47E-14	1.29E-14
280 kts	2.96E-09	2.27E-09	9.72E-10	1.62E-10	1.54E-11	2.4E-12	4.3E-13	8.93E-14	2.13E-14
285 kts	3.03E-09	2.43E-09	1.21E-09	2.34E-10	2.31E-11	3.75E-12	6.86E-13	1.44E-13	3.45E-14
290 kts	3.1E-09	2.58E-09	1.46E-09	3.31E-10	3.74E-11	5.76E-12	1.08E-12	2.29E-13	5.54E-14
295 kts	3.14E-09	2.72E-09	1.7E-09	4.62E-10	6.34E-11	8.67E-12	1.67E-12	3.61E-13	8.8E-14
300 kts	3.15E-09	2.85E-09	1.93E-09	6.34E-10	9.74E-11	1.28E-11	2.55E-12	5.61E-13	1.38E-13
305 kts	3.14E-09	2.96E-09	2.15E-09	8.45E-10	1.43E-10	1.85E-11	3.81E-12	8.55E-13	2.13E-13
310 kts	3.19E-09	3.07E-09	2.35E-09	1.1E-09	2.08E-10	2.64E-11	5.65E-12	1.3E-12	3.27E-13

Table C-19: Worst Winds without Controller Intervention at 4800’

Turn Radius

Groundspeed	1 NM	1.5 NM	2 NM	2.5NM	3 NM	3.5 NM	4 NM	4.5 NM	5 NM
150 kts	7.03E-11	1.2E-11	3.54E-12	1.2E-12	4.47E-13	1.84E-13	8.29E-14	4E-14	2.04E-14
155 kts	7.99E-11	1.37E-11	4.07E-12	1.39E-12	5.19E-13	2.15E-13	9.71E-14	4.71E-14	2.4E-14
160 kts	1.06E-10	1.83E-11	5.56E-12	1.92E-12	7.25E-13	3.03E-13	1.38E-13	6.73E-14	3.46E-14
165 kts	1.41E-10	2.53E-11	7.64E-12	2.67E-12	1.02E-12	4.3E-13	1.97E-13	9.69E-14	5.02E-14
170 kts	1.84E-10	3.6E-11	1.03E-11	3.66E-12	1.41E-12	6.01E-13	2.78E-13	1.37E-13	7.17E-14
175 kts	2.35E-10	5.3E-11	1.38E-11	4.95E-12	1.93E-12	8.27E-13	3.85E-13	1.92E-13	1.01E-13
180 kts	2.96E-10	7.75E-11	1.81E-11	6.61E-12	2.59E-12	1.12E-12	5.27E-13	2.64E-13	1.4E-13
185 kts	3.66E-10	1.05E-10	2.35E-11	8.71E-12	3.45E-12	1.51E-12	7.12E-13	3.59E-13	1.91E-13
190 kts	4.47E-10	1.36E-10	3.03E-11	1.13E-11	4.54E-12	2E-12	9.5E-13	4.82E-13	2.58E-13
195 kts	5.37E-10	1.72E-10	4.03E-11	1.46E-11	5.9E-12	2.61E-12	1.25E-12	6.4E-13	3.45E-13
200 kts	6.37E-10	2.15E-10	5.72E-11	1.86E-11	7.58E-12	3.39E-12	1.63E-12	8.4E-13	4.55E-13
205 kts	7.5E-10	2.65E-10	7.96E-11	2.34E-11	9.65E-12	4.34E-12	2.11E-12	1.09E-12	5.95E-13
210 kts	8.79E-10	3.22E-10	1.05E-10	2.92E-11	1.22E-11	5.51E-12	2.7E-12	1.4E-12	7.7E-13
215 kts	1.03E-09	3.86E-10	1.34E-10	3.62E-11	1.52E-11	6.94E-12	3.42E-12	1.79E-12	9.87E-13
220 kts	1.21E-09	4.58E-10	1.68E-10	4.64E-11	1.88E-11	8.66E-12	4.29E-12	2.26E-12	1.25E-12
225 kts	1.41E-09	5.38E-10	2.07E-10	6.24E-11	2.31E-11	1.07E-11	5.35E-12	2.83E-12	1.58E-12
230 kts	1.6E-09	6.26E-10	2.51E-10	8.26E-11	2.81E-11	1.32E-11	6.61E-12	3.52E-12	1.97E-12
235 kts	1.76E-09	7.25E-10	3.01E-10	1.06E-10	3.41E-11	1.6E-11	8.1E-12	4.34E-12	2.44E-12
240 kts	1.9E-09	8.38E-10	3.55E-10	1.32E-10	4.19E-11	1.94E-11	9.86E-12	5.31E-12	3.01E-12
245 kts	2.03E-09	9.63E-10	4.13E-10	1.61E-10	5.29E-11	2.33E-11	1.19E-11	6.46E-12	3.68E-12
250 kts	2.14E-09	1.1E-09	4.75E-10	1.92E-10	6.58E-11	2.78E-11	1.43E-11	7.81E-12	4.46E-12
255 kts	2.25E-09	1.25E-09	5.42E-10	2.27E-10	8.24E-11	3.3E-11	1.71E-11	9.38E-12	5.39E-12
260 kts	2.35E-09	1.41E-09	6.1E-10	2.64E-10	1.05E-10	3.93E-11	2.03E-11	1.12E-11	6.46E-12
265 kts	2.45E-09	1.58E-09	6.83E-10	3.06E-10	1.27E-10	4.8E-11	2.4E-11	1.33E-11	7.7E-12
270 kts	2.54E-09	1.75E-09	7.68E-10	3.5E-10	1.51E-10	5.94E-11	2.81E-11	1.57E-11	9.12E-12
275 kts	2.63E-09	1.91E-09	8.76E-10	3.97E-10	1.76E-10	7.09E-11	3.28E-11	1.84E-11	1.08E-11
280 kts	2.7E-09	2.07E-09	1.02E-09	4.45E-10	2.04E-10	8.55E-11	3.83E-11	2.15E-11	1.26E-11
285 kts	2.76E-09	2.2E-09	1.18E-09	4.97E-10	2.34E-10	1.05E-10	4.59E-11	2.5E-11	1.47E-11
290 kts	2.8E-09	2.33E-09	1.37E-09	5.61E-10	2.66E-10	1.25E-10	5.63E-11	2.89E-11	1.71E-11
295 kts	2.83E-09	2.44E-09	1.57E-09	6.41E-10	3E-10	1.45E-10	6.66E-11	3.33E-11	1.98E-11
300 kts	2.82E-09	2.54E-09	1.77E-09	7.49E-10	3.36E-10	1.66E-10	7.63E-11	3.86E-11	2.29E-11
305 kts	2.81E-09	2.64E-09	1.96E-09	8.9E-10	3.74E-10	1.89E-10	8.79E-11	4.59E-11	2.62E-11
310 kts	2.85E-09	2.73E-09	2.14E-09	1.07E-09	4.2E-10	2.14E-10	1.05E-10	5.51E-11	2.99E-11

Table C-20: Worst Winds without Controller Intervention at 5300’

Turn Radius

Groundspeed	1 NM	1.5 NM	2 NM	2.5NM	3 NM	3.5 NM	4 NM	4.5 NM	5 NM
150 kts	3.59E-11	7.28E-12	2.1E-12	7.09E-13	2.61E-13	1.06E-13	4.7E-14	2.23E-14	1.12E-14
155 kts	4.41E-11	8.35E-12	2.43E-12	8.26E-13	3.05E-13	1.25E-13	5.54E-14	2.64E-14	1.33E-14
160 kts	6.52E-11	1.14E-11	3.37E-12	1.16E-12	4.32E-13	1.78E-13	7.98E-14	3.83E-14	1.94E-14
165 kts	8.98E-11	1.55E-11	4.71E-12	1.64E-12	6.17E-13	2.56E-13	1.16E-13	5.59E-14	2.85E-14
170 kts	1.2E-10	2.09E-11	6.46E-12	2.28E-12	8.67E-13	3.63E-13	1.65E-13	8.03E-14	4.13E-14
175 kts	1.57E-10	2.86E-11	8.74E-12	3.13E-12	1.2E-12	5.07E-13	2.32E-13	1.14E-13	5.88E-14
180 kts	2.02E-10	4.11E-11	1.16E-11	4.24E-12	1.64E-12	6.98E-13	3.22E-13	1.59E-13	8.26E-14
185 kts	2.55E-10	6.06E-11	1.53E-11	5.66E-12	2.21E-12	9.48E-13	4.4E-13	2.18E-13	1.14E-13
190 kts	3.16E-10	8.69E-11	1.99E-11	7.46E-12	2.94E-12	1.27E-12	5.94E-13	2.97E-13	1.56E-13
195 kts	3.87E-10	1.15E-10	2.55E-11	9.72E-12	3.87E-12	1.69E-12	7.93E-13	3.99E-13	2.11E-13
200 kts	4.67E-10	1.48E-10	3.25E-11	1.25E-11	5.04E-12	2.21E-12	1.05E-12	5.29E-13	2.82E-13
205 kts	5.55E-10	1.85E-10	4.22E-11	1.6E-11	6.48E-12	2.87E-12	1.37E-12	6.96E-13	3.73E-13
210 kts	6.55E-10	2.29E-10	5.83E-11	2.02E-11	8.27E-12	3.68E-12	1.77E-12	9.05E-13	4.88E-13
215 kts	7.69E-10	2.79E-10	8.13E-11	2.52E-11	1.04E-11	4.68E-12	2.26E-12	1.17E-12	6.31E-13
220 kts	9.02E-10	3.36E-10	1.08E-10	3.13E-11	1.31E-11	5.9E-12	2.87E-12	1.49E-12	8.1E-13
225 kts	1.06E-09	4E-10	1.38E-10	3.84E-11	1.62E-11	7.38E-12	3.62E-12	1.88E-12	1.03E-12
230 kts	1.23E-09	4.71E-10	1.72E-10	4.68E-11	2E-11	9.16E-12	4.51E-12	2.36E-12	1.3E-12
235 kts	1.39E-09	5.49E-10	2.1E-10	5.88E-11	2.44E-11	1.13E-11	5.58E-12	2.94E-12	1.63E-12
240 kts	1.53E-09	6.36E-10	2.53E-10	7.81E-11	2.96E-11	1.38E-11	6.86E-12	3.63E-12	2.02E-12
245 kts	1.65E-09	7.33E-10	2.99E-10	1.03E-10	3.56E-11	1.67E-11	8.37E-12	4.46E-12	2.49E-12
250 kts	1.77E-09	8.34E-10	3.49E-10	1.29E-10	4.26E-11	2.01E-11	1.01E-11	5.43E-12	3.05E-12
255 kts	1.88E-09	9.46E-10	4.01E-10	1.57E-10	5.06E-11	2.41E-11	1.22E-11	6.58E-12	3.71E-12
260 kts	1.99E-09	1.07E-09	4.55E-10	1.87E-10	6.15E-11	2.87E-11	1.46E-11	7.92E-12	4.49E-12
265 kts	2.08E-09	1.21E-09	5.12E-10	2.21E-10	7.65E-11	3.39E-11	1.74E-11	9.47E-12	5.39E-12
270 kts	2.16E-09	1.36E-09	5.75E-10	2.56E-10	9.43E-11	3.99E-11	2.06E-11	1.13E-11	6.45E-12
275 kts	2.23E-09	1.51E-09	6.5E-10	2.93E-10	1.18E-10	4.67E-11	2.43E-11	1.33E-11	7.66E-12
280 kts	2.3E-09	1.65E-09	7.43E-10	3.33E-10	1.41E-10	5.52E-11	2.84E-11	1.57E-11	9.07E-12
285 kts	2.36E-09	1.78E-09	8.64E-10	3.75E-10	1.66E-10	6.67E-11	3.31E-11	1.84E-11	1.07E-11
290 kts	2.42E-09	1.91E-09	1.01E-09	4.22E-10	1.92E-10	7.94E-11	3.84E-11	2.14E-11	1.25E-11
295 kts	2.46E-09	2.02E-09	1.18E-09	4.77E-10	2.19E-10	9.28E-11	4.43E-11	2.49E-11	1.46E-11
300 kts	2.48E-09	2.12E-09	1.35E-09	5.5E-10	2.48E-10	1.07E-10	5.1E-11	2.87E-11	1.69E-11
305 kts	2.47E-09	2.22E-09	1.52E-09	6.42E-10	2.78E-10	1.26E-10	5.98E-11	3.3E-11	1.95E-11
310 kts	2.48E-09	2.3E-09	1.69E-09	7.64E-10	3.14E-10	1.49E-10	7.19E-11	3.78E-11	2.24E-11